TABLE OF CONTENTS

1.0 MIT Research Reactor

1.1 Introduction

This preliminary Safety Analysis Report (SAR) is intended to support a future application to the U.S. Nuclear Regulatory Commission (NRC) by the Massachusetts Institute of Technology (MIT) for the licensing of its research reactor, the MITR, for conversion from High Enriched Uranium (HEU) to Low Enriched Uranium (LEU) Fuel. The preliminary SAR is based on the guidance of NUREG-1537 [1-1, 1-2] and updates required for LEU conversion to the current MITR-II HEU SAR [1-3]. In the course of analysis, it was determined that a power level increase from 6,000 kW (HEU core) to 7,000 kW (LEU core) is required, in order to maintain core neutronic flux performance [1-4].

The Massachusetts Institute of Technology Reactor (MITR) is a heavy-water reflected, light-water cooled and moderated nuclear research reactor that utilizes flat, plate-type fuel elements. The MITR is owned and operated by the Massachusetts Institute of Technology, a non-profit educational institution. The MITR is the major experimental facility of the MIT Nuclear Reactor Laboratory, which is an interdepartmental laboratory that functions as a center for both education and research for many MIT departments as well as local-area universities and hospitals. The reactor facility is located on the MIT Campus at 138 Albany Street in Cambridge, Massachusetts. The MITR design includes a number of inherent (i.e., passive) safety features. The principal safety features are negative reactivity temperature coefficients of both the fuel and moderator, a negative void coefficient of reactivity, the location of the core within two concentric tanks, the use of anti-siphon valves to isolate the core from the effect of breaks in the coolant piping, a core-tank design that promotes natural circulation, and the presence of a full containment building. A unique design feature of the MITR is the fuel elements with rhomboidal cross-sections, which permits the core to be arranged in a hexagonal close-packed array. It should be noted that the fuel element has been redesigned and that the longitudinal fins, which exist in the HEU 15-plate fuel element, are removed in the 19-plate LEU design. This is due to fabrication and economic considerations, as well as the efforts of standardizing the non-finned fuel plate design of all five U.S. High Performance Research Reactors (HPRRs).

1.2 Summary and Conclusions of Principal Safety Considerations

This section summarizes safety criteria, the principal safety considerations, and the resulting conclusions of the preliminary SAR. Detailed information is given in the subsequent chapters of this report.

1.2.1 Consequences from Operation and Use

The principal conclusion of the safety analysis contained in this report is that operation and use of the MITR with LEU fuel will result in considerable benefit without any significant cost to public health or the environment. Specific conclusions are as follows:

a) Operation and use of the MITR with LEU fuel will provide significant benefits in terms of education, research, and the medical applications of radiation.

b) The facility's purpose is within the scope of Sections 104a (medical therapy) and 104c (research and development) of the Atomic Energy Act of 1954, as amended. Moreover, the facility will be operated in conformity with that Act, as amended.

c) Operation and use of the MITR with LEU fuel will be conducted without consequences to the health and safety of the public. Nor will there be any significant environmental impact from the facility.

The basis for these conclusions is the careful review of the MITR design and operational safety that is documented in this SAR. Areas reviewed include the site characteristics, the design basis for facility structures, the core and the coolant systems, engineered safety features, instrument and control systems, electrical power and auxiliary support systems, and experimental facilities. In addition, administrative elements of design and operation such as radiological safety programs, operating procedures, accident scenarios, technical specifications, and financial qualifications, were reviewed as part of the process that lead to the above conclusions.

1.2.2 Safety Considerations on Choice of Site, Fuel, and Power Level

The MITR is situated on the MIT campus, which is located within a metropolitan area. This site was selected to promote the exchange of ideas between educators and researchers at both MIT and other local-area universities. A further reason for choosing this site was its proximity to many major medical centers. Such proximity is necessary in order to foster scientific collaboration, to provide the timely delivery of short-lived isotopes for medical research, and to permit patient therapy using neutron beams. In view of the urban setting for the MITR, a full containment structure was chosen. The building is a domed cylindrical airtight structure. The cylindrical portion is made of 3/8-inch thick steel plate that surrounds a 2.0-foot thick concrete wall. The dome portion is made of 5/8-inch steel plate. The containment building, which is equipped with both underpressure protection and an overpressure relief system, is designed to protect the public from radioactive effluents in the event of a facility accident. A complete description of the containment building is given in Section 6.5 of this report. The site itself is described in Chapter 2 of the SAR.

The reactor is a tank-type design that uses light water as a moderator and coolant and heavy water as a reflector. The tank-type design coupled with the separation of the moderator/coolant from the reflector offers several safety advantages. First, the reactor core is contained within a closed system. This serves to prevent the release of fission products and provides a simple method for the detection of incipient fuel cladding failures. Namely, the coolant and/or cover gas contained within the tank can be sampled for abnormal activity. Second, there are two metal tanks, that of the primary system and that of the reflector system, surrounding the core. This reduces the likelihood of a loss-of-coolant accident. Third, tritium production from the activation of heavy water is limited to the heavy-water reflector system, and the heavy-water reflector is a closed system.

Conversion of the MITR from an HEU fuel system to an LEU fuel system has required redesign of the MITR fuel element. Reducing the enrichment to 19.75 wt. % U-235 led to changing the fuel-bearing region of the MITR plates from a dispersion cermet fuel form to an alloy of uranium and 10 wt. % molybdenum, referred to as the U-10Mo monolithic fuel foil. This high-density

U-10Mo monolithic alloy fuel is currently under development and qualification. The monolithic U-10Mo alloy density of 17.02 gU/cm^3 is adequate for all U.S. High Performance Research Reactors (USHPRRs), including the MITR.

The maximum power level allowed by the Code of Federal Regulations for a research reactor is ten megawatts. The analysis presented in Chapter 4 of the SAR demonstrates that the MITR can be safely operated with the existing heat removal equipment at a steady-state power level of 8.68 MW. The planned power level for MITR operation is 7.0 MW. This provides a 17% increase in power over the HEU core power level of 6.0 MW. The power level increase to 7.0 MW operations is required to maintain performance of the reactor for both researchers and the facility's medical therapy capability. In addition, it maintains a substantial safety margin as established in the safety analyses.

1.2.3 Inherent Safety Features

The MITR's design includes a number of inherent safety features listed here:

a) The reactor core is designed so that there are negative reactivity coefficients associated with both its fuel and moderator temperatures. These mitigate the consequences of any reactivity excursion and promote self-regulation of the reactor. These negative coefficients arise because the core is intentionally under-moderated and its design is such that some neutron leakage occurs.

b) The reactor core is designed so that there is a negative coefficient of reactivity associated with the formation of voids. This feature also mitigates the consequences of any reactivity excursion.

c) There should be no mixing of the light-water moderator and the heavy-water reflector because the tanks and systems are separate and isolated. However, should any leaking or mixing occur, the result will be the insertion of negative reactivity. The leakage of light water into the heavy water reflector would cause greater neutron absorption of the already-thermalized neutrons. The leakage of heavy water into the light water moderator would result in less moderation of the still fast neutrons. Hence, in both cases, the fission rate will be reduced.

d) The reactor core is contained within two concentric tanks, one for the light water that serves as both coolant and moderator and one for the heavy-water reflector. The concentric configuration of the two tanks greatly reduces the likelihood of a loss-of-coolant accident.

e) Piping penetrations to the primary core tank (for the coolant/moderator) are all located above the core. Where appropriate, the core tank penetrations are equipped with anti-siphon valves. With these design features, a pipe break cannot result in uncovering of the core.

f) The reactor is housed in a containment building that contains redundant (main and auxiliary) sets of dampers on both the inlet and exhaust ventilation penetrations. The main dampers are interlocked with the effluent radiation monitoring system and will

close, thereby sealing the building, if abnormal radiation levels are detected. If these dampers fail to close within a specified time interval, the auxiliary dampers are signaled to close. The main dampers are hydraulically operated. The auxiliary dampers are gravity-operated. Both sets close on loss of electricity.

g) The geometrical arrangement of the core relative to the core housing and tank was chosen to promote natural circulation in the event of a loss-of- flow accident. In addition, there are specially designed natural circulation valves that facilitate establishment of natural convection heat removal in the absence of forced circulation of the coolant.

h) The reactor control blades, which are used to maintain criticality during operation and shutdown the reactor when needed, are held in place by electromagnets. Upon de-energizing the electromagnets, the blades drop by force of gravity into the core thereby making it subcritical.

i) The reactivity worth of the heavy water reflector is substantial and its removal makes the reactor subcritical even if the control blades are still withdrawn. The reflector can be rapidly "dumped" to a holding tank by means of a solenoid-controlled air-operated valve. Loss of electrical power, loss of compressed air supply, or manual action will result in the reflector being dumped to the holding tank.

j) The containment building is protected against excessive vacuum forces by two sets of redundant spring-loaded vacuum relief breakers.

1.2.4 Design Features for Safe Operation and Shutdown

There are a number of design features and design bases of systems and components associated with the MITR that promote safe operation and shutdown. These include:

a) Reactor Control System: The reactor control system consists of both shim blades and a regulating rod. The former are used to attain criticality, to compensate for fission product poisoning and fuel depletion, and to accomplish major changes of reactor power. The latter is used for the fine adjustment of reactor power and is operated by the auto control system to maintain a constant power level. The six shim blades are connected to drive mechanisms by electromagnets. Hence, on loss of electrical power, all blades drop into the core under the force of gravity. The reactor control system restricts reactivity insertion by permitting only one shim blade to be withdrawn at a time. All six blades can be driven in simultaneously to shut the reactor down. In an emergency, all six can be simultaneously dropped into the core.

b) Reflector Dump Capability: The heavy-water reflector can be dumped to a holding tank away from the core. Loss of the reflector shuts the reactor down, so this capability is a backup shutdown mechanism.

c) Reactor Protection System: The reactor protection system consists of the nuclear and process safety systems that monitor parameters that are important to reactor safety including reactor power and period, coolant outlet temperature and flow, and core tank level. The system uses a one-out-of-one logic. Hence, even if a particular signal is

measured by redundant instruments, any single out-of-specification signal will cause a shutdown. Actuation of the protection system causes the shim blade electromagnets to be de-energized, thereby dropping the six shim blades into the core, shutting down the reactor.

d) Emergency Core Cooling System: The passive safety features (the natural convection and anti-siphon valves) are sufficient to ensure that the core is adequately cooled upon a loss of forced convection. The presence of both a core tank and a reflector tank as well as the use of anti-siphon vales greatly reduces the likelihood that the core would ever be uncovered. Nevertheless, an emergency core cooling system has been installed. This system, which requires manual initiation, sprays water from one of multiple sources on to the core at a rate sufficient to remove decay heat.

e) Containment Building Pressure Differential: The control damper, from the containment ventilation system, is adjusted to maintain building pressure slightly below atmospheric pressure. Hence, any air leakage will be into the building rather than out of the building.

f) Containment Building Isolation: Operation of the ventilation exhaust dampers, which close on loss of electrical power, was described above in Section 1.2.3(f) of this report. An engineered safeguards feature is associated with this system. The exhaust ventilation flows through a holdup plenum. Effluent radiation monitors are located at the entrance to this plenum and the ventilation system's isolation dampers are located at the exit. The air flow delay through the plenum is such that if abnormal activity is detected, the building will be sealed by the isolation damper system before it can be released.

g) Containment Pressure Relief: The containment building is equipped with a pressure relief system that processes exhaust air for the removal of radioactive particulates and iodine. This system can be placed on line manually without entry to the containment building. Once on line, flow through the system is established by the pressure difference between the building and the environment. Its purpose is to permit building pressure to be maintained at or below a pre-determined allowed value in the event that the building is sealed.

1.2.5 Potential Accidents

The maximum hypothetical accident (MHA) for the MITR is that some foreign material becomes lodged beneath the core where it causes partial blockage of fuel element channels. Because of the size of the openings in the nozzles at the end of each fuel element, any piece of foreign material that could pass through the nozzles would not be large enough to restrict flow in more than six coolant channels of one element. Hence there could be, at most, the overheating of a maximum of five fuel plates. The MHA conservatively assumes that the entire active portions of all five plates melt completely. Analysis of this accident is given in Section 13.2.1 of this report. The calculated maximum Total Effective Dose Equivalent (TEDE) to an individual located at the nearest points of public occupancy during the first two hours following the MHA (the time allowed for protective actions to be implemented) is 302.1 mrem at 8 m (back fence) and 392.8 mrem at 21 m (front fence). The maximum TEDE is less than 480 mrem at 16 m (peak

dose location), which is well bounded by the 500 mrem TEDE limit goal for public exposure cited from NUREG-1537.

Other accidents that are evaluated in Chapter 13 of this SAR include insertion of excess reactivity, loss of primary coolant, loss of primary coolant flow, malfunction of fuel, loss of normal electrical power, external events, and equipment malfunctions. These evaluations demonstrate that none of these accidents will result in a safety hazard to the public or the environment. It should be recognized that some of these accidents, such as a loss of coolant flow or a loss of offsite electrical power, have occurred and are expected to occur again. The MITR was designed with this expectation so that no safety hazards or environmental effects will result.

1.3 General Description of the Facility

The original MIT Reactor, MITR-I, was both heavy-water moderated and cooled with an open array of plate-type fuel elements. It was surrounded by a graphite reflector. This original core attained criticality in July 1958 and operated at power levels of up to 5 MW until May 1974. The MITR-II core (from 1975 to present) differs significantly from the original design in that it uses light water to cool and moderate a close-packed array of finned, plate-type fuel elements that are surrounded by a heavy-water reflector which is in turn surrounded by the original graphite reflector. This core design was chosen to maximize the thermal neutron flux in the reflector regions where the experimental beam ports are located. The current effort is to convert the MITR-II core with unfinned U-10Mo LEU fuel.

The MITR LEU core has several unique features. First, the fuel elements are rhomboid in cross-section. This allows arrangement of a hexagonal-shaped core that contains twenty-seven element spaces grouped in three concentric rings. The A-ring (inner-most) contains three elements, the B-ring contains nine elements, and the C-ring (outer-most) contains fifteen elements. Second, the control devices (six shim blades and a fine-control regulating rod) are all located on the core periphery in the space between the C-ring and the light-water core tank. Third, the beamports are aligned so that they point to a position below the core where the thermal flux is at a maximum because of water peaking effects. Those locations also improve the quality of the flux provided to experimenters because all neutrons entering a beam port must have undergone at least one thermalizing collision.

The MITR is located in the northwest section of the MIT campus in Cambridge, Massachusetts. The site is urban with activities related to both manufacturing and retail sales located nearby. In addition, there are other MIT-owned properties adjacent to the reactor site. These include administrative and teaching facilities, dormitories, and other laboratories. An advantage to this urban setting is the proximity of the site to security, fire, and medical assistance should those services be needed.

The meteorological and seismic characteristics of the site are those of the northeastern United States. Hurricanes and winter storms do occur. However, extreme weather conditions, such as tornadoes, are not a factor. There has been low to moderate seismic activity in historic time both to the north and south of the Cambridge-Boston area. However, Cambridge itself lies in a basin that has been largely free of such activity. The MITR site is drained by the Charles River immediately before it flows into the Atlantic Ocean. Hence the site is not subject to flooding.

The principal design criterion is that reactor operation should not result in any fuel damage. As a practical matter, this means that the thermal-hydraulic, reactor control, and reactor protection systems are designed to prevent the occurrence of critical heat flux (CHF). To assure further the safe operation of the MITR, limiting safety system settings (LSSS) are selected to prevent the onset of nucleate boiling (ONB) anywhere in the core. For the transients listed above in Section 1.2.5 of this report, a reactor scram at the LSSS will prevent exceeding temperature safety limits of the fuel plates.

According to the results in Chapter 4 of this report, the MITR is capable of operating at a steady-state power level of 8.68 MW (8,680 kW). It is planned to operate at no more than 7.0 MW (7,000 kW) thereby providing a substantial safety margin. The reactor is not designed for pulsed operation. Its principal operating characteristics are negative coolant and fuel temperature coefficients of reactivity, a negative void coefficient, a negative change of reactivity should there be any accidental mixing of the light-water moderator and heavy-water reflector, the inability to attain criticality on withdrawal of a single control device, and the capability of making the facility subcritical by an amount equal to or greater than the required shutdown margin through use of either the control devices or dumping of the heavy-water reflector.

The principal safety systems are (1) the reactor protection system, which is used to monitor both core neutronic performance and the status of the various process systems especially those associated with heat removal; (2) the reactor control and reflector dump system, which provides the means to make the reactor subcritical even with all absorbers fully withdrawn; and (3) the containment ventilation isolation and pressure relief systems, which ensure the retention of any abnormal radioactivity within the containment building itself.

The reactor is equipped with a number of passive and engineered safety systems. The former were enumerated above in Section 1.2.3 of this report. The latter include:

a) Emergency core cooling that, upon manual initiation, sprays water onto the core to remove decay heat.

b) Emergency battery backup electrical power that, upon loss of the normal electrical power supply, picks up the loads that are important to reactor and personnel safety.

c) Containment isolation that, upon actuation by an effluent radiation monitor, seals the building.

d) Containment pressure relief that, upon manual initiation, relieves pressure in the containment building by passively discharging air through filters that remove particulates and iodines.

The MITR has five major instrumentation systems. These are the reactor control system, the reactor protection system, engineered safeguards actuation system, the control console display instruments, and the radiation monitoring system. These systems utilize redundancy to avoid single-point failures and diversity to preclude common mode failures. Most instruments indicate remotely in the reactor control room. Signals that are of importance to the operator-in-charge for the manipulation of reactor power are displayed on the console. These include indications of reactor power and period, control device position, coolant temperature, and process system flows.

Also provided at or near the console are readouts from the effluent and area radiation monitors, an annunciator panel that reflects the status of the process systems, and the outputs of the nuclear safety system.

Control of the MITR is at all times under the direct observation of a licensed reactor operator. That operator may, depending on the circumstances, either perform the needed manipulations manually or employ an automatic controller. The principal modes of control are:

a) Startup: Upon completion of mechanical and instrumentation checklists, the operator may take the reactor critical and raise its power level. This is done by withdrawing each of the shim blades, one at a time. The withdrawals are done in small increments with each blade being moved in sequence to maintain a uniform bank height. A number of interlocks must be satisfied in order to initiate a startup. These ensure that the requisite initial conditions (e.g., all process and instrumentation system operating) are satisfied.

b) Power Adjustment: Major adjustments of reactor power are normally performed manually by moving one of the shim blades to establish the requisite period. Movement of the blade is limited to a certain increment (either above or below) the bank height. Once the new power level is attained, the blade is returned to the bank and the regulating rod adjusted to make the reactor exactly critical before returning the reactor to auto-control.

c) Steady-State: Steady-state operation is usually achieved via an automatic controller that moves the fine-control regulating rod in response to a deviation between the measured power and the specified power setting. In the event of a sudden large deviation, auto-control will trip automatically to manual and sound an alarm. Steady-state operation can also be done manually.

d) Shutdown: Reactor shutdown can be accomplished in several different ways. First, the operator can perform a shutdown manually by driving each blade in sequentially in small increments to maintain a uniform bank height during the shutdown. Second, all blades can be inserted simultaneously at their normal speed. Third, the reactor can be scrammed by two available methods. A "minor" scram causes all blades to drop. A "major" scram does that and also dumps the reflector and seals the containment building. Fourth, the reflector can be dumped without other action such as building isolation.

e) Digital Automatic Control: The MITR has approval for the digital control of both its regulating rod and its shim blades. Two types of controllers are possible. For the first category, safety is assured by limiting the net reactivity worth of the control element (blade or regulating rod) that is associated with the automatic controller. For the second category, safety is assured by designing the controller in accordance with the concept of "feasibility of control." (See Section 10.2.10 of this report.) This ensures that it will always be possible to achieve some equilibrium state before a limiting condition is attained.

Offsite electricity is supplied by two 13.8 kV power lines that feed separate 1,200 ampere circuit breakers. These breakers are interlocked so that only one is closed at a time. A transformer

reduces the voltage to 480 V and supplies separate load centers. One load center provides electrical power to the Nuclear Reactor Laboratory's administrative building. The others supply various reactor loads. In addition to the normal electrical power supply, there is an emergency distribution system. An emergency backup battery bank supplies a motor-generator (MG) set that in turn provides AC power to vital loads. On loss of normal off-site power, the MG set starts automatically and essential loads transfer to it. These include the minimum complement of instrumentation needed to ensure reactor safety, the minimum complement of radiation monitors, essential lighting, communications equipment, and the decay heat removal pump.

Heat produced from fission in the MITR core is deposited in the primary, heavy-water reflector, and shield systems. All three are equipped with heat removal systems. The primary heat removal system is the largest because it transports the bulk of the fission energy. It consists of two centrifugal pumps, heat exchangers, a cleanup loop, and a storage tank that both allows for volume changes and provides a reserve. In addition to removing heat from the core, primary coolant is circulated through the light-water shutter that controls the neutron beam to the medical irradiation room that is located in the reactor basement. Primary coolant from the storage tank can also be supplied to the emergency core cooling system although the normal lineup for this system is from city water. The coolant systems for the heavy water reflector and shield system are similar except that they each utilize a single pump and heat exchanger. Each has its own cleanup loop and storage tank.

The MITR generates high-level waste (spent fuel) and low-level waste. The latter may be solid, liquid, or gaseous. The spent fuel is returned to the U.S. Department of Energy as discussed below in Section 1.7 of this report. The low level waste is treated as follows:

a) Solid waste (rags, dewatered resins, contaminated tools, etc.) is compacted, and either stored on-site for decay or shipped off-site to an approved disposal site.

b) Liquid waste is held in one of two storage tanks for decay. It is then recirculated to ensure uniformity, filtered, sampled, and discharged to the sanitary sewer.

c) Gaseous waste is filtered for the removal of particulates and iodines and then discharged via the containment building stack.

Both liquid and gaseous discharges are continuously monitored for radiation level. Interlocks will halt the discharge if any abnormal activity is detected.

A radiation protection program for those who work at the facility is designed and administered by an on-site group – Reactor Radiation Protection – that is part of the MIT Environment, Health and Safety (EHS) Office. EHS reports to the Executive Vice President and Treasurer and hence is independent of Reactor Operations.

The MITR is equipped with a number of experimental facilities as listed here:

a) Medical Irradiation Rooms: Two such facilities are available. One is located in the basement and uses a neutron beam from the reactor core. The other is located on the reactor floor and uses a beam produced by a fission converter that in turn is driven by neutrons from the core. The basement facility's beam may be either thermal or epithermal

depending on the filters that are used. The fission converter beam is epithermal. Both facilities have previously been used to support research in the medical uses of neutrons in cancer therapy.

b) Beam Ports: Numerous beam ports penetrate the reactor's shield, graphite reflector, and heavy-water reflector. These provide a high-quality neutron flux for such endeavors as neutron scattering, prompt- gamma analysis, and neutron physics.

c) Automatic Sample Transfer: The MITR is equipped with pneumatically-operated horizontal tubes that allow samples to be exposed to various neutron fluxes. These facilities are used to activate samples, including medical isotopes, and to support the neutron activation analysis of environmental samples such as air pollutants.

d) Graphite Reflector: Vertical irradiation thimbles penetrate the graphite reflector that surrounds the reactor tanks. These are used for the activation of specimens that require a uniform, thermal flux.

e) In-Core Sample Assemblies: There are twenty-seven fuel element positions. Of these, only twenty-three or twenty-four, depending on fuel burnup, are required to achieve criticality. The other three or four positions can be occupied by in-core sample assemblies that are used for major experiments such as in-core loops that simulate conditions in pressurized or boiling water reactors.

1.4 Shared Facilities and Equipment

The MITR is located within its own containment building. As a result, it shares few systems or equipment with other facilities. Those that are shared are as follows:

a) Electricity Supply: Off-site electricity for both the reactor building and an adjoining administrative building is brought into the utility area that adjoins the containment building. The electric power is distributed among six circuits. Five of these supply the reactor and its associated load centers. The sixth provides electrical power to the administrative building.

b) Water Supply: Off-site water is supplied to the reactor building and cooling tower makeup system. A backflow preventer precludes the possibility of any water being returned to the potable water supply.

c) Heating: Heat for the reactor containment building is provided by steam from the MIT Cogeneration Plant and an on-site backup boiler.

d) Compressed Air: The reactor building has a dedicated supply of compressed air from on-site main and backup compressors. Should that supply be lost, the distribution network can be cross-connected to a supply that is normally used for nearby laboratories.

e) Sanitary Sewer: Liquid discharges from the reactor building are directed, after processing, to a common sanitary sewer.

In addition to the shared items, certain other services originate outside the containment building even though they are dedicated systems. These include the helium and CO_2 cover gas supplies, purified water for use as makeup, and a capability to transfer irradiated samples via pneumatic tubes. Each of these systems is equipped with either manual or solenoid-operated valves, or both, so that containment integrity is maintained.

There is a hot cell facility located within the containment building on the main floor. It is used to service in-core experiments. It has its own ventilation, fire-protection, and radiation- monitoring system.

1.5 Comparison with Similar Facilities

The MITR is one of many operating research reactors that are located on university campuses. Others are located at hospitals, industrial sites, and research laboratories. In addition, there are more than fifty research reactors operating overseas. The power levels of these facilities range from a few watts to 10 MW, the maximum allowed power level for research reactors stipulated by the Code of Federal Regulations. In general, research reactors may be divided into two groups: those that use TRIGA fuel and those that use Material Test Reactor (MTR) fuel. The former often have a pulse capability whereas the latter do not. The MITR is among the latter group. The safety record for both types of research reactor has been excellent. This reflects both the actions of the individual licensees and the robust design of these reactors.

1.6 Summary of Operation

The mission of the MITR is to support the educational and research programs of the Massachusetts Institute of Technology. A related objective is to support similar programs at other local-area universities and hospitals. To this end, the MITR currently operates twenty-four hours per day, seven days a week. The reactor is operated on a quarterly cycle with shutdowns of 2–3 weeks every quarter in order to conduct tests and calibrations, perform maintenance and refueling, and remove or install experiments. The major experimental capabilities include:

a) In-core loops that replicate the environment of pressurized or boiling water reactors. The objectives include the study of mechanisms for materials failures and methods for improving water chemistries.

b) Medical therapy facilities for the treatment of certain cancers such as metastic melanoma and glioblastoma multiforme using neutron capture therapy.

c) Beam tubes for the conduct of neutron scattering experiments.

d) Irradiation facilities for the conduct of neutron activation analysis and for the production of short-lived medical isotopes.

1.7 Nuclear Waste Policy Act of 1982

The MIT Research Reactor (MITR) is owned and operated by the Massachusetts Institute of Technology, a non-profit university. Fuel for the operation of the MITR (and also the heavy water for the reflector) was originally provided by the U.S. Atomic Energy Commission (AEC).

The U.S. Department of Energy (DOE) is the successor agency to the AEC and it now provides both the fuel and heavy water. It also retains title to both. It is MIT's understanding that DOE informs NRC of the title arrangement and that MIT and DOE have a contractual arrangement whereby DOE retains title to the fuel and is obligated to take the spent fuel and/or high-level waste for storage or reprocessing. All of the MITR-I fuel and much of the MITR-II spent fuel has been returned to DOE pursuant to this arrangement. A copy of the contract between MIT and DOE for fuel assistance is available from MIT's Office of Sponsored Programs.

1.8 Facility Modifications and History

On May 7, 1956, the United States Atomic Energy Commission (AEC) issued Construction Permit No. CPRR-5 to the Massachusetts Institute of Technology (MIT). Construction then began on the original reactor, the MITR-I. The MITR-I was heavy-water cooled and moderated. On June 9, 1958, the AEC issued Facility Operating License No. R-37, which authorized operation at power levels up to 1 MW. The license was effective on its date of issuance and it was to expire at midnight May 7, 1996. Initial criticality was achieved on July 21, 1958. In June 1961, an increase in the allowed operating power to 2 MW was approved. In October 1965, a further increase to 5 MW was authorized. On April 9, 1973, Construction Permit No. CPRR-118 was issued to MIT by the AEC. This permit authorized the modifications to create the present MITR. At 1618 May 24, 1974, the original MITR-I was shut down for the last time and further operation was precluded until the construction specified in Permit No. CPRR-118 was complete. Permit No. CPRR-118 authorized modification to a light-water cooled and moderated facility with a heavy-water reflector. The new design, known as the MITR-II, offered higher flux levels for the same power as well as significantly reduced tritium production. On July 23, 1975, the U.S. Nuclear Regulatory Commission (NRC) issued Amendment No. 10 to Facility Operating License No. R-37. This amendment authorized operation of the modified reactor at power levels up to 5 MW. Initial criticality of the MITR-II was achieved on August 14, 1975. Significant regulatory actions that occurred after 1976 were the approval to conduct digital control experiments on the MITR, the authorization to use the medical facility for neutron capture therapy for humans, the safety evaluation of a fission converter facility, and the extension of the operating license to August 1999 to recover time spent in construction. Renewal of the MITR-II operating license and a power uprate to 6 MW was issued on November 1, 2010.

References

[1-1] Guidelines for Preparing and Reviewing Applications for the Licensing of Non-Power Reactors, Standard Format and Content, NUREG-1537, Part 1, United States Nuclear Regulatory Commission, February 1996.

[1-2] Guidelines for Preparing and Reviewing Applications for the Licensing of Non-Power Reactors, Standard Review Plan and Acceptance Criteria, NUREG-1537, Part 2, United States Nuclear Regulatory Commission, February 1996.

[1-3] MITR-Staff, Safety Analysis Report for the MIT Research Reactor, MIT-NRL-13-01, 2013, MIT Nuclear Reactor Laboratory.

[1-4] A. Bergeron, E.H. Wilson, G. Yesilyurt, F.E. Dunn, J.G. Stevens, L. Hu, and T. H. Newton, "Low Enriched Uranium Core Design for the Massachusetts Institute of Technology Reactor (MITR) with Un-finned 12 mil-thick Clad UMo Monolithic Fuel", ANL/GTRI/TM-13/15, Argonne National Laboratory, November 2013.

2.0 Site Characteristics

There are no changes to Chapter 2 (Site Characteristics) as a result of LEU conversion; information on this subject can be found in the current MITR-II SAR.

3.0 Design of Structures, Systems, and Components

There are no changes to in Chapter 3 (Design of Structures, Systems, and Components) **except Sections 3.1.1.1 and 3.5** as a result of LEU conversion; information on this subject can be found in the current MITR-II SAR.

3.1 Design Criterial

3.1.1 Prevention of Release of Radioactive Material

3.1.1.1 Fuel and Cladding

Specifications for the MITR LEU U-10Mo monolithic alloy fuel are currently under development. It is a joint effort led by MIT-NRL with assistance from Argonne National Laboratory (ANL). Specifications for the MITR LEU fuel will be maintained by Idaho National Laboratory (INL). More detailed information, including the specification number, will be provided in the later version of the SAR.

3.5 Systems and Components

a) Design criteria for systems and components that are important to safety and which have not been previously discussed in this chapter are provided here. There are three types of plates in the MITR LEU fuel element design. Those with thin fuel thickness (0.013 inch) are designated as T-plate, intermediate fuel thickness (0.017 inch) as Y-plate, and the full thickness of fuel (0.025 inch) as designated F-plate. Each plate type has the same total plate thickness (0.050 inch).

   Fuel: The specification for the fuel and cladding is described in Section 3.1.1.1 of this report. It addresses all aspects of the fuel's manufacture. In addition, a limit is observed on the maximum fission density to be consistent with planned fuel qualification irradiations. Parameters enumerated in the specification include:

   (i) Form: U-10Mo monolithic with nominal of 10 wt. % molybdenum in the fuel core alloy. The alloy shall have a nominal density of 17.02 g/cm^3.

   (ii) Interlayer: A nominal 0.001-inch layer of zirconium shall be intimately bonded to each face of the U-10Mo alloy foil by co-rolling.

   (iii) Cladding: Aluminum with a nominal cladding thickness of not less than 0.011 inches.

   (iv) U-235 Loading: 967.7 grams per element
   30.02 grams in T-plates
   39.26 grams in Y-plates
   57.74 grams in F-plates

(v) Fission Density: 5.0×10^{21} fissions/cc for T-plates,
4.4×10^{21} fissions/cc for Y-plates,
3.6×10^{21} fissions/cc for F-plates.

b) Control Device Scram: The time from initiation of a scram signal for a shim blade to go from its full-out position to its 80% inserted position shall be less than 1.0 second. The term "initiation of a scram signal" refers to the time at which the true value of the parameter in question attains its scram setting.

Design bases for other systems and structures important to safety, such as emergency core cooling, containment, and ventilation isolation, are provided in Section 3.1 of this report.

4.0 Reactor Description

There are no changes to Chapter 4 (Reactor Description) as a result of LEU conversion **except Sections 4.1, 4.2, 4.2.1, 4.2.5.1, 4.3.1.1, 4.5, and 4.6**; information on this subject can be found in the current MITR-II SAR.

4.1 Summary Description

The MIT Research Reactor (MITR) is intended to operate at or below a steady-state thermal power level of 7.0 MW with a primary coolant flow rate of 2,400 gpm, a coolant outlet temperature of 55 °C, and a coolant level at overflow. The corresponding limiting safety system settings are 8.68 MW, 2,200 gpm, 60 °C, and 4 inches below overflow. The licensed power is 7.0 MW. The reactor utilizes flat, plate-type, aluminum-clad fuel elements that have U-235 enriched to less than 20% (i.e., LEU). The elements are rhomboid in shape and each contains nineteen plates [4-1]. The rhomboid shape allows arrangement of a hexagonal-shaped core that is contained in a tank as opposed to an open pool. Both forced and natural-convection cooling are possible. The former is the normal mode of operation. The latter is used only at power levels of less than 100 kW. Both the coolant and moderator are light water. There are two reflectors. The inner one is heavy water that is contained in a reflector tank that surrounds the light-water core tank. The outer one is made of graphite blocks. The MITR is equipped with a variety of experimental facilities including beam ports, irradiation tubes, and medical irradiation rooms. The beam ports are aligned with radial reentrant thimbles that are welded to the inside of the heavy water reflector tank. This feature maximizes the thermal neutron flux available at the experimental ports. All pneumatic sample irradiation tubes are located in the graphite reflector except one that utilizes a reentrant thimble and terminates in the D_2O reflector. Irradiation facilities can also be installed within the core by replacing a fuel element with an irradiation thimble. These are referred to as in-core sample assemblies or ICSAs. There are two medical irradiation rooms, one located below the core in the basement and one located to the side of the core on the main floor. The latter is driven by a fission converter.

The MITR is not designed to be pulsed.

Table 4-1 lists major reactor parameters. Figure 4-1 is a vertical cross-section of the MITR. As shown in the figure, the reactor core is contained within two concentric tanks and a core shroud. The outer tank, the four-foot diameter D_2O reflector tank, is used to maintain a constant D_2O level for neutron reflection. The inner tank contains light water that serves as both the primary coolant and the moderator. The D_2O reflector tank is in turn surrounded by a graphite reflector that extends approximately two feet in the radial direction and is blanketed with CO_2 or an inert cover gas. Numerous experimental ports penetrate through the graphite region to the D_2O reflector tank. Welded into the D_2O reflector tank – and in line with the experimental ports – are the radial reentrant thimbles.

Outside the graphite reflector region is a thermal shield that consists of 1.5 inches of lead supported on either side by two-inch steel plates. The thermal shield is cooled by demineralized water that circulates through cooling coils embedded in the lead. A dense concrete biological

shield, approximately 5.5 feet thick, surrounds the thermal shield, and makes the reactor about twenty feet wide overall.

Table 4-1. Major Reactor Parameters of the MITR LEU Core

No.	Parameters	Values
1.	Steady-State Operating Power	7.0 MW
2.	Primary Coolant Flow	2400 gpm
3.	Coolant Outlet Temperature	55 °C
4.	Limiting Safety System Settings Power Flow Temperature Level	 8.68 MW (Max.) 2,200 gpm (Min.) 60 °C (Max.) 4 inches (Min.) below overflow, which is 10 feet above top of the fuel plates
5.	Coolant and Moderator	Light Water
6.	Reflector	Heavy Water / Graphite
7.	Reactor Type	Tank
8.	Fuel Type	U-10Mo Monolithic Alloy
9.	Fuel Geometry	Unfinned Plate, Rhomboidal Cross-section

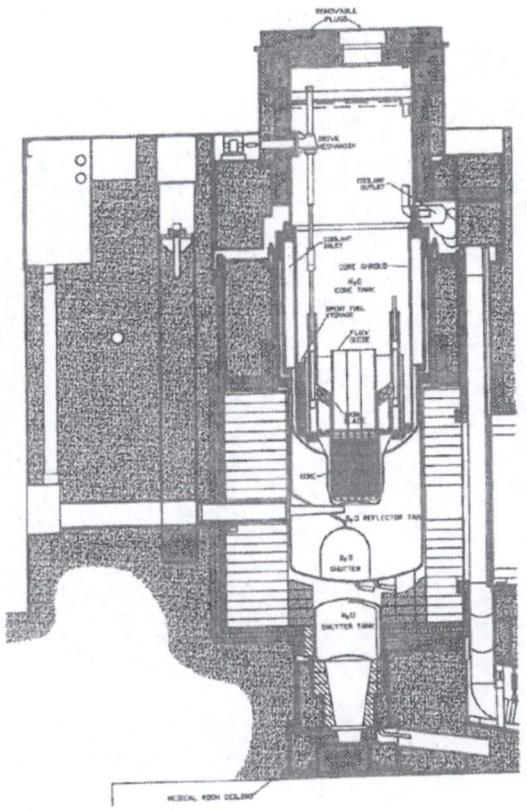

Figure 4-1. Vertical Cross-Section of the MITR

4.2 Reactor Core

Figure 4-2 is a cross-sectional diagram of the reactor core. There are twenty-seven fuel element positions arranged in three rings. There is a central group of three elements, the A-Ring. This is enclosed by a group of nine elements, the B-Ring, which is in turn surrounded by a group of fifteen elements, the C-Ring. Each element is rhomboidal in shape with the result that the core as a whole forms a hexagon. Fuel element positions may be occupied by fuel elements, in-core sample assemblies (ICSAs), or dummy elements. The thimbles and dummies have the same exterior shape as a fuel element. This is done to prevent excessive bypass flow and to limit moderation. There is no limit on the number of non-fueled positions provided that thermal-hydraulic, reactivity, and shutdown margin requirements are met. However, to assure proper flow distribution, all fuel elements positions are occupied when the reactor is operating.

The location of both the control and flux-shaping components are also shown in Figure 4-2. The control elements consist of six boron-impregnated stainless steel shim blades and one cadmium regulating rod. The six blades are used for the attainment of criticality, for the performance of major changes in power level, and for compensation of reactivity changes that occur as the result of xenon and temperature. The regulating rod is used for fine adjustments of power. The regulating rod and all six blades are located on the core perimeter.

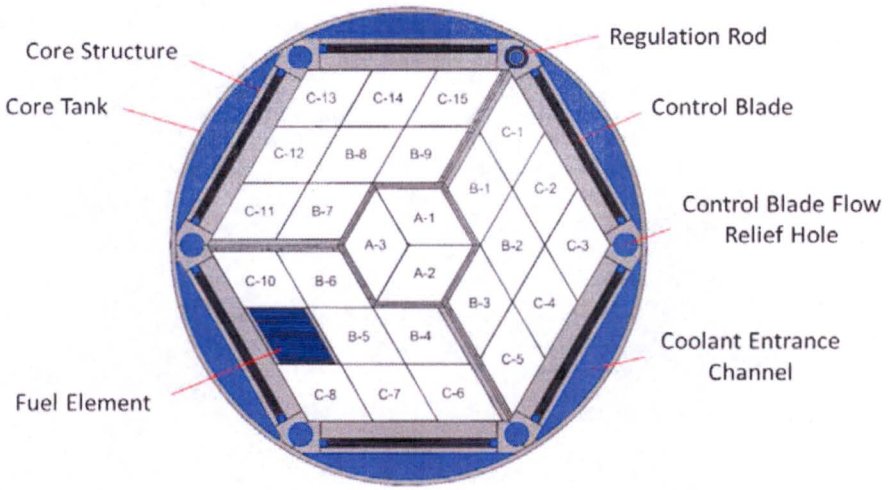

Figure 4-2. Horizontal Cross-Section of the MITR Core

The MITR was designed with a provision to install fixed neutron absorbers in the upper half of the core. The objective is to poison the upper half of each fuel element, thereby maximizing the leakage flux into the D_2O reflector beneath the core at the ends of the radial re-entrant thimbles. At present, boron-impregnated stainless steel absorbers are installed in the upper four inches of the radial portion of the core housing so that they are adjacent to the B- and C-Ring elements.

Heat generated by the fission of U-235 is removed from the core by means of the light-water primary cooling system. Coolant enters the reactor through the inlet plenum, flows into the annular region between the core tank and the core shroud, and then moves downward to the bottom of the core tank through the six coolant inlet channels formed by the hexagonal core support housing assembly as shown in Figure 4-2. The coolant is then directed upward through the fuel elements that are held in the core support housing assembly. It was determined during the MITR-II start up testing that a small portion of the primary flow bypasses the fuel elements through the natural convection valves. The coolant flow exiting the core then enters the core tank through a hexagonal flow guide that is about 39 cm from flat to flat and 76 cm high. The flow guide protects the shim blades from flow-induced vibration. Water then moves at lower velocity upwards within the space contained by the core shroud to the three exit ports that form the outlet plenum. This plenum is located above the level of the inlet plenum. The coolant passes out of the reactor and flows through two parallel pumps and the primary heat exchangers to form a common line back to the reactor, thereby forming a closed loop. A detailed description of the flow system is given in Chapter 5 of the SAR.

4.2.1 Reactor Fuel

MITR fuel elements have one unique design feature. First, the elements are both radially and axially symmetric so that they can be both rotated and inverted in order to equalize the effect of flux peaks on burnup.

Figure 4-3 is a diagram of an MITR LEU fuel element. The MITR utilizes flat, plate-type, aluminum-clad fuel elements that are U-235 enriched to 19.75 wt. %. Each fuel element consists

of nineteen fuel plates. The fuel plates are assembled between two grooved side plates which are 0.188 inches thick. The fuel plates are 0.049 inches thick, 23.00 inches long and are spaced 0.0746 inches apart to form eighteen cooling water passages 2.308 inches wide. Within an element, the spacing between the fuel plates is maintained by the grooves in the side plates. Between elements, end nozzles, which are designed to provide structural rigidity for the element, maintain the necessary spacing. The fuel elements are rhombic in shape with a perpendicular distance between the flats of 2.380 inches. The overall length, including the end nozzles, is 26.25 inches. Each element has similar nozzles at both ends, thereby allowing it to fit into the lower matrix and to mate with the upper hold-down grid.

Each fuel element contains 968 grams of U-235. The amount of U-235 is not evenly distributed among each fuel plate, where three different fuel core thicknesses are adopted. T-plates (Plate No. 1 and 19, yellow-color plates in Figure 4-3b) have a fuel core thickness of 0.013 inch. Four Y-plates (Plate No. 2, 3, 17, and 18, orange-color plates in Figure 4-3b) have 0.017 inch. Thirteen F-plates (Plates No. 4 – 16, red-color plates in Figure 4-3b) have a fuel thickness of 0.025 inch. The fuel core is LEU enriched to 19.75 wt. % U-235 in the form of a U-10Mo monolithic alloy. Like the HEU fuel, each plate has fuel 22.375 inches long and 2.082 inches wide. Plates remain clad with 6061 aluminum alloy (AA 6061) with 0.001-inch zirconium interlayers between the fuel and cladding. The nominal thickness of the AA 6061 cladding and zirconium for T-plates, Y-plates, and F-plates are 0.018, 0.016, and 0.012 inch, respectively, so that the total thickness of each plate is identical regardless of its position. Eventually there will be a specification that includes the degree of centering of the fuel foil within the plate and minimum AA 6061 cladding thickness requirements.

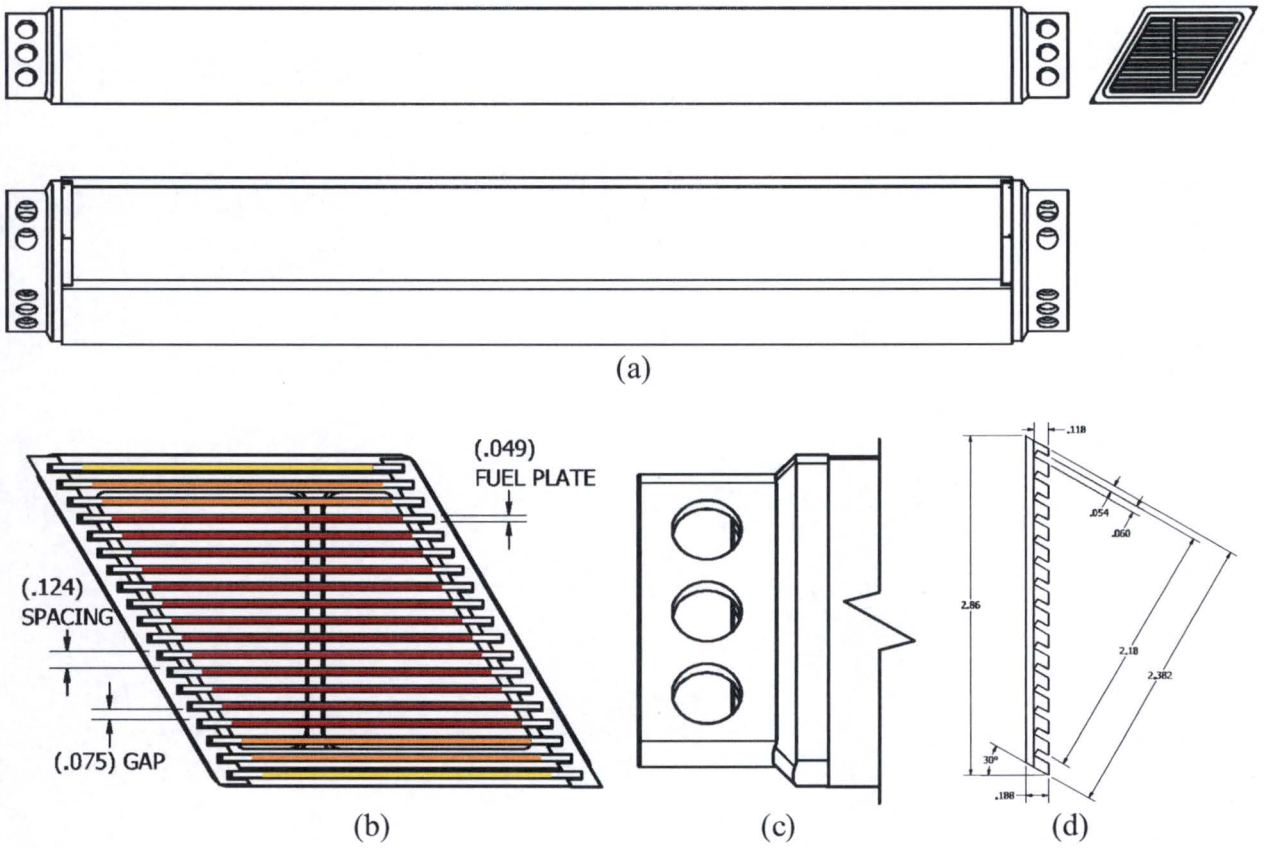

Figure 4-3. Diagram of an MITR LEU Fuel Element (a) Full Element Assembly, (b) Assembly Cross-Section, (c) Assembly Nozzle, and (d) Side-Plate.

This high-density U-10Mo monolithic alloy fuel will be adopted for the MITR LEU conversion. The maximum allowed local fission density is 5.0×10^{21} fissions/cc for T-plates, 4.4×10^{21} fissions/cc for Y-plates, and 3.6×10^{21} fissions/cc for F-plates. [4-2] Fuel plate performance associated higher burnup has also been evaluated. Film formation on the fuel cladding would present a significant heat transfer resistance because of its relatively small thermal conductivity compared to that of the aluminum fuel cladding. Oxidation of the aluminum has been identified as the major contributor to the film growth on the fuel cladding. The reaction rate of the oxidation process depends on the thermal (temperature and/or heat flux), hydraulic (flow velocity), and chemical (pH) conditions [4-3, 4-4]. A film thickness of 0.002 inches or less is recommended which is based on the limit to prevent spallation that could lead to the release of radioactive gas [4-5].

The MITR fuel elements do not contain any burnable poisons and/or moderating materials. In addition, there are no partial elements or control rod elements. An instrumented element was fabricated for the initial start-up of the MITR-II in 1974/1975. Thermocouples were crimped between the fins of an otherwise standard element. This element was then used to measure fuel plate temperatures. The thermocouples were subsequently removed and the element was used in the same way as any other element. Another special element was fabricated for the MITR-II's initial startup. This element had removable fuel plates. It was used for flux mapping and peaking factor determination, and is currently in storage at a DOE facility.

Table 4-2 lists materials and physical properties of the MITR fuel.

Table 4-2. Material and Physical Properties of MITR LEU Fuel

No.	Property	Value
A.	***Aluminum (6061)***	
A1.	Melting Point	660 °C
A3.	Heat Capacity	915 J/kg-°C
A4.	Thermal Conductivity	186 W/m-°C
B.	***Fuel***	
B1.	U-235 Mass	967.7 g/element
B2.	U-235 Enrichment	19.75 ± 0.20 wt. %
B3.	Molybdenum	10.0 ± 1.0 wt. %
B4.	Density	17.02 g/cm^3

Fresh MITR elements may be stored in the following locations: in the reactor core provided that the reactivity is below the shutdown margin requirement, in the cadmium-lined fuel storage ring attached to the flow shroud, or in the storage safe in the containment building.

Irradiated fuel may be stored in the reactor core provided that the reactivity is below the shutdown margin requirement, in the cadmium-lined fuel storage ring attached to the flow shroud, in the spent fuel storage tank in the basement of the reactor building, in the fuel element transfer cask or other proper shield within the controlled area, or in the fission converter tank.

The principal concerns associated with these storage areas are that criticality considerations be addressed and that the fuel will not be subject to chemical attack or other forms of deterioration. The criticality issue is addressed by requiring that the k-effective of all storage locations be less than 0.9 [4-6, 4-7]. The corrosion issue is addressed as follows: elements placed in the storage safe are left in the plastic wrap provided by the manufacturer, an element in the transfer cask is surrounded by air, and the medium in all other storage locations is light water for which the chemical purity is maintained in accordance with the specifications for primary coolant. (Refer to Section 5.2.2.1 of the SAR.)

MITR fuel is subject to stringent quality assurance. Much of this is performed by the manufacturer in accordance with the requirements of the U.S. Department of Energy, the agency that owns the fuel. In instances where a question exists as to the compliance of a given fuel plate with the design specifications, radiographs are forwarded to MIT for review. Upon receipt at MIT, each element is surveyed for radiation. Table 4-3 lists the surveys that are performed. These are done in accordance with good health physics practice and to satisfy the shipping requirements of the U.S. Department of Transportation. In addition, they serve to confirm the absence of any "tramp" uranium that might be on the surface of an element. Elements are then inspected visually to verify the absence of damage to the cladding. This inspection is, of course, limited to accessible surfaces. Irradiated fuel is inspected visually through water for evidence of

corrosion and/or cladding defects. These examinations are performed quarterly in conjunction with an inspection of all in- core components. One of the tests that is performed is to observe the core with the only source of illumination being Cherenkov radiation. This process can detect foreign material or cladding blisters that might be blocking a fuel element channel.

Table 4-3. Surveys Performed on Receipt of Un-irradiated Fuel Elements

Survey	Location
γ radiation levels	1 meter from surface of shipping containers Contact with surface of shipping containers
Gross removable α / β contamination	Surface and interior of each container
β / γ radiation levels	1 meter from element Contact with element
Gross removable α / β contamination	Surface of element and all accessible plates or portions thereof
Direct fixed α survey	Exterior plates of element

4.2.5 Core Support Structure

4.2.5.1 Design Considerations

The core support housing is designed to ensure that all fuel elements, dummy elements, and in-core experimental facilities are properly secured against all anticipated loads including both the buoyant force of the coolant and the hydraulic forces associated with primary flow. The principal feature for achieving this is a heavy grid structure that is positioned at the top of the core and which serves as a hold-down assembly. This grid is designed to lock down the fuel and other core components during reactor operation and to prevent accidental disassembly of the core by the hydraulic lifting force if a primary coolant pump were to be started during a refueling. The grid structure and its associated interlocks are described in Section 4.2.5.2 of the SAR.

The total mass of an MITR fuel element is 7.94 kg [4-7]. Hence, these elements are held down by gravity with a force of 77.8 N. Upon initiation of primary flow, elements will rise by less than 0.25 inches as a result of the flow through the grid. Similar considerations apply to solid aluminum dummies. The forces to which an in-core assembly are subject depend on the assembly's design. These assemblies are normally secured by means of a metal tab that protrudes from the outer thimble and which fits under the grid. A description of the method used to secure a particular assembly is included in the safety evaluation that is written for each such assembly. (See Section 13.2.6 of the SAR.)

4.3 Reactor Tanks

4.3.1 Light-Water Core Tank

4.3.1.1 Design Considerations

The design pressure of the light-water core tank is 60 psig. The core tank is rated for 24 psig at 150 F. The maximum hydrostatic pressure, which occurs at the bottom of the tank, is 5.4 psig. The maximum hydrodynamic pressure, which occurs with a primary coolant flow of 2400 gpm, is 16.9 psig. The design pressure (60 psig) is the pressure at which it exhibits ductile failure. The rated pressure (24 psig) is the steady-state operating pressure. The working pressure (flow present) is 16.9 psig. So, the ratio of design to working pressure is 60/16.9 = 4.01. The rated pressure is higher than the normal operating pressure by 42%. (Note: (24 psig – 16.9 psig) / 16.9 psig = 0.42.)

The pH of the primary coolant is slightly acidic, typically 5.5–6.5. This minimizes corrosion of aluminum. Radiation damage to the core tank is discussed in Section 16.3.1.6 of the SAR. Correlations developed at the Brookhaven National Laboratory [4-8] have been applied to the MITR's operating history. The material properties of the present light-water core tank will remain satisfactory for at least twenty more years with the reactor operated at 10 MW [4-9].

4.5 Nuclear Design

Many research reactors select a limiting core configuration that yields the highest power density for the specified fuel. Other configurations are allowed if they are within the envelope of this limiting one. For the MITR, the limiting core would be the one with the maximum number of non-fueled positions because the power density in the fuel elements would be at its highest. Criticality considerations restrict MITR operation to a maximum of five non-fueled positions. Such a core was installed and operated following the initial startup of the MITR-II. The same 22 fresh fuel elements core configuration will be adopted for the LEU core startup. A more routine configuration is three non-fueled positions. However, other core configurations have also been demonstrated that had either two or four non-fueled positions.

The power peaking factors used for the thermal-hydraulic analysis given in Section 4.6 of this report are from the core with five non-fueled positions and hence is the worst case. Limiting thermal-hydraulic conditions are then developed as a function of the maximum power deposited in a coolant channel. Cores other than the limiting one are evaluated by verifying that these limiting core conditions are met. An analysis is then performed to evaluate every channel in a proposed core to ensure that these limiting conditions are not exceeded. If so, the proposed core is acceptable. The principal steps in the analysis are:

a) A three-dimensional computational model of the core is developed. The model specifies the physical layout of the core components (fuel, control devices, moderator, housing, reflectors, etc.), the material composition of each component (uranium, aluminum, water, boron, etc.), and the number density of each composition. Provisions exist to include xenon and other fission products.

b) A numerical code is used to obtain the k-effective, neutron flux distribution, and power density distribution of the modeled core. The codes used for this purpose are ones obtained from the Radiation Safety Information Computational Center (RSICC at Oak Ridge National Laboratory). MCNP5/1.60, the general purpose Monte Carlo code, is currently in use at the MITR for neutronic calculations [4-10]. The standard ENDF/B-VII.0 nuclear data library has been adopted.

c) The proposed core's thermal-hydraulic limits are evaluated using the calculated power distribution for every channel derived from the MCNP simulation. If all channels pass the safety limits and limiting safety system settings (LSSS) criteria, then the proposed core is considered acceptable. The MULCH-II code is used for the steady-state thermal-hydraulic calculations [4-11].

d) All the computational models have been validated against MITR-II cores to the best extent. These models are directly adopted for the LEU calculations. Experimental validations will be performed during the reactor startup testing before the final SAR was issued.

The above approaches are computationally intensive. However, they offer flexibility in terms of modelling and evaluating both in-core experiments and fuel utilization.

4.5.1 Normal Operating Conditions

4.5.1.1 Core Components

Core components are described in Section 4.2 of the SAR.

4.5.1.2 Planned Core Configurations

There are no pre-planned core configurations for the MITR. Rather, any configuration is acceptable provided the following criteria are met:

a) Safety limits and limiting safety system settings (LSSS) -related thermal-hydraulic parameters must not be exceeded in any channel in the core.

b) Each of the twenty-seven positions within the core must contain a fuel element, a solid aluminum dummy, or an approved in-core sample assembly (ICSA). (Note: A neutron source tube is also acceptable as discussed in Section 4.2.4 of the SAR.)

c) The shutdown margin requirement is met.

d) No fuel element, or any portion thereof, exceeds the fission density limit as discussed in Section 4.2.1 of the current report.

4.5.1.3 Reactor Operating Characteristics

MITR fuel management policy is, in general, to place fresh fuel in the B-ring where peaking factors are the lowest and to place partially-spent fuel in the A- and C-rings where peaking tends to be greater. The net result is that power is concentrated in the core interior when a core is newly installed. As the fuel depletes the average height of the shim bank increases. All six shim blades are located in the core periphery. As shim blades and/or fixed absorbers are raised, the following occurs:

a) The axial spatial location of the point of maximum flux rises vertically.

b) The magnitude of this maximum decreases.

c) The magnitude of the thermal neutron flux available at the beam port reentrant thimble tips decreases.

d) Power density decreases in the A- and B-rings and rises in the C-ring. The average power density for the core decreases as the same total power is being produced in what is, effectively, a larger volume.

These same studies have established that insertion of fresh fuel in a given position increases the power density in that position at the expense of neighboring positions, and that replacement of a solid dummy and/or experimental facility with fuel increases the power density in the neighboring elements.

4.5.1.4 Effect of Fuel Burnup

The MITR operates 24 hours per day, seven days per week. Refueling is performed every quarter and may involve replacement of spent fuel with fresh or partially used fuel, shuffling of fuel to achieve better overall burnup, rotation of individual elements to offset the effect of radial flux gradients, and inversions (flipping) of individual elements to negate the effect of axial flux gradients. Detailed analyses of these refueling strategies are available in Ref [4-12].

The effect of fuel depletion on reactivity has been quantified. The change in reactivity with core energy production is –0.125 mβ/MWH. Plutonium buildup is about 50 g per 7900 MWH fuel cycle. Detailed depletion results at equilibrium can be found in Ref [4-13].

4.5.1.5 Kinetic Behavior / Requirements and Features of Control Devices

Figure 4-4 and Figure 4-5 show the integral and differential reactivity worth of the MITR's shim bank at the beginning-of-life (BOL) and middle-of-life (MOL) states, respectively. The MOL state (see definition in Ref [4-13]) represents a typical equilibrium fuel cycle, with 24 fuel elements in core. It should be noted that all the presented reactivity worth in Figures 4-4 and 4-5 has a standard statistical deviation of less than 15 mβ (i.e., Monte-Carlo method-based statistical error). The integral worth of the shim bank is ~ 13 β at BOL and slightly less than 12 β at MOL. The reduced shim bank worth in the equilibrium fuel cycle state is because the neutron flux is more concentrated in the core center due to the addition of two new fuel elements in the B-ring. As discussed in the current MITR-II SAR [4-14] the worth of the shim bank will vary with the

radial power distribution. The typical range of shim bank worth is usually 11.5–13.0 β, and a similar range is expected with an LEU-fueled core. The shim bank worth is a function of the energy and magnitude of the flux to which the blades are exposed. The high differential worth that exists in the mid-range of blade travel corresponds to a maximum in axial flux shape.

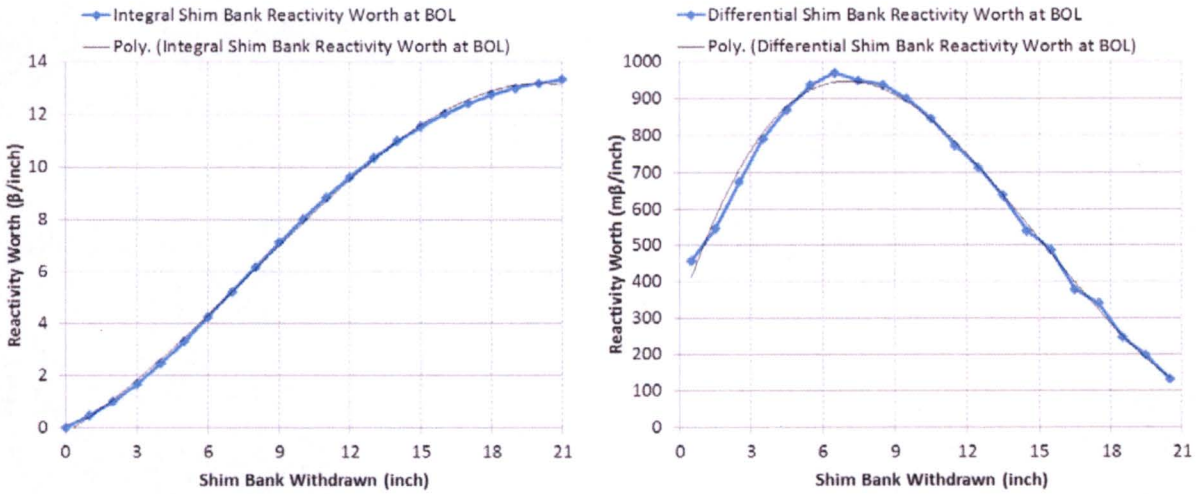

Figure 4-4. MITR LEU core shim bank integral (left) and differential (right) worth at BOL

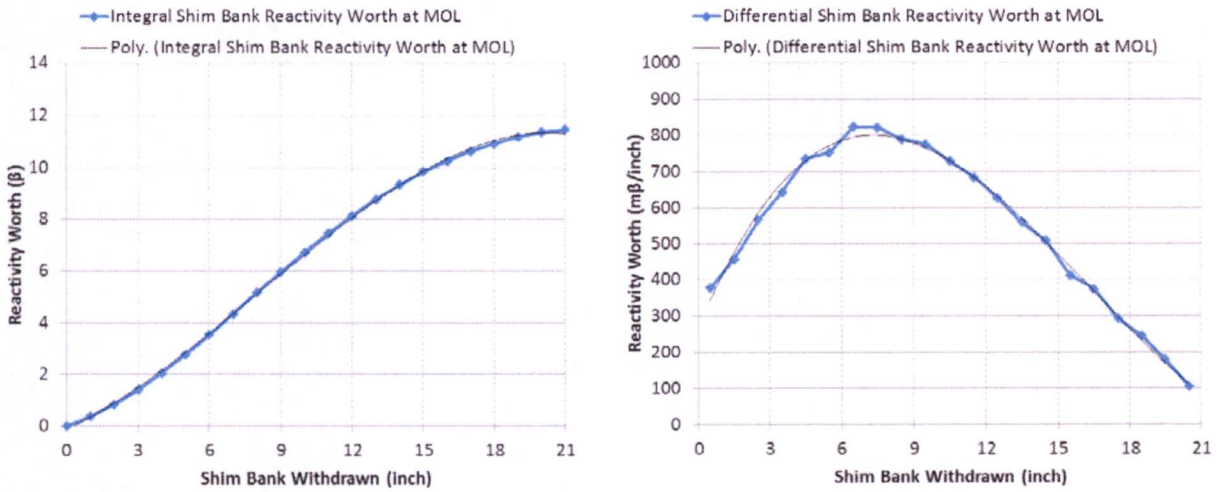

Figure 4-5. MITR LEU core shim bank integral (left) and differential (right) worth at MOL

Figure 4-6 and Figure 4-7 show the integral and differential reactivity worth of the MITR's regulating rod at BOL and MOL, respectively. The fine-control regulating rod is normally worth less than 300 mβ. The peak in the differential regulating rod worth curve occurs at a low rod height because the full-in position for the regulating rod is located six inches above the bottom of the fuel elements, and because once the regulating rod is withdrawn any appreciable amount, it is heavily shadowed by the adjacent shim blades. It should be noted that all the presented reactivity worth in Figures 4-6 and 4-7 has a standard statistical deviation of less than 15 mβ (i.e., Monte-Carlo method-based statistical error).

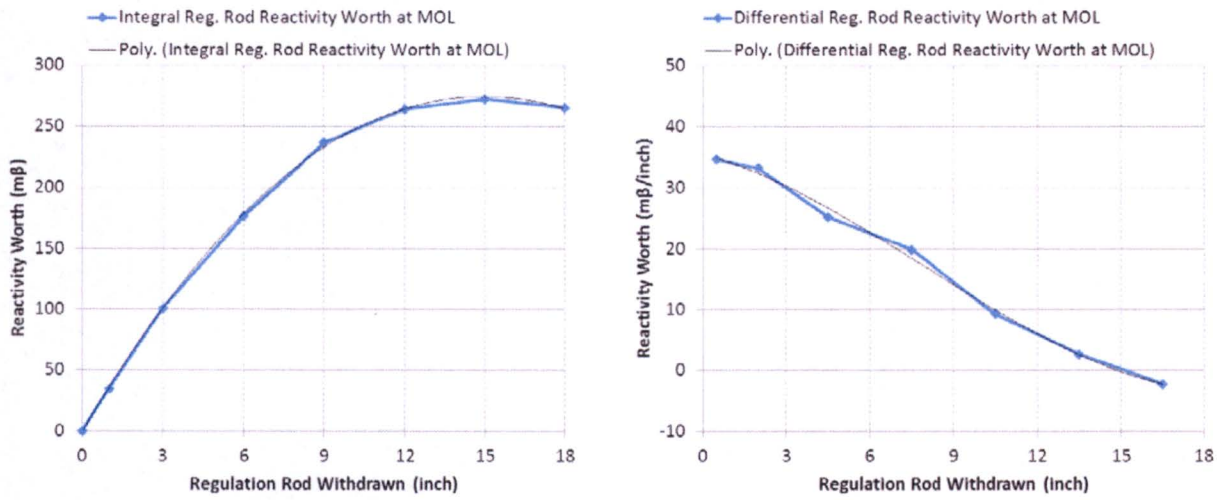

Figure 4-6. MITR LEU core regulating rod integral (Left) and differential (Right) worth at MOL with the shim bank withdrawn 12 inches

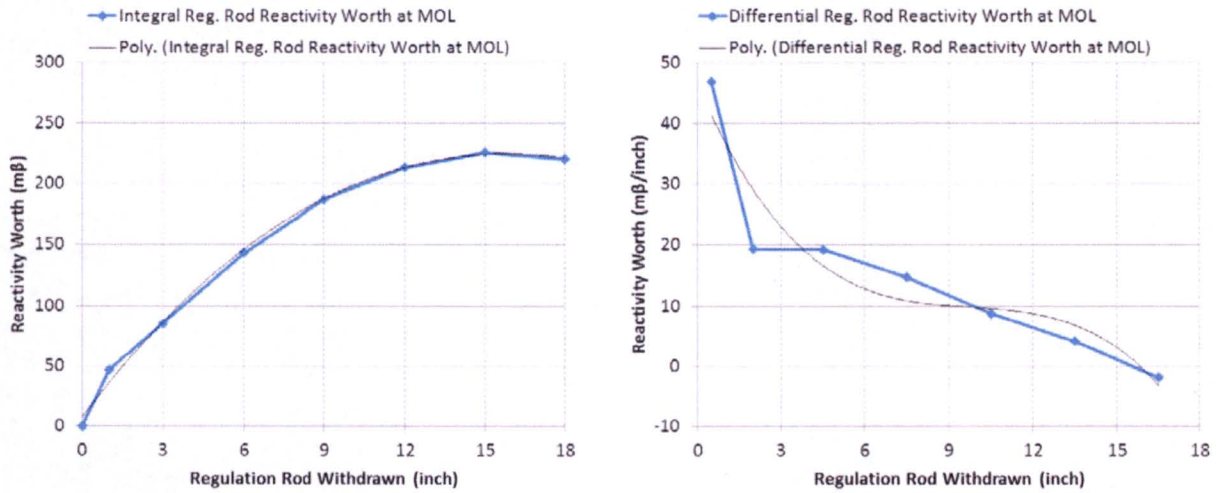

Figure 4-7. MITR LEU core regulating rod integral (Left) and differential (Right) worth at MOL with the shim bank withdrawn 8 inches

MITR refueling is normally designed so that the core at the beginning of a new cycle will reach criticality at a shim bank height of 8 to 10 inches. Considerations that limit the shim bank height at which criticality is attained include the subcritical limit interlock and the shutdown margin. At 8.0 inches, the shim bank worth is about 6 β. The reactivity worth of equilibrium xenon concentration at 6 MW is slightly less than 4 β. Hence, the core will operate at a bank height of about 13 inches. The shim bank height will gradually increase as the fuel depletes. Refueling is normally performed when it is no longer possible to compensate for the negative xenon reactivity worth when the reactor is restarted several hours after a shutdown. Increases of reactor power are accomplished subject to the following administrative limits:

a) A reactor scram will occur at a period between 10 and 11 seconds.

b) The minimum allowed dynamic period is 30 seconds.

c) If reactor power is less than 80% of the target, the steady period shall be longer than 50 s.

d) If reactor power is within 80% of the target, the steady period shall be longer than 100 s.

Either a shim blade or the regulating rod may be used to accomplish a reactor power adjustment. The choice is at the discretion of the licensed console operator. (Note: The term "steady period" implies a non-zero reactivity and the absence of control device movement. The term "dynamic period" implies the presence of control device movement with or without a nonzero reactivity.)

4.5.1.6 Interactions of Fuel / Moderator / Reflector / Control Devices

The criticality of any given core configuration is a function of certain interactions between some of the core components. These include:

a) Moderator/Reflector Temperature: The MITR is designed to be under-moderated so that there is a negative reactivity coefficient associated with the temperature of both the moderator (coolant) and the reflector. This temperature coefficient of reactivity encompasses two distinct phenomena. The first is the temperature rise of the light water due to an increase in the thermal power output of the reactor core resulting in a decrease in water density and a reduction in moderation, and thus hardening of the neutron spectrum. The second phenomenon is the heating of the heavy water reflector that adds negative reactivity by increasing neutron leakage. Temperature rise in the reflector lags any temperature rise in the light water in the core proper. The temperature coefficient of reactivity associated with the entire reactor (H_2O and D_2O) heat-up varies from -8 mβ/°C to -20 mβ/°C over the normal band of operating temperatures from 25 °C to 50 °C. This is depicted in Figure 4-8. It should be noted that the reactivity worth in Figure 4-8 has a standard statistical deviation of less than 15 mβ.

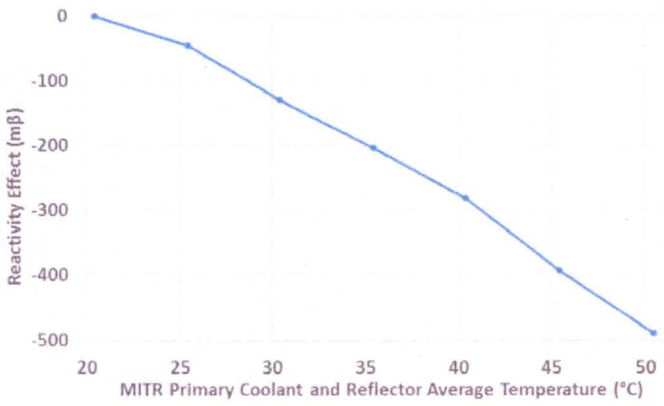

Figure 4-8. MITR LEU core primary coolant and heavy water temperature reactivity effect

b) Heavy Water Reflector Dump: The portion of the MITR's heavy water that is above the bottom plane of the fuel elements (approximately 2 feet) is the volume of heavy water that may be dumped. Because the shim blades also operate in the region between the core and the radial heavy water reflector, the reactivity worth of dumping the reflector is

dependent on the position of the shim bank. This effect is the result of the shadowing effect that the shim bank has on the reflector's worth. The reactivity worth of dumping the radial reflector with the shim bank at different heights is given in Table 4-4. Calculated heavy-water reflector dump worth for MITR LEU core.

Table 4-4. Calculated heavy-water reflector dump worth for MITR LEU core

Shim Bank Height	**Reflector Dump Worth (β)** Fresh Core – 22 fuel elements
Fully Withdrawn (21-inch)	-8.80
12-inchWithdrawn	-8.23
Critical Height (8.73-inch)	-7.14
Fully Inserted	-4.09

It should be noted that all the presented reactivity worth in Table 4-4 has a standard statistical deviation of less than 15 mβ. These results show that the reactivity worth of dumping the radial heavy water reflector when the shim bank is fully inserted is about two-thirds that of the corresponding value when the bank is withdrawn by 12 inches. Safety considerations dictate that the radial heavy water reflector be pumped up with the shim bank in the full-inserted position. This ensures that the reactivity insertion for this process will not occur when the reactor is or could go critical.

c) Effects of Coolant and Reflector Leakage: Light water has both higher moderating power and a higher neutron absorption cross-section than that of heavy water. In an under-moderated core with a hardened neutron energy spectrum such as that of the MITR, the effect of the high moderating power of light water outweighs its absorption effects, and consequently, replacement of the coolant in the core with heavy water will result in a negative reactivity effect. However, in the exterior regions of the light water core tank, where the neutron energy spectrum is much softer, the absorption by light water outweighs the effect of its high moderating power. Replacement of light water with heavy water in the plenum above the fuel elements and along the walls and bottom of the core tank would result in a momentary positive reactivity effect that is followed by a negative reactivity effect as the heavy water enters the core proper. Replacement of the heavy water in the reflector tank with light water will always result in a negative reactivity effect. The detailed calculations of the heavy water and light water mixing accident is addressed in Section 13.2.9.4 of this report.

d) In-Core Facilities: The reactivity limit for an in-core experimental facilities having "movable" nature is discussed in Section 10.3.2.6 of the MITR-II SAR.

e) Doppler Effect: The fuel temperature reactivity effect (i.e., Doppler Effect) is expected to be more pronounced in the LEU fuel. However, it is still overall insignificant and predominantly shadowed by the much stronger coolant density reactivity effect. The reasons are 1) the absorption reactions are mostly contributed from the 19.75 wt.% enriched U-235 and 2+ the fuel operation temperature range is considerably low (peak steady-state temperature less than 100° C).

4.5.1.7 Safety Considerations for Different Core Configurations

The approach utilized to ensure the safety of every MITR core configuration is discussed in the introduction to Section 4.5 of this report.

4.5.1.8 Reactivity Worth

Reactivity data on LEU fueled MITR core, void coefficients, and in-core facilities has been estimated by MCNP calculations in advance of the conversion. This data will be subsequently confirmed by measurement during startup tests after the conversion.

Table 4-5. Calculated reactivity worth for adding U-235 in various positions presents the reactivity worth for adding U-235 in various rings at the LEU core. It should be noted that the calculated reactivity effect takes into account the combination of adding U-235 and removing equivalent amount of fission products. The presented reactivity worth per g-U235 in Table 4-5 has a standard statistical deviation of less than 0.15 mβ/g-U235.

Table 4-5. Calculated reactivity worth for adding U-235 in various positions

Location	Reactivity Effect (mβ/g-U235)
A1	+4.14
B4	+3.33
B5	+3.04
C6	+2.00
C7	+1.98
C8	+1.59
A-ring Average	+4.14
B-ring Average	+3.19
C-ring Average	+1.86

Table 4-6. Calculated reactivity worth for coolant voiding at different locations presents the reactivity worth for voiding coolant channels in the LEU core. It should be noted that the calculated void effect assumes nominal coolant density at room temperature (294 K). The presented reactivity worth per cubic-centimeter (cm^3) in Table 4-6 has a standard statistical deviation of less than 0.02 $m\beta/cm^3$.

Table 4-6. Calculated reactivity worth for coolant voiding at different locations

Location	Reactivity Effect (mβ/cm^3)
A-ring Full Channel Average	-1.97
B-ring Full Channel Average	-1.77
C-ring Full Channel Average	-1.09
A-ring Bottom 6-inch Average	-1.90
B-ring Bottom 6-inch Average	-1.77
C-ring Bottom 6-inch Average	-1.19

Table 4-7. Calculated reactivity worth for coolant voiding at different locations presents the reactivity worth for voiding H_2O and D_2O shutter/blister tanks with the LEU core. The reactivity worths in Table 4-7 have a standard statistical deviation of less than 15 mβ. However, comparing to the small reactivity effect of dumping the tanks, the statistical uncertainties is relatively significant.

Table 4-7. Calculated reactivity worth for coolant voiding at different locations

Location	Reactivity Effect (mβ)
H_2O Shutter Tank	-4
D_2O blister Tank	-46

Table 4-8. Calculated reactivity worth for experimental facilities presents the reactivity worth of introducing U-235 and cadmium in the experiment channel in the LEU core. The former represents fissile materials; whereas the latter is a currently used neutron absorber at the MITR. Two types of experiment environments have been examined: an inert gas environment in the A-ring and a pressurized water environment in the B-ring. It should be noted that the reactivity worth per unit mass is largely experiment-dependent. The size and the shape of experimental samples will have significant impact on spatial self-shielding. The presented values in Table 4-8 are obtained from the reactivity worth of PWR fuel rodlet like samples. They can only provide a rough estimate of the reactivity effect. Problem-dependent analysis must be performed in advanced of each in-core experiment. The presented reactivity worth per unit mass has a standard statistical deviation of less than 1.5 mβ/g-U235 or 0.5 mβ/g-Cd. The relatively large statistical uncertainty is due to the relatively small PWR pellet-like sample size.

Table 4-8. Calculated reactivity worth for experimental facilities

Location	Reactivity Effect
A-ring (inert gas environment)	+2.3 mβ/g-U235
	-2.0 mβ/g-Cd
B-ring (pressurized water environment)	+4.9 mβ/g-U235
	-2.0 mβ/g-Cd

4.5.1.9 Core Reactivity

Core reactivity is not established in advance because there are no pre-defined core configurations. Instead, the following analysis will be performed and documented for every planned core configuration in order to be certain that the core is appropriately configured:

a) The expected reactivity change for the proposed refueling will be calculated by MCNP, with the fuel management capability of MCODE-FM [4-15]. Alternatively, the expected reactivity change may be derived by combining estimates of the change in grams of U-235 with the reactivity coefficients given in Table 4-5.

b) The shutdown margin for the refueled core will be calculated and verified to be acceptable.

c) Items (a) and (b) above will be documented and reviewed by someone other than the individual who did the calculations.

d) The refueling will be performed.

e) The reactivity change will be measured and compared to the predicted estimate.

f) The shutdown margin will be recalculated using the measured reactivity change. It is again verified to be acceptable.

g) Items (e) and (f) will be documented and reviewed.

4.5.1.10 Administrative and Physical Constraints

Both administrative and physical constraints preclude the inadvertent addition of positive reactivity:

a) Administrative: Movement of fuel is not permitted in the core or the fuel storage pool without the prior written approval of the Reactor Superintendent or his/her designate. All such approvals include a schedule of the authorized moves.

b) Physical: The k-effective of all areas where fuel may be stored (except the core itself) is less than 0.9. The principal concern is therefore the core. Changes to the core configuration are not possible when the reactor is operating because of the grid-latch

mechanical interlock. In order to obtain a "reactor start" condition, the upper grid plate must be in the latched position. When the grid is latched, no fuel element positions are accessible. That is, fuel can neither be inserted nor removed. This eliminates movement of fuel as a means of inserting positive reactivity during reactor operation. That leaves the possibility of manipulating a sample in an in-core sample assembly (ICSA). All manipulations are scheduled in writing by the Reactor Superintendent or his/her designate. In addition, ICSAs are not accessible unless either a reactor top lid penetration or other equivalent shielding is removed. This requires both use of the overhead crane and access to the reactor top. Use of the former is under the control of the licensed console operator. Entry to the latter triggers an alarm in the control room.

4.5.2 Reactor Core Physics Parameters

4.5.2.1 Effective Delayed Neutron Fraction and Neutron Lifetime

The effective delayed neutron faction (β_{eff}) and prompt neutron lifetime have been calculated for the LEU core. In addition to the fresh core (i.e., BOL), two equilibrium cores (i.e., MOL) and end-of-life (i.e., EOL), have also been investigated (see definitions in Ref [4-13]). The broader consideration aims to evaluate the impact of plutonium build-up post LEU conversion on the core kinetics parameters. As seen in Table 4-9. Calculated effective delayed neutron faction and prompt neutron life time, the β_{eff} remains fairly constant at different fuel cycle states indicating that plutonium build-up has a relatively small effect on β_{eff}. On the other hand, the prompt neutron life time varies between 55 and 65 μs for the three studied cases. It should be noted that the kinetics parameters are calculated for a critical LEU core. The presented β_{eff} has a standard statistical deviation of less than 0.00008 and the standard statistical deviation for the obtained prompt neutron life time is less than 0.36 μs.

Table 4-9. Calculated effective delayed neutron faction and prompt neutron life time

Fuel Cycle State	Effective Delayed Neutron Fraction	Prompt Neutron Life Time (μs)
BOL (Fresh Core – 22 Elements)	0.00762	64.05
MOL (Equilibrium – 24 Elements)	0.00747	55.13
EOL (Equilibrium – 24 Elements)	0.00727	64.32

4.5.2.2 Coefficients of Reactivity

Values and signs for coefficients of reactivity were given in Section 4.5.1.8. These reactivity data for the LEU-fueled MITR core, void coefficients, and in-core facilities have been estimated by MCNP calculations in advance of the conversion. All of them will be subsequently confirmed by measurement during startup tests after the conversion.

The test method for experimental verification used is as follows:

a) Reactor operation is restricted to low power so that there is no xenon production and/or temperature-dependent reactivity feedback.

b) The reactor is made critical and critical data (shim blade and regulating rod height, coolant temperature, etc.) are recorded.

c) The reactor is shut down.

d) An adjustment is made that affects reactivity (for example, a shutter may be opened or a portion of an in-core sample facility voided).

e) The reactor is again made critical and critical data is recorded.

f) The reactivity worth of the adjustment is determined by comparison of the two sets of critical data.

LEU calculated values for fuel and void reactivity in the fuel region were given in Tables 4-5 through 4-8. Changes with fuel burnup will be verified after depletion of an LEU core.

4.5.2.3 Flux Distributions

At present, the Monte-Carlo code MCNP is being used in the fuel management of the MITR. Very detailed three-dimensional neutron flux distributions can be calculated at different fuel cycle states. The axial heat flux profiles of the 7 MW LEU core at the peak stripe (1 stripe = 1/4 channel) locations (i.e., stripes with peak integral power for both interior and end channels) have been presented and discussed in Section 4.6.1 and more details can be found in Ref [4-13].

At the time the LEU conversion is completed, measurements of axial and radial neutron flux will be part of the startup testing. The experiment data will serve as validation for the MCNP calculations.

4.5.3 Operating Limits

Safety is ensured by observance of a substantial shutdown margin requirement as well as by specifying a minimum shim bank height (i.e., the subcritical limit interlock) below where the reactor cannot attain criticality.

4.5.3.1 Reactivity Conditions

The current discussion follows Section 4.5.1.5, which shows the shim bank and regulating rod reactivity worth. The cited results are for purposes of illustration and are not intended as limiting values.

As discussed in Section 4.5.1.5, MITR refueling is normally designed so that the new core will go critical at a shim bank height of 8 to 10 inches (taking into account the reactivity penalty from in-core experiments). Typically the BOL critical absorber configuration is 8.0 inches on the shim bank and 2.0 inches on the regulating rod with a coolant/reflector temperature of 20 °C. Accordingly, the reactivity inserted to attain criticality is 7.1 β (shim bank) and 0.1 β (regulating rod) for a total of 7.2 β. The total reactivity worth of the shim bank and regulating rod are 11.5 β and 0.2 β, respectively. Hence, the excess reactivity in this example is 4.5 β. The reactivity associated with the attainment of the normal operating temperature (50 °C) for the coolant and

reflector is -0.5 β. The estimated equilibrium xenon worth at 7.0 MW is -2.6 β. The remaining excess reactivity once equilibrium operating conditions have been attained is 1.4 β. Fuel depletion accounts for average of -0.125 mβ/MWH. Hence, if no reactivity was needed to override peak xenon after shutdown, the core could be operated for 11,200 MWH or 66.7 days at 7.0 MW. This is a relatively short operating cycle and suggests that the excess reactivity available for MITR operation is quite modest.

4.5.3.2 Excess Reactivity

Excess reactivity and the effect of temperature, xenon, and experiments on excess reactivity are discussed in the Section 4.5.3.1 of this report. A typical value for the MITR's excess reactivity is 6 to 7 β. However, it may be larger because the integral worth of the control devices (shim blades and regulating rod) is more than 13.4 β for the fresh core and more than 11.5 β for the equilibrium cores (see Section 4.5.1.5). Two provisions in the MITR's design and operation limit the excess reactivity that is potentially available. First, the subcritical interlock, as described in Section 7.3.1.2 of the SAR, is observed during startups. Specifically, if the reactor should attain criticality at a shim bank height of less than 5.0 inches, it is to be shutdown. The requirement has the effect of reducing the maximum possible excess reactivity from 13.4 β to about 10.1 β. Second, only one shim blade can be withdrawn at a time. This fact, coupled with the identical nature of the six blades and the requirement that they be operated as a bank when above the subcritical interlock, limits the excess reactivity per blade to about 1.7 β. This is the amount that could – in a worst-case scenario – be inserted.

4.5.3.3 Shutdown Margin

The shutdown margin requirement for the MITR is that it be possible to shut the reactor down by at least 1% Δk/k using shim blades from the cold (10 °C), xenon-free condition with both the most reactive blade and the regulating rod fully withdrawn and all movable and non-secured samples in their most reactive state.

The shutdown margin was calculated for the LEU core, using configurations at BOL (fresh core – 22 fuel elements) and MOL (equilibrium core – 24 fuel elements), respectively. There are no movable samples present in the current calculations. The results are shown in Table 4-10 and it should be noted that all the presented values have a standard statistical deviation of less than 0.07% Δk/k. The lowest shutdown margin (2.72% Δk/k) occurs at the MOL state, when shim blade No. 5 and the regulating rod are fully withdrawn, which satisfies the minimum shutdown margin requirement of 1% Δk/k.

Table 4-10. Calculated shutdown margin for LEU core at BOL and MOL (SB and RR stand for Shim Blade and Regulating Rod)

Scenarios	BOL (%Δk/k)	MOL (%Δk/k)
SB#1 & RR Out	3.03	2.88
SB#2 & RR Out	3.17	3.00
SB#3 & RR Out	3.16	2.91
SB#4 & RR Out	3.24	2.74
SB#5 & RR Out	3.11	2.72
SB#6 & RR Out	3.09	2.76

The availability of normal electric power (or emergency backup electric power) has no effect on the capability of the MITR to meet the shutdown margin. As discussed in Section 4.2.2.7 of the SAR, the blades drop into the core under the influence of gravity upon loss of power to electromagnets.

As noted in Section 4.5.1.9 of this report, the shutdown margin is determined prior to every refueling. It is verified following every refueling using the measured worth of the refueling.

The error of the shutdown margin calculation is the result of uncertainties associated with the measurement of the individual reactivity values that are used in the computation. These in turn reflect the accuracy with which the control device, temperature, and xenon reactivity worth curves are determined as well as the correctness of measurements of the shim blade and regulating rod height, coolant and reflector temperature, and the time since shutdown. An error analysis of these factors was performed as part of the fuel management studies for the MITR-II [4-12]. The MITR uses the power doubling time method (once equilibrium conditions have been established) to measure the reactivity of the control devices. This method is believed accurate to be within ±10%.

4.5.3.4 Limiting Core Configuration for Thermal-hydraulic Analysis

For the same nominal reactor power, neutron flux and thermal power density increase with the number of non-fueled assemblies in the core. The HEU core has been operated with two, three, four, and five non-fueled positions. In each case, analysis showed that no thermal-hydraulic and nuclear safety limits were exceeded. The thermal-hydraulic analysis of the LEU core has been performed based on five and three non-fueled locations, representing the fresh and equilibrium cores respectively.

The power peaking factors are a function of both the number of non-fueled positions and the shim bank height. As described in Section 4.5.1.3 of this report, power peaking is greater in the inner fuel rings at low shim bank height. The peaking shifts to the outer fuel ring as the shim bank is withdrawn. Other factors that affect power peaking include the location of the non-fueled positions within the core, the burnup of each element, and the presence of in-core sample assemblies. Accordingly, the BOL, MOL, and EOL cores were analyzed. It has been found that the stripes (¼ plate) peak integral power and the peak power spot both occur at the beginning-of-

life (BOL) state because only 22 fuel elements are loaded (compared to 24 elements in equilibrium/depleted cores), so the average heat flux per element is higher. More detailed information is available in Ref [4-13].

During standard operation, all six shim blades are maintained within 2 inches of the average shim bank height. It is rare for a shim blade to be inoperable. If an inoperable blade is below the bank average, then the reactor is not to be operated at power levels in excess of 1 kW. This precludes the possibility of a skewed flux profile that could alter the calculated peaking factors. Operation with an inoperable blade at or above the bank average is permitted because this will not significantly alter the flux density distribution. Section 13 of this report discusses an analysis of operation with the shim blades in a non-uniform bank position.

4.5.3.5 Transient Analysis

The continuous withdrawal of the most reactive shim blade would create a ramp reactivity addition. Failure of an in-core experiment could create either a fast or a slow ramp reactivity insertion depending on the cause of the failure. Both ramp reactivity additions are analyzed in Section 13 of this report. In neither case is the reactor damaged or fuel integrity compromised.

4.5.3.6 Redundancy and Diversity of Reactor Shutdown Mechanisms

The MITR's shutdown mechanisms are both redundant and diverse. Redundancy is provided by six identical shim blades that operate in parallel. Diversity is provided by a completely separate means of shutting the MITR down. This is the capability to dump the portion of the heavy water reflector that surrounds the fuel to a tank located well below the core.

Electrical power is required to energize both the electromagnets that support the shim blades and the solenoid that controls the air pressure that keeps the reflector dump valve closed. Hence, on loss of electrical power, the MITR shuts down automatically.

4.6 Thermal-hydraulic Design

The thermal-hydraulic design of the MITR LEU core is described in this section. The MITR may be operated under either forced or natural convection and both modes are addressed here. The MITR does not have a pulse capability and hence only steady-state operation conditions are described. The description of end channel configuration and the details in determination of hot stripes for interior and end channels can be found in Ref [4-13].

4.6.1 Design Basis

The basis for the MITR's thermal-hydraulic design is that, under conditions of forced convection, the primary coolant system can remove the fission energy produced during steady-state 7.0 MW operation and transfer it to the secondary coolant system without the onset of nucleate boiling in the core region. Another design feature is that the system can remove at least 100 kW of heat from the fuel elements by natural convection without the onset of nucleate boiling. Provisions are also taken into account in the coolant system design so that fuel integrity is maintained during all credible transients, such as a loss of primary coolant flow because of a pump coast-

down (Section 13.2.4 of this report). Sufficient margin for the possible deviation of design parameters is taken into account in the thermal-hydraulic limit calculations.

The objective of the thermal-hydraulic design is to guarantee the structural integrity of the fuel elements which are made of a monolithic U-Mo matrix enclosed in an aluminum alloy 6061 cladding. There are several heat transfer phenomena that must be avoided in steady-state. These are:

a) Critical Heat Flux (CHF): During the initial state of nucleate boiling, vapor bubbles form on the fuel cladding surface and increases heat transfer because of the latent heat that is removed by bubble formation. When the heat flux rises, the bubbles coalesce to form a vapor film and heat transfer then deteriorates because of the low thermal conductivity of vapor. CHF leads to a fuel temperature excursion and subsequent fuel damage. CHF is a function of flow rate and coolant temperature.

b) Onset of Flow Instabilities (OFI): Flow instability refers to the phenomenon where a large amount of vapor forms in a coolant channel which results in channel blockage and reduces coolant flowing to the channel in question and more to adjacent ones. OFI is a possibility in cores with a multi-channel design.

Although CHF is widely used as the criterion of fuel temperature excursions for nuclear reactors, OFI is identified as the mechanism that may lead to premature CHF due to transient flow reduction in the hot channel. Empirical correlations exist to predict both CHF and OFI, which are calculated in Section 4.6.6 and used in order to establish the MITR's safety limits.

4.6.1.1 Core Characteristics

The reactor is typically filled with 24 fuel elements. The three grid positions that are not occupied by fuel elements can be filled with solid aluminum dummies or approved units such as in-core sample assemblies (Section 10.3.2.6 of the SAR) to prevent excessive bypass flow through the non-fueled positions. The MITR can be operated with forced flow or natural convection flow. The former is provided by two primary pumps that are operated in parallel. The nominal flow rate is 2400 gpm. The latter is accomplished by a natural convection flow path in the core tank that is established by the four natural convection valves and the two anti-siphon valves. Natural convection is driven by the buoyant force from the heated (therefore less dense) coolant exiting the core region rising to the top of the core tank, cooling down, and flowing back down to the bottom of the tank, establishing a flow loop. Chapter 6 of the SAR has a detailed description of the operation of the natural convection and anti-siphon valves.

4.6.1.2 Thermal Power Density Distribution

The thermal power density distribution is assumed to be proportional to the fission density or the neutron flux distributions that are calculated by neutronics codes. In this report, the Monte Carlo transport code MCNP5 version 1.60, which enables three-dimensional modeling of the exact geometry of the MITR, is adopted for computing the thermal power density distribution. The thermal power distribution is a function of fuel depletion, fuel element orientation, and shim bank height. Therefore, the power distribution is divided into several independent parameters to characterize a bounding power distribution. These are: radial power peaking factor (F_r), lateral

power peaking factor (F_s), and axial power distribution $\theta(z)$. The radial power peaking factor is defined as the ratio between the power generated by a fuel plate and the average power per fuel plate in the entire core. The lateral power peaking factor is defined as the ratio between the heat flux of a lateral section (i.e. a stripe) and the average heat flux in a particular fuel plate. Thus,

$$F_{r,i} = \frac{P_i}{P_{avg}} \qquad \textbf{Eq. 4-1}$$

$$F_{s,i} = \frac{q''_s}{q''_{avg,i}} \qquad \textbf{Eq. 4-2}$$

where P_i is power generated by fuel plate i,

P_{avg} is the average power generated by each fuel plate in entire core,

q''_s is the axially-averaged heat flux of a lateral section of fuel plate i,

$q''_{avg,i}$ is the axially-averaged heat flux along fuel plate i.

The axial power distribution in a lateral section of a fuel plate can be written as:

$$q''_s(z) = F_{r,i} F_{s,i} \theta(z) q''_{avg} \qquad \textbf{Eq. 4-3}$$

where q''_{avg} is the average heat flux of all fuel plates and $\theta(z)$ is the normalized axial power distribution.

Because q''_{avg} is constant for a given reactor power and core configuration, the three-dimensional power distribution can be represented by the combination of the three dimensionless factors $F_{r,i}$, $F_{s,i}$, and $\theta(z)$.

Power distributions calculated using MCNP5 define each of the factors $F_{r,i}$, $F_{s,i}$, and $\theta(z)$ (defined in Eq. 4-1, 4-2, and 4-3) in a power profile with geometry and materials specific to the core modeled for fuel depletion, fuel element orientation, and shim bank height. Power distributions for a series of 7 MW fresh and equilibrium LEU cores at different fuel cycle states have been investigated in Ref [4-13]. It has been found that the stripes peak integral power for both interior and end channels occur at the BOL state. This is because only 22 fuel elements are loaded (comparing to 24 elements in equilibrium cores), so that the average power and heat flux per element is higher. The respective power distributions are shown in Figure 4-9. Axial heat flux profile of the 7 MW LEU core at hot stripe locations. It should be noted that A1 and C15 represent element positions, 's' stands for the Stripe Number, and 'p' is the Plate Number. In addition, thermal-hydraulic analysis of the studied cases indicates that the stripe with peak integral power corresponds to the most limiting scenario with $F_r F_s = 1.677$ for interior channels and $F_r F_s = 1.455$ for end channels.

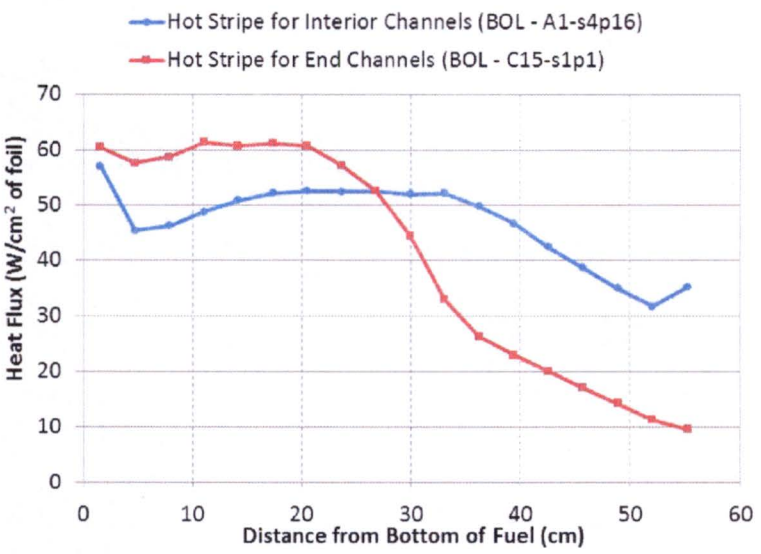

Figure 4-9. Axial heat flux profile of the 7 MW LEU core at hot stripe locations

4.6.2 Major Correlations Used in the Thermal-Hydraulic Limit Calculations

Critical heat flux (CHF) denotes the condition at which the heat transfer of two-phase flow deteriorates substantially and subsequently leads to elevated fuel temperatures. CHF may occur because of either vapor film formation on the cladding surface or dryout of the liquid film. Because the rise in temperature quickly follows CHF, it is desirable to use some other phenomenon, one that occurs earlier, as the basis for a thermal-hydraulic limit. If the energy flux to a heated surface is increased slowly, the first two-phase behavior that is observed is onset of nucleate boiling (ONB), also called incipient boiling. It defines the conditions where bubbles first start to form on the heated surface. Because most of the liquid is still subcooled, the bubbles do not detach but grow and collapse while attached to the wall. ONB is followed by onset of significant voiding (OSV) which describes the condition where the bubbles grow larger on the heated surface and detach regularly. OSV leads to onset of flow instability (OFI) which describes the condition when the mass flow rate decreases with increasing vapor content in the coolant flow. This type of flow excursion will lead to an elevated fuel temperature (or premature CHF) because of an abrupt drop in the coolant flow rate. Experimental studies have shown that OFI tends to occur closely after OSV when the increase in vapor content results in a higher friction pressure drop [4-16].

Correlations are enumerated below for ONB, OFI, and CHF.

4.6.2.1 Correlation for Onset of Nucleate Boiling (ONB)

Sudo *et al.* suggested the Bergles-Rohsenow correlation for the prediction of ONB for narrow rectangular coolant channels [4-17]. This suggestion was based on comparisons of several existing correlations with experimental data. Sudo *et al.* also concluded that the Bergles-Rohsenow correlation predicts the lower limits of the measured ONB temperatures for given heat fluxes and that there exists a margin between the predicted and measured ONB temperatures.

The Bergles-Rohsenow correlation predicts the fuel cladding temperature at which ONB occurs.

$$T_{clad,ONB} = T_{sat} + 0.556 \cdot \left[\frac{q''}{1082 \cdot p^{1.156}} \right]^{0.463 \cdot p^{0.0234}} \quad \textbf{Eq. 4-4}$$

where $T_{clad,ONB}$ is the fuel cladding temperature (°C) at which ONB occurs,

T_{sat} is the saturation temperature (°C)

q'' is the local heat flux (W/m^2), and

p is the pressure (bar).

The Bergles-Rohsenow correlation is applicable to both forced convection and natural circulation.

4.6.2.2 Correlation for Onset of Flow Instability (OFI)

Low pressure systems such as the MITR are susceptible to a form of static flow instability known as flow excursion or Ledinegg instability. This type of instability is very important when the gas-to-liquid density ratio is low. This flow excursion instability can be described in terms of a plot of channel pressure drop versus mass flow rate as shown in Figure 4-10. Channel pressure drop – mass flow rate behavior [4-18]. The two-phase flow region with a negative slope is the unstable region. Were the hot channel to be operated in this region at point B, it is possible that the operating condition would be shifted to point B' by a small perturbation. Operation at point B' will lead to critical heat flux. Onset of flow instability (OFI) defines the point of inception of this excursion instability.

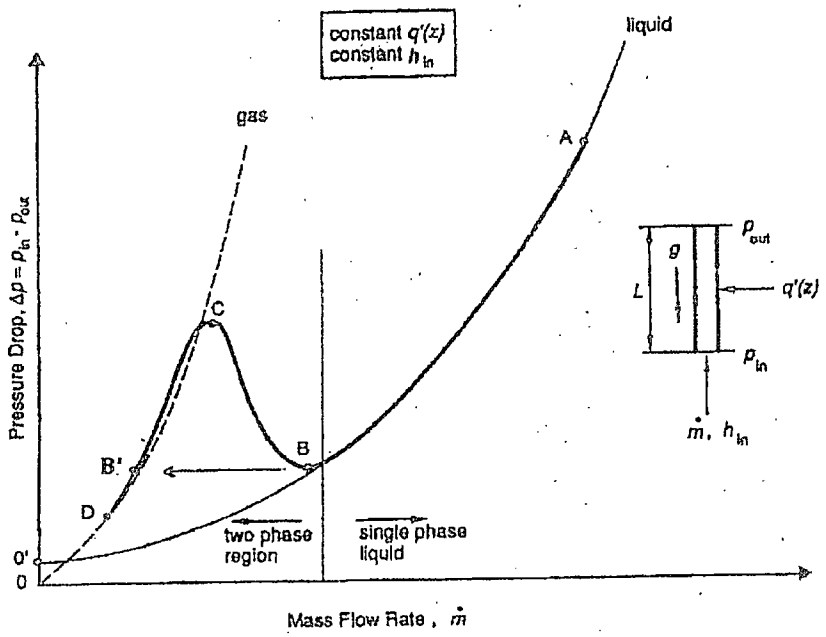

Figure 4-10. Channel pressure drop – mass flow rate behavior [4-18]

The OFI point was determined in previous studies using a steady-state energy conservation equation [4-16]:

$$\dot{m}_{OFI} = \frac{Q}{Rc_p(T_{sat} - T_{in})} \qquad \textbf{Eq. 4-5}$$

where $\dot{m}_{OFI}$ is the channel mass flow rate when OFI occurs (kg/s),

Q is the channel power (W),

R is the channel outlet sub-cooling ratio, $R = (T_{out} - T_{in}) / (T_{sat} - T_{in})$

c_p is the coolant specific heat (J/kg/°C),

T_{sat} is the saturation temperature (°C),

T_{in} is the channel inlet temperature (°C), and

T_{out} is the channel outlet temperature (°C).

The channel outlet sub-cooling ratio, R, can be determined from the following relations:

$$R = \frac{1}{1 + 25\frac{D_e}{L_h}}, \text{ from Ref [4-16]} \qquad \textbf{Eq. 4-6}$$

$$R = 0.21 \cdot \ln\left(\frac{L_h}{D_e}\right) - 0.258, \text{ for } 70 < \frac{L_h}{D_e} < 250, \text{ from Ref [4-19]} \qquad \textbf{Eq. 4-7}$$

$$R = 0.697 + 0.00063\left(\frac{L_h}{D_e}\right), \text{ for } 100 < \frac{L_h}{D_e} < 200, \text{ from Ref [4-16]} \qquad \textbf{Eq. 4-8}$$

where L_h is the heated length of the coolant channel (m), and

D_e is the equivalent diameter of the coolant channel (m).

The above relations do not include the effect of axial power distribution. This is addressed in Ref [4-18] by calculating the pressure drop at OFI using different power profiles and a uniform one was found to be limiting. Thus only total channel power is required in the evaluation of OFI.

Because L_h/D_e of the LEU fuel element is 135.3 for the interior channel and 76.8 for the end channel. The former is within the applicable range of all three above equations (i.e., Eqs. 4-6 to 4-8) and the latter is only applicable to the first two.

4.6.2.3 Correlation for Critical Heat Flux (CHF)

Critical heat flux (CHF) denotes the conditions at which the heat transfer of the two-phase flow deteriorates substantially and subsequently leads to elevated fuel temperatures. A CHF correlation scheme was proposed for vertical rectangular channels in research reactors by Sudo and Kaminaga [4-19]. This correlation scheme is based on experimental data that covers the operating conditions of the MITR. For a forced convection up-flow condition, the CHF is calculated as a function of mass flux (G) and the outlet sub-cooling ($\Delta T_{SUB,o}$). The correlation is:

$$q^*_{CHF,1} = 0.005 \cdot G^{*0.611}\left(1 + \frac{5000}{G^*} \cdot \Delta T^*_{SUB,o}\right) \qquad \textbf{Eq. 4-9}$$

Sudo and Kaminaga also suggested a minimum CHF which corresponds to a zero or blocked flow condition and which can be used to analyze natural convection. It was noted experimentally that when the flow becomes stagnant, a situation could develop where a downward movement of water co-existed with an upward flow of bubbles or steam generated in the channel. This is referred to as a flooding condition because the flow channels are submerged in a pool of coolant.

$$q^*_{CHF,2} = 0.7 \cdot \frac{A_{XS}}{A_H} \cdot \frac{\sqrt{W/\lambda}}{\left[1 + (\rho_g/\rho_f)^{0.25}\right]^2} \qquad \textbf{Eq. 4-10}$$

The dimensionless heat flux and mass flux are defined as:

$$q^*_{CHF} = \frac{q''_{CHF}}{h_{fg}\sqrt{\lambda g \rho_g (\rho_f - \rho_g)}} \quad \textbf{Eq. 4-11}$$

$$G^* = \frac{G}{\sqrt{\lambda g \rho_g (\rho_f - \rho_g)}} \quad \textbf{Eq. 4-12}$$

$$\Delta T^*_{SUB,o} = \frac{c_{pf}}{h_{fg}} \cdot (T_{sat} - T_{out}), \text{ and} \quad \textbf{Eq. 4-13}$$

$$\lambda = \left[\frac{\sigma}{g \cdot (\rho_f - \rho_g)}\right]^{0.5} \quad \textbf{Eq. 4-14}$$

where:

A_H is the heat transfer area,

A_{XS} is the cross section area,

g is the acceleration due to gravity,

h_{fg} is the enthalpy difference between fluid and gas phases,

ρ_f is the liquid density,

ρ_g is the vapor density,

W is the coolant channel width, and

σ is the surface tension.

Eqs. 4-9 and 4-10 can be plotted as shown in Figure 4-11. G^*_0 is the intersection of $q^*_{CHF,1}$ and $q^*_{CHF,2}$. When the mass flux drops below G^*_0, the fuel will be cooled by countercurrent flow (flooding). For the geometry of the MITR LEU fuel element, G^*_0 is calculated to be 3.50 kg/m^2-s, which is less than 0.2% of the nominal flow. The calculated $q^*_{CHF,2}$ is 4.220×10^4 W/m^2, which corresponds to a reactor power of 595 kW with a hot stripe factor of 1.677. It should be noted that the CHF correlation is applicable to forced convection ($q^*_{CHF,1}$) and natural convection ($q^*_{CHF,2}$).

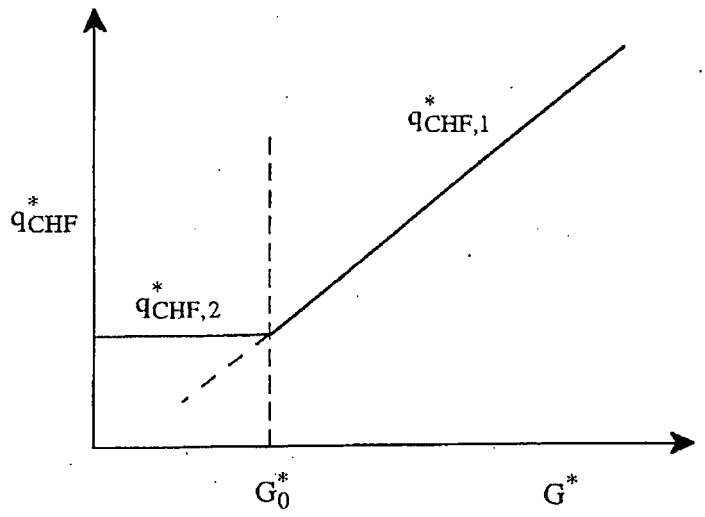

Figure 4-11. CHF correlation scheme for up-flow proposed by Sudo and Kaminaga [4-19] for forced convection ($q^*_{CHF,1}$) and natural convection ($q^*_{CHF,2}$)

4.6.3 Reactor Power Deposition and Core Flow Distribution

The correlations described above are to be used to obtain the thermal hydraulic limits based on the most limiting core configuration as described in Section 4.6.1.2 of this report. The flow rate and heat generation are represented as a function of the reactor primary coolant flow rate and reactor power because these are the parameters that are measured by the reactor instrumentation. This representation is achieved by using a set of factors that are derived from either calculations or experimental data.

4.6.3.1 Reactor Power Deposition

The energy produced by the reactor consists of the kinetic energy of the fission fragments, beta particles, prompt and delayed gammas, prompt and delayed neutrons, and neutrinos. Kinetic energy of the fission fragments and beta particles make up about 90% of the total fission power and is deposited in the fuel because of the short travel range of these particles. A small percentage of the fission power is deposited outside the core region because of the long mean-free-path of gammas and fast neutrons compared to the small size of the core. The kinetic energy from neutrinos is not deposited. The core deposition factor (F_{core}) defines the fraction of the fission power deposited in the reactor core region (both fuel and coolant) of the core tank. The fuel deposition factor (F_{fuel}) defines the fraction of the core power deposited in the fuel elements. The average heat flux can be calculated using

$$q''_{avg} = \frac{P}{N_f A_H} F_{core} F_{fuel} \qquad \textbf{Eq. 4-15}$$

where: P is the reactor power,

N_f is the total number of fuel plates in the core,

A_H is the total heat transfer area for one fuel plate.

MCNP calculations showed that ~ 95% of the total fission energy is deposited in the fuel, cladding, and light water in the coolant channels (see Table 4-11. Fission energy depositions in different components for LEU equilibrium core). The product of F_{core} and F_{fuel} is thus estimated to be 0.95.

Table 4-11. Fission energy depositions in different components for LEU equilibrium core

Equilibrium Core	Fuel	Cladding	Channel H2O	Structure & H_2O pockets	D2O	Graphite	Total
	(MeV/f)	(MeV/f)	(MeV/f)	(MeV/f)	(MeV/f)	(MeV/f)	(MeV/f)
Neutron	175.75	0.07	2.78	1.03	0.57	0.01	180.21
Photon	9.50	0.98	1.50	4.50	2.20	1.21	19.89
Both	185.25	1.05	4.29	5.53	2.77	1.21	200.10
	(%)	(%)	(%)	(%)	(%)	(%)	(%)
Neutron	87.8	0.03	1.4	0.5	0.3	0.003	90.1
Photon	4.7	0.5	0.8	2.3	1.1	0.6	9.9
Both	92.6	0.5	2.1	2.8	1.4	0.6	100.0

4.6.3.2 Core Flow Distribution

Ideally, the core region should be designed so that 100% of the coolant flows through the fuel elements. However, in reality part of this flow bypasses the core region through the natural circulation and anti-siphon valves, and because of design/manufacturing tolerances, such as clearances, between the fuel elements. The coolant flow factor (F_f) is defined as the ratio of the primary coolant flow that actually cools the core region to the total flow. The coolant flow factor was determined experimentally during the initial startup testing of the MITR HEU core to be $F_f = 0.921$ [4-14].

The channel flow disparity factor (d_f) is defined as the ratio of the minimum flow to the average flow in a fuel assembly. The flow distribution in the reactor core was measured during the MITR HEU core initial startup testing to be $d_f = 0.93$.

The fraction of the coolant channel flow in the stripe region (f_{sf}) accounts for neglecting the flow between the side plate and the edge of the fuel foil. $f_{sf} = 0.91$ is recommended in Ref [4-2].

Therefore, the average flow rate per coolant channel in the fuel assembly is:

$$\dot{m}_{avg} = \frac{W_p F_f}{N_c} d_f \cdot f_{sf} \qquad \textbf{Eq. 4-16}$$

where: W_p is the total primary flow rate, and

N_c is the number of coolant channels in the core region.

Within the fuel assembly, the flow distribution among each coolant channel depends predominantly on channel gap distance. For a constant friction pressure drop, the flow rate is proportional to channel gap distance. The channel flow rate as a function of channel gap can be derived as [4-21]:

$$\dot{m} = \dot{m}_{avg}\left(\frac{\delta}{\overline{\delta}}\right)^{1.714} \qquad \textbf{Eq. 4-17}$$

where: δ is the actual coolant gap size, and

$\overline{\delta}$ is the nominal coolant gap of 74.6 mil and 65.7 mil for interior and end channel.

It should be noted that even though the core tank configuration will not be changed, the different pressure drop of the new LEU fuel element will lead to changes of several important parameters, (e.g., F_f and d_f). These parameters will be determined through detailed modeling or measurements before or during the reactor startup testing before the final Safety Analysis Report (SAR) issued [4-20].

4.6.4 Engineering Hot Channel Factors and Uncertainty Treatments

The engineering hot channel factors (EHCF) account for possible deviations from nominal design specifications that may affect the thermal-hydraulic calculations. Specifically, they are defined for channel enthalpy rise, film temperature difference, and heat flux [4-18]. These parameters encompass sub-factors that can be combined either multiplicatively or statistically to obtain the engineering hot channel factors. It has been concluded that it is overly conservative to combine the sub-factors multiplicatively [4-18, 4-22]. A statistical approach (for sub-factors combination) to determine a fixed EHCF has been used in the current LSSS analysis. Table 4-12 is a summary of the engineering hot channel factors.

Table 4-13. Engineering hot channel factors applied in thermal-hydraulic calculations

Hot Channel Factor	Enthalpy Rise	Film Temperature Rise	Heat Flux
Reactor power measurement	1.05	1.05	1.05
Power density measurement / calculation	1.10	1.10	1.10
Plenum chamber flow	1.08	1.06	—
Flow measurement	1.05	1.04	—
Fuel density tolerances	1.026	1.05	1.05
Flow channel tolerances	1.089	1.124	—
	F_H, statistical* 1.173	**$F_{\Delta T}$, statistical 1.189**	**F_Q, statistical 1.123**

* The engineering hot channel factors are obtained by combining the sub-factors statistically using the equation $F = 1 + \left[\sum_j (f_j - 1)^2\right]^{0.5}$, where f_j denotes sub-factors [4-18].

The engineering hot channel sub-factors considered in the current analysis include those for reactor power measurement, power density measurement/calculation, fuel density (homogeneity or loading specification) tolerances, pump flow rate, flow channel tolerances, and heat transfer coefficient prediction. Numerical values for these sub-factors were mostly adopted from the MITR-II SAR [4-14].

A "vertical" approach is used in the current analysis to calculate the maximum fuel cladding temperature and the maximum coolant temperature using the engineering hot channel factors. This approach is the standard conventional method noted in Ref [4-18]. To calculate the maximum coolant temperature, use

$$T_{c,M} = T_{in} + F_H \cdot \Delta T_c \quad (\text{or } H_{c,M} = H_{in} + F_H \cdot \Delta H_c, \text{ if boiling occurs}) \qquad \textbf{Eq. 4-18}$$

To calculate the maximum cladding (or wall) temperature, use:

$$T_{w,M} = T_{in} + F_H \cdot \Delta T_c + F_{\Delta T} \cdot \Delta T_w \qquad \textbf{Eq. 4-19}$$

where T_{in} is the coolant channel inlet temperature,

H_{in} is the coolant enthalpy at the channel inlet,

ΔT_c is the coolant temperature rise,

ΔH_c is the coolant enthalpy rise,

ΔT_c is the film temperature rise (temperature difference between coolant and cladding),

F_H is the engineering hot channel factor for enthalpy rise,

$F_{\Delta T}$ is the engineering hot channel factor for film temperature rise,

$T_{c,M}$ is the maximum coolant temperature because of design / manufacture deviations,

$H_{c,M}$ is the maximum coolant enthalpy because of design / manufacture deviations,

$T_{w,M}$ is the maximum cladding temperature because of design / manufacture deviations.

The quantities ΔT_c (or ΔH_c), and ΔT_w are calculated for every axial node in the hot channel with the operating limits taken into account, $T_{c,M}$ is then calculated and checked if the LSSS are exceeded.

Detailed descriptions for calculating the LSSS with use of engineering hot channel factors are presented in Section 4.6.7.

For analysis of safety limits, a methodology based on statistically combining the parametric uncertainties is adopted in order to explicitly quantify both measurement and calculation uncertainties. Each parameter is treated as a distribution (e.g., normal or Gaussian distribution). When several parameters are included in an equation and cannot be solved analytically, they can be analyzed using Monte Carlo uncertainty propagation. This method is similar to one adopted for advanced reactor analysis. Measurement and calculation uncertainties based on the 99.7% confidence level (or 3-σ deviation) that are incorporated in the safety limit analysis are:

- Reactor power measurement: ±5%
- Power density measurement/calculation: ±10%
- Local fuel homogeneity: ±10%
- Primary flow measurement: ±5%
- Heat transfer coefficient: ±20%
- Coolant channel flow distribution: ±13%

Reactor power measurement and primary flow measurement errors are dependent on instrument specifications and performance. Operational experience and instrument calibration data from the MITR have demonstrated that the measurement errors from these safety channels are within 5%. Typical uncertainty for full three-dimensional power density calculation using MCNP code is within 10%. Correlations used for heat transfer coefficient analysis were obtained from a wide range of experimental data with an uncertainty of ±20% [4-23].

The dominant factor for coolant channel flow distribution uncertainty is the fabrication tolerance associated with the size of a coolant channel gap. Historical data obtained from MITR HEU fuel element certification reports indicated that the 3-σ deviation of the nominal HEU water gap is 5.4 mils. The coolant channel flow distribution uncertainty corresponding to this fabrication tolerance is 13% [4-23]. It should be noted that the obtained 13% is based on historical data from MITR finned fuel elements. The fabrication tolerance associated with the un-finned MITR LEU fuel is not yet derived. The preliminary coolant channel 3-σ uncertainties for un-finned MITR LEU fuel have been defined in Ref [4-1]: 0.0041 inches for interior channels and 0.017 inches for end channels. As the next step, additional data will be analyzed during U.S. High Performance Research Reactors fuel element fabrication campaigns.

Detailed descriptions for deriving the safety limits using the Monte Carlo uncertainty propagation method are presented in Section 4.6.6.

4.6.5 Thermal-Hydraulic Limits

The MITR is designed to operate in a safe manner under all credible conditions. The thermal-hydraulic design limits were chosen to provide a safe margin beyond the desired operating range. Calculations of the design limits also include considerations for deviations from design specifications.

Safety limits are established to maintain the integrity of the fuel cladding. Critical heat flux (CHF) is normally used as the criterion of fuel overheating. However, because the coolant flow path in the MITR core is a multi-channel design, there exists the possibility that flow instabilities could occur before reaching CHF limitations. If onset of flow instability (OFI) did occur first, it would have the effect of lowering the flow rate to the hot channel significantly and thus lowering the critical heat flux. In the safety limit calculations, both CHF and OFI are calculated and the one that would occur first is used to determine the safety limits.

The limiting safety system settings (LSSS) are established to allow a sufficient margin between normal operating conditions and the safety limits. Onset of nucleate boiling (ONB) is chosen as the criterion for the LSSS derivation. This guarantees that boiling will not occur anywhere in the fueled region as long as the limits are not exceeded.

Specifically, the LSSS for forced flow operations is set for:

a) The maximum reactor power,

b) The maximum steady-state average core outlet temperature,

c) The minimum primary flow rate, and

d) The minimum coolant level in the core tank.

The LSSS for natural-convection operation is set for:

a) The maximum reactor power,

b) The maximum steady-state average core outlet temperature, and

c) The minimum coolant level in the core tank.

The MITR can operate with all four/three parameters simultaneously approaching their limits without there being boiling in the fueled region. Each of these parameters is protected by more than one reactor scram.

Derivation of the safety limits using the Monte Carlo uncertainty propagation method is based on the following assumptions:

a) All parametric uncertainties are modeled as normal distributions as described in Section 4.6.4. The parameters that are treated as probability distributions are reactor power <P>, primary flow rate $<W_p>$, and coolant channel gap size $<\delta>$.

b) A "hot stripe" is defined as the most limiting lateral fuel plate section and coolant channel for the thermal hydraulic limits analysis. The power density of the hot stripe is based on a 7 MW depleted LEU core analysis as described in Section 4.6.1.2. The following assumptions are made about the hot stripe:

- It has no lateral heat conduction within the fuel plate to adjacent stripes (shown to be a conservative assumption in Ref [4-1])
- It is adjacent to an interior or end coolant channel, with both sides of the coolant channel having the same heat flux profile.
- It has no coolant mixing (shown to be a conservative assumption in Ref [4-19]).

4.6.6 Derivation of the Safety Limits

4.6.6.1 Comparison of OFI and CHF

The value of minimum CHF ratio (MCHFR) is determined for the CHF correlation to account for the lower bound of the experimental data used to develop the CHF correlation. It is suggested by Sudo and Kaminaga that MCHFR of 1.5 should be used. CHF and OFI heat flux are calculated by Eqs. 4-9 and 4-5 respectively for different mass flux G, and Figure 4-12 shows the comparison of the minimum CHF and the OFI heat flux. Property parameters (e.g., h_{fg}, ρ_f, ρ_g, and etc.) of saturated water (coolant height 10 feet above top of fuel plates) and the channel inlet temperature calculated by MULCH-II for steady state (which is 43.6 °C) are used in the calculation. It should also be noted that the maximum R-value (which is 0.8440) calculated using Eqs. 4-6 through 4-8 has been adopted here, since it leads to the lowest ratio between CHF and OFI heat flux.

As shown in Figure 4-12, the ratio between CHF and OFI is about 2.64 at a mass flux of 2,100 kg/m^2-s, which corresponds to the mass flux in a coolant channel receiving the least flow at a total primary flow of 2,200 gpm. Upon dividing by the maximum axial peaking factor of 1.45 (obtained from the BOL core model) this ratio becomes 1.82. This adjustment is made because CHF is used for local heat flux and OFI is a channel-average quantity. This represents

an estimate of CHF that is about 100% higher than that of OFI. It is concluded that OFI is a more conservative estimate than CHF for the MITR and therefore OFI should be used as the basis of the safety limits for the MITR instead of CHF. (Note: This conclusion applies only to forced convection because the OFI correlation does not extrapolate to natural convection conditions.)

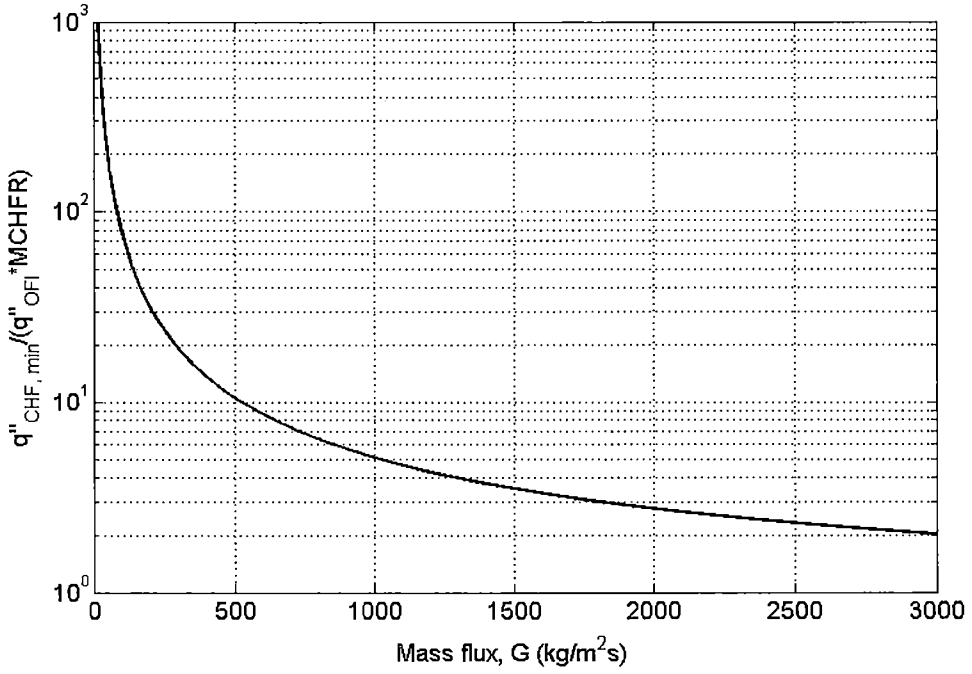

Figure 4-12. Comparison of the ratio of CHF to OFI heat flux for forced flow conditions

4.6.6.2 Calculation of the Safety Limits for Forced Convection

The coolant channel flow rate $<\dot{m}>$ and its power <Q> can be written as functions of total primary flow rate $<W_p>$ and coolant channel tolerance $<\delta_n>$, and reactor power <P> using the following equations:

$$<\dot{m}>=\frac{<W_p>}{N_c}F_f d_f f_{sf} <\delta_n> \qquad \textbf{Eq. 4-20}$$

where $<\delta_n>=(<\delta>/\bar{\delta})^{1.714}$ is the dimensionless channel flow disparity distribution due to channel gap tolerance. $\bar{\delta}$ is the nominal coolant gap which is 0.746 inches for interior channels and 0.0656 inches for end channels. $<\delta>$ is the coolant gap distribution with nominal distance 0.0746 inches with one standard deviation of 0.00137 inches for interior channels, and nominal distance 0.0656 inches with one standard deviation of 0.00567 inches for end channels.

The channel power < Q > for interior channels:

$$< Q >= \frac{< P >}{N_c} F_{core} F_r F_s$$ **Eq. 4-21**

The channel power for end channels is divided by a factor of 2 to account for the fact that the end channel is a half channel:

$$< Q >= \frac{< P >}{2N_c} F_{core} F_r F_s$$ **Eq. 4-22**

Core inlet temperature can be written as a function of core outlet temperature, reactor power, and total primary flow rate using an energy balance.

$$T_{in} = T_{out} - \frac{< P > F_{core}}{< W_p > c_p}$$ **Eq. 4-23**

Upon combining Eqs. 4-20 through 4-23 with Eq. 4-5, the equation for the safety limit to avoid OFI is derived as follows:

For interior channels,

$$\frac{< P >}{< W_p >} = \frac{c_p (T_{sat} - T_{out})}{F_{core} \left(\frac{F_r F_s}{F_f d_f f_{sf} < R >< \delta_n >} - 1 \right)}$$ **Eq. 4-24**

For end channels,

$$\frac{< P >}{< W_p >} = \frac{2 c_p (T_{sat} - T_{out})}{F_{core} \left(\frac{F_r F_s}{F_f d_f f_{sf} < R >< \delta_n >} - 1 \right)}$$ **Eq. 4-25**

The safety limits are calculated assuming $F_r F_s = 1.677$ for interior channels and $F_r F_s = 1.455$ for end channels (corresponding to the stripe with peak integral power at BOL), $F_f d_f f_{sf} = 0.779$, and $F_{core} = 0.952$.

The water gap δ is assumed to be Gaussian distributed, i.e. $\delta \sim N(0.0746, 0.00137^2)$ (inches) for interior channels, and $\delta \sim N(0.0656, 0.00567^2)$ (inches) for end channels [4-1]. L_h/D_e used to calculate the channel outlet sub-cooling ratio R is a function of δ:

$$\frac{L_h}{D_e} = \frac{L_h P_h}{4 \delta w}$$ **Eq. 4-26**

where L_h is the channel heated length,

P_h is the channel heated perimeter, and

w is the channel width.

Specifically, $L_h/D_e = 0.2564/\delta$ for interior channels and $L_h/D_e = 0.1282/\delta$ for end channels. According to the applicable range of Eqs. 4.6 – 4.8 and the dimensions of coolant channels, < R > is calculated using Eqs. 4-6 through 4-8 for the interior channels, and Eqs. 4-6 and 4-7 for end channels.

Two coolant heights are considered, namely 10 and 6 feet above fuel plates, corresponding to saturation temperatures T_{sat} of 107.4 °C and 105.0 °C, respectively.

The results correspond to three standard deviations of the calculated ratio of reactor power to primary flow, which is obtained by the Monte Carlo sampling-based method. The coolant height is the elevation from the top of the fuel plates to the air/water interface on the top of the core tank. A coolant height of 10 feet corresponds to 4 inches below the overflow level. A coolant height of 6 feet corresponds to 5 inches below the anti-siphon valves. In summary, the safety limits for end channels with < R > calculated using Eq. 4-7 gives the most limiting results (see Figure 4-13). This solution should be adopted as the MITR LEU core safety limits for forced flow operation. The comprehensive results can be found in Ref [4-13].

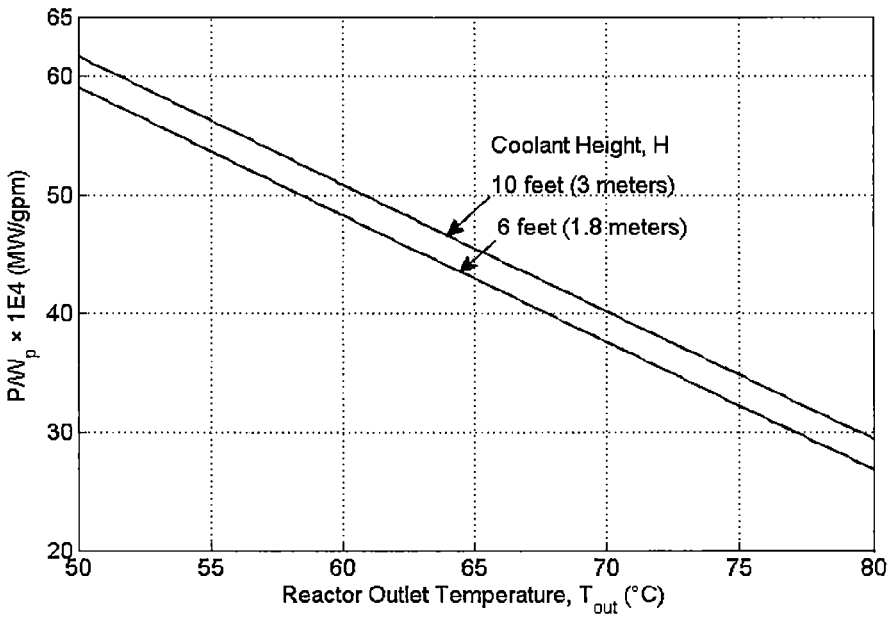

Figure 4-13. Safety limits for forced flow operation

4.6.6.3 Calculation of the Safety Limits for Natural Convection

The safety limit for natural convection operation is calculated using the Sudo and Kaminaga CHF correlation in Eq. 4-27 derived for a zero-flow or blocked-flow condition:

$$q^*_{CHF,2} = 0.7 \frac{A_{XS}}{A_H} \frac{\sqrt{W/\lambda}}{\left[1+(\rho_g/\rho_f)^{0.25}\right]^2} \quad \text{Eq. 4-27}$$

where

$$q^*_{CHF} = \frac{q''_{CHF}}{h_{fg}\sqrt{\lambda g \rho_g (\rho_f - \rho_g)}} \quad \text{Eq. 4-28}$$

$$\lambda = \sqrt{\frac{\sigma}{g(\rho_f - \rho_g)}} \quad \text{Eq. 4-29}$$

Property parameters at saturation temperature T_{sat} = 105.0 °C (corresponding to coolant height H = 6 feet) are used. The dimension parameters of interior channels and end channels are summarized in Table 4-14.

Table 4-14. AXS and AH for interior and end channels

	Interior channels	End channels
A_{XS} (m^2)	1.111×10^{-4}	9.782×10^{-5}
A_H (m^2)	6.013×10^{-2}	3.005×10^{-2}

Substituting all these parameters into Eq. 4-27. The CHF flux for interior channels and end channels under natural convection conditions are calculated to be 4.220×10^4 W/m^2 and 7.434×10^4 W/m^2, respectively. Interior channels are the limiting case, and therefore the corresponding reactor power is then derived accounting for the hot strip factor and axial peaking factor.

$$P = \frac{q''_{CHF}}{F_r F_s F_a} N_c A_H \quad \text{Eq. 4-30}$$

Using the hot strip factor of 1.677 and the axial peaking factor of 1.45 (obtained from the BOL state), the maximum reactor power is calculated to be 595 kW. After considering the uncertainties associated with local power (14%, which is the root mean square combination of an assumed 10% uncertainty in the calculated power distribution, and a 10% uncertainty in the local fuel homogeneity in a 0.5-inch diameter area) [4-1], the reactor power corresponding to a dry-out condition is 457 kW. A reactor power of 400 kW is conservatively adopted as the safety limit, as shown in Table 4-15.

Table 4-15. Proposed safety limits for natural convection operation

Variable	**Safety Limits** (Natural Convection)
Power	400 kW (Max.)
Coolant Height	6 feet above top of fuel plates (Min.)

The core outlet temperature and the coolant height do not affect the natural convection dry-out limit, as long as the core is covered with coolant. The coolant height is conservatively set at 6 feet above the top of the fuel plates to ensure an adequate coolant inventory.

4.6.7 Calculation of the Limiting Safety System Settings

Onset of nucleate boiling (ONB) is chosen as the criterion for the limiting safety system settings (LSSS). This guarantees that boiling will not occur anywhere in the core and that the safety limits will not be approached. The ONB limit is calculated based on the cladding temperature. The following equation needs to be satisfied in order to prevent ONB.

$$T_{clad}(z) \le T_{clad,ONB}(z) \qquad \textbf{Eq. 4-31}$$

where $T_{clad}(z)$ is the cladding temperature at axial location z of a hot stripe, and

$T_{clad,ONB}(z)$ is the predicated cladding surface temperature at which ONB occurs.

$$T_{clad,ONB} = T_{sat} + 0.556\left[\frac{q''}{1082p^{1.156}}\right]^{0.463p^{0.0234}} \qquad \textbf{Eq. 4-32}$$

The axial heat flux distribution of the core hot stripe is given as:

$$q''(z) = \frac{P}{N_f A_H} F_{core} F_{fuel} F_r F_s \theta(z) \qquad \textbf{Eq. 4-33}$$

The cladding temperature can be obtained from energy balance and convective heat transfer equations:

$$T_{clad}(z) = T_{in} + \frac{F_H}{\dot{m} c_p} \int_0^z P_H q''_{hs}(z) dz + F_{\Delta T} \frac{q''_{hs}(z)}{h} \qquad \textbf{Eq. 4-34}$$

P_H is the heat transfer perimeter of a coolant channel. T_{in} is the core inlet coolant temperature and can be written as a function of reactor power and core outlet temperature using the following equation:

$$T_{in} = T_{out} - \frac{P F_{core}}{W_p c_{pf}} \qquad \textbf{Eq. 4-35}$$

Upon combining equations Eq. 4-4 and Eqs. 4-33 through 4-35, and treating reactor power, primary flow, channel mass flow rate, heat flux, and heat transfer coefficient as probability distribution functions and Eq. 4-31 becomes

$$T_{out} - \frac{PF_{core}}{W_p c_{pf}} + \frac{F_H}{\dot{m} c_p} \int_0^z P_H q''_{hs}(z)dz + F_{\Delta T} \frac{q''_{hs}(z)}{h} \le T_{sat}(z) + 0.556 \left[\frac{q''_{hs}(z)}{1082 p^{1.156}} \right]^{0.463 p^{0.0234}} \quad \textbf{Eq. 4-36}$$

The appropriate thermal properties based on the bulk coolant temperature and pressure at each axial location are used to calculate the cladding and ONB temperatures. A coolant height of 10 feet (3 meters) above the top of the fuel plates or 4 inches below overflow provides a head pressure of 1.3 bar.

4.6.7.1 Calculation of the Limiting Safety System Settings for Forced Convection

Interior channel with peak integral power is found to be the most limiting case for LSSS calculation [4-13]. Key parameters in the input file for LSSS determination using MULCH-II are summarized in Table 4-16. Figure 4-14 shows the calculated LSSS for two-loop (i.e., both pumps in service) operation according to Eq. 4-36. Table 4-1 lists the proposed LSSS points for forced convection operation.

Table 4-16. Key input parameters used in the LSSS search

Channel geometry	Interior channel	
Fuel configuration	F-plate (with fuel thickness 0.025 inch)	
Hot channel factor	1.677	
Primary flow	2,200 gpm	
Coolant height	10 feet above the top of fuel plates	
Power distribution	Stripe with peak integral power at BOL	
Engineering hot channel factors	Enthalpy rise	1.173
	Film temperature rise	1.275
	Heat Flux	1.123

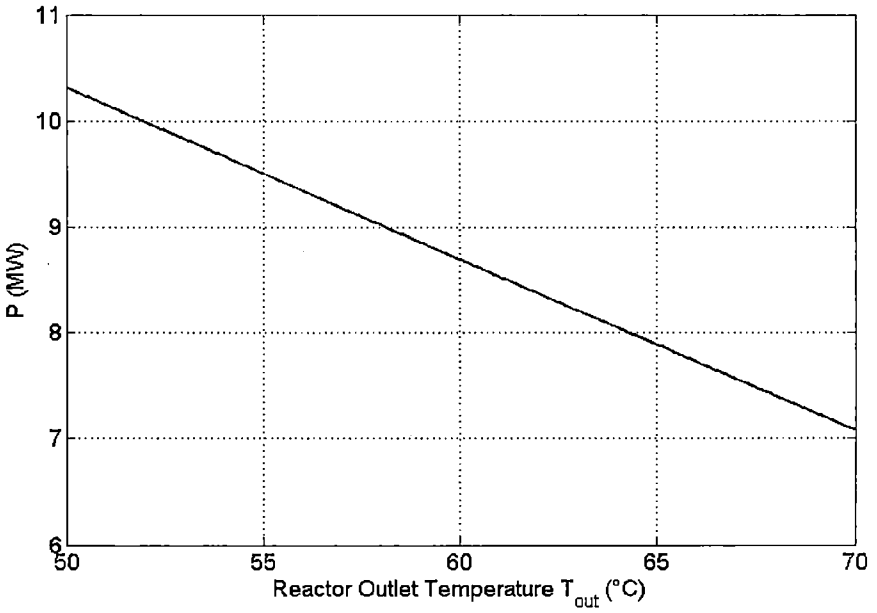

Figure 4-14. MITR LEU core limiting safety system settings for forced flow operation

Table 4-17. Limiting safety system settings for forced convection operation

Parameter	**LSSS (forced convection)**
Power	8.68 MW (Max.)
Primary Coolant Flow	2,200 gpm (Min.)
Steady-State Core Outlet Temperature	60 °C (Max.)
Coolant Height	4" below overflow (Min.), or 10 feet above top of fuel plates

The comprehensive results, including the LSSS search, can be found in Ref [4-13].

4.6.7.2 Calculation of the Limiting Safety System Setting for Natural Convection

The MULCH-II code was used for accident analysis to demonstrate that there is enough ONB margin for natural convection cooling with the remaining reactor power after a loss of primary flow accident at 100 kW. It has been concluded in Ref [4-13] that long-term decay power in the case of P_0 = 5 MW is well below 100 kW. As a result, the natural convection flow rate derived from the 5 MW decay power case will be smaller (i.e., more conservative) than that in the actual case with 100 kW remaining power, and thus the natural convection flow rate was determined in this way. Two cases were considered in the natural convection (i.e. without forced flow) analysis: (1) all 4 natural convection valves (NCVs) and 2 anti-siphon valves (ASVs) open, and (2) only NCVs open. ONB margins are calculated with a maximum natural convection power of 100 kW,

and coolant inlet temperature of 60 °C. The axial power distribution is set to be uniform, which leads to more conservative conditions. The results are listed in Table 4-18.

Table 4-18. Calculated coolant temperature rise and film temperature rise for natural convection operation

		NCV & ASV	NCV only
Flow rate through core (kg/s)		1.81	1.35
T_{in} (°C)		60	60
	$T_{out,max}$ (°C)	86.1	94.6
	$T_{clad,max}$ (°C)	94.2	102.7
T_{ONB} (°C)		108.6	108.6
ONB margin ΔT_{ONB} (°C)		14.4	5.1

Table 4-19 lists the proposed LSSS points for natural convection operation.

Table 4-19. Limiting safety system settings for natural convection operation

Parameter	LSSS (Natural convection)
Power	100 kW (Max.)
Steady-State Average Core Outlet Temperature	60 °C (Max.)
Coolant Height	4" below overflow (Min.), or 10 feet above top of fuel plates

4.6.8 Refueling Considerations

There is no set of pre-planned core configurations for the MITR. Rather, any configuration is acceptable if certain criteria are met. These include:

a) Each of the twenty-seven positions within the core must contain a fuel element, a solid aluminum dummy, or an approved in-core experiment. There should be 24 fuel elements in the equilibrium core (22 in the fresh core).

b) Refueling can be performed by replacement of spent fuel with fresh or partially used fuel, shuffling, rotation, and inversion (flipping) of individual elements to minimize the effect of radial and axial flux gradients.

c) Thermal-hydraulic parameters (including safety limits and LSSS) must not be exceeded for any channel in the core.

d) No fuel element, or any portion thereof, can exceed the fission density limit during the projected operation cycle.

e) The shutdown margin requirement is met. The expected reactivity change for the proposed refueling is calculated. This can be done by comparing the k-effective from

calculations of the core before and after the refueling is done. Alternatively, it could be done by combining estimates of the change in grams of U-235 with the reactivity coefficients given in Section 4.5.2.

f) Items (c) through (e) above are documented and reviewed by someone other than the individual who did the calculations. Each movement of the fuel elements is planned so that only one fuel element is moved at a time.

g) The refueling is performed.

h) The reactivity change is measured and compared to the predicted estimate.

i) The shutdown margin is recalculated using the measured reactivity change. It is again verified to be acceptable.

j) Items (h) and (i) are documented and reviewed.

If any fuel element is to be moved to the spent fuel pool, requirements are imposed to limit decay heat before the fuel transfer to prevent excessive temperature.

References

[4-1] A. Bergeron, E.H. Wilson, G. Yesilyurt, F.E. Dunn, J.G. Stevens, L. Hu, and T. H. Newton, "Low Enriched Uranium Core Design for the Massachusetts Institute of Technology Reactor (MITR) with Un-finned 12 mil-thick Clad UMo Monolithic Fuel", ANL/GTRI/TM-13/15, Argonne National Laboratory, November 2013.

[4-2] K. Sun, Y. Zeng, T. Newton, L. Hu, A. Bergeron, F. Dunn, and E. Wilson, Neutronic and Thermal-Hydraulic Analyses for Conversion of the MIT Research Reactor (MITR) from Highly Enriched Uranium to Low Enriched Uranium using an Unfinned Fuel Element, MIT-NRL-16-01, Rev.1, May, 2016.

[4-3] S.J. Pawel, D.K. Felde, R.E. Pawel, Influence of Coolant pH on Corrosion of 6061 Aluminum Under Reactor Heat Transfer Conditions, ORNL/TM-13083, Union Carbide Corp., Oak Ridge National Lab. Oct. 1995.

[4-4] R.E. Pawel, G.L. Yoder, D.K. Felde, B.H. Montgommery, M.T. McFee, The Corrosion of 6061 Aluminum Under Heat Transfer Conditions in the ANS Corrosion Test Loop, Oxydation of Metals, Vol. 36, 1991.

[4-5] J.C. Griess et al., Effect of Heat Flux on the Corrosion of Aluminum by Water: Part III Final Report on Tests Relative to the High Flux Isotope Reactor, ORNL-3230, Union Carbide Crop., Oak Ridge National Laboratory, Dec. 1961.

[4-6] S. Dinsmore et al., MITR-II Criticality Safety Evaluation of Storage Locations for 510 Gram Fuel Elements, MITR SR# O-80-13, August 11, 1980.

[4-7] MIT-NRL File Memo, Mass of MITR Fuel Elements for HEU and LEU Cores. December 15, 2016.

[4-8] J.R. Weeks, C.J. Czajkowski, and P.R. Tichler, "Effects of High Thermal Neutron Fluences on Type 6061 Aluminum", BNL-46330, 1993.

[4-9] J.T. Hwang, A Study of MITR-II Core Tank Aging for Relicensing Consideration, Course 22.39 Report, MIT NED, December 1992.

[4-10] X-5 Monte Carlo Team, MCNP – A General Monte Carlo N-Particle Transport Code, Version 5, Volume II: User's Guide. April 24, 2003.

[4-11] L.-W. Hu and J. A. Bernard, "Development and Benchmarking of a Thermal-Hydraulics Code for the MIT Nuclear Research Reactor," Proceedings of the ANS Joint International Conference on Mathematical Methods and Super-Computing for Nuclear Applications, pp 1117-1127, Saratoga, NY, Oct. 5-7, 1997.

[4-12] J.A. Bernard, Jr., MITR-II Fuel Management, Core Depletion, and Analysis: Codes Developed for the Diffusion Theory Program CITATION, S.M. Thesis, MIT NED, 1979.

[4-13] K. Sun, Y. Zeng, T. Newton, L. Hu, A. Bergeron, F. Dunn, and E. Wilson, Neutronic and Thermal-Hydraulic Analyses for Conversion of the MIT Research Reactor (MITR) from Highly Enriched Uranium to Low Enriched Uranium using an Unfinned Fuel Element, MIT-NRL-16-01, Rev.1, May, 2016.

[4-14] MITR-Staff, Safety Analysis Report for the MIT Research Reactor, MIT-NRL-13-01, 2013, MIT Nuclear Reactor Laboratory.

[4-15] K. Sun, M. Ames, T. Newton, L. Hu. Validation of a fuel management code MCODE-FM against fission product poisoning and flux wire measurement of the MIT Reactor. Progress in Nuclear Energy, vol. 75: pp. 42-48, 2014.

[4-16] R. H. Whittle and R. Forgan, A Correlation for the Minima in the Pressure Drop Versus Flow Rate Curves for Sub-Cooled Water Flowing in Narrow Heated Channel, Nuclear Engineering and Design, Vol. 6, 1967.

[4-17] Y. Sudo et al., "Experimental Study of Incipient Nucleate Boiling in Narrow Vertical Rectangular Channel Simulating Subchannel of Upgraded JRR-3", J. of Nuclear Science and Technology, 23[1], Jan. 1986.

[4-18] N.E. Todreas and M.S. Kazimi, Nuclear Systems I – Thermal Hydraulic Fundamentals, Hemisphere Publishing, 1990.

[4-19] Y. Sudo and M. Kaminaga, A New CHF Correlation Scheme Proposed for Vertical Rectangular Channels Heated From Both Sides in Nuclear Research Reactors, Journal of Heat Transfer, Vol. 115, May 1993.

[4-20] L. Hu and K. Sun, Parameters Used in LEU Preliminary Safety Analysis Report, MIT-NRL File Memo, December 2017.

[4-21] J. Stillman et al., Accident Analyses for Conversion of the University of Missouri Research Reactor (MURR) from Highly-Enriched to Low-Enriched Uranium, ANL/GTRI/TM-14/5, Revision 1, February 2017.

[4-22] J.H. Rust, Nuclear Power Plant Engineering, Haralson Publishing Co., 1979.

[4-23] K-Y. Chiang, "Thermal hydraulic limits analysis for the MIT Research Reactor low enrichment uranium core conversion using statistical propagation of parametric uncertainties," SM. Thesis, Nuclear Science and Engineering Department, Massachusetts Institute of Technology, 2012.

5.0 Reactor Coolant Systems

There are no changes to Chapter 5 (Reactor Coolant Systems) as a result of LEU conversion **except Section 5.2.1.1, Table 5-1, and Table 5-2**; information on this subject can be found in the current MITR-II SAR.

5.2 Primary Coolant System

5.2.1 Main Flow System

5.2.1.1 Design Bases/Functional Requirements

The primary coolant system can transfer at least 7 MW of heat from the primary to the secondary coolant system with a minimum forced flow of 2,200 gpm and maintain the core free of boiling under steady-state operation. The primary coolant system fulfills several other functions:

a) The coolant pool above the core provides biological shielding for the reactor top.

b) The coolant pool above the core serves as a reservoir of coolant for emergency conditions and for natural circulation cooling

c) The system would slow the escape of fission products and hence serves as a second barrier to fission product release (the fuel element cladding being the first and the containment building being the third).

d) The coolant is also the neutron moderator.

Table 5-1. Primary coolant system design and operation parameters

Parameter		Specification or Range
Material		
Coolant		Light Water
Piping		6061 Aluminum and Stainless Steel
Flow Rate		
Minimum		2,200 gpm
Nominal		2,400 gpm
Temperature		
ΔT at 2,200 gpm		11 °C
ΔT at 2,400 gpm		10 °C
Elevation Above Top of Fuel Plates		
Overflow Line		10.3 ft
Anti-siphon Valves		6.7 ft
Inlet Penetration		6.0 ft
Construction Materials		
Core Tank / Housing		6061 Aluminum
Storage Tank		Stainless Steel
Pressure		
Pump Discharge		17 psig
Top of Core Outlet Plenum		Atmospheric
Chemistry		
pH		5.5 – 7.5
Conductivity		< 5 μS/cm
Chlorides		< 6 ppm
Level		
Nominal		Overflow of Core Tank
Reactor Scram		4" below Overflow

Table 5-2. Calculated coolant temperature rise and film temperature rise for natural convection operation

Parameter	Designation	Function / Setpoint***
Flow	MP-6*, MP-6A*	Scram on low pressure reactor inlet at pressure corresponding to 2,200 gpm or higher
	MF-1*	Scram on low flow at 2,200 gpm or higher
Level	ML-3	Scram on low level at -4 inches below overflow
Temperature	MTS-1**, MTS-1**	Scram on high reactor outlet temperature at 60 °C or lower
	MT-5A**	Scram on high reactor outlet temperature at 60 °C or lower

* Two out of three required
** Two out of three required
*** Value cited is the LSSS

6.0 Engineered Safety Features

There are no changes to Chapter 6 (Engineered Safety Features) as a result of LEU conversion **except Section 6.4**; information on this subject can be found in the current MITR-II SAR.

6.4 Emergency Core Cooling System

A scenario that requires an ECCS for the MITR is not considered credible because the core is contained within two concentric tanks (the primary and reflector tanks) and siphoning is prevented by passive safety features. Specifically, a leak from the core tank itself will result in mixing of the light-water coolant and heavy-water reflector and not in a major loss of coolant from the core tank. Also, the helium vent lines at the top of the reflector tank and above the reflector level sight glass are designed to prevent the possibility of siphon action and hence to limit the loss of water to the level of the primary coolant inlet and outlet pipes. (See Section 13.2.3.2 of this report.) Similarly, a rupture of the primary inlet piping would not cause a major loss of coolant because the anti-siphon valves would stop the siphon effect and stop the coolant loss at 1.8 m (6.0 ft) above the top of the fuel plates. For both cases, natural convection cooling is sufficient to remove the decay heat from the core region with a pool of water remaining above the core. A complete loss of coolant accident requires one of the following incredible scenarios:

a) A simultaneous rupture of the core tank and the reflector tank.

b) A rupture of the inlet pipe below the core level, together with a failure of both anti-siphon valves to open.

c) A core tank puncture caused by an explosion at one of the beam port reentrant thimbles that extend inward from the reflector tank. (See Section 13.2.3.3 of this report for analysis of this scenario.)

A detailed description of the ECCS is given in Section 5.2.5 of the MITR-II SAR [6-1] and the schematic of the primary coolant system (i.e., Figure 5-1) includes a diagram of the ECCS. To summarize, there are two independent subsystems, each with its own spray nozzle. Water for the system is available from either of two sources: city water or the primary storage/makeup water tanks. The possible lineups are:

a) City Water: Flow is initiated by use of either of two quick-connect hoses, each with special couplings and a pair of valves. The source of the flow is city water pressure. No pump is needed. There are two possible initiation points for this flow. One is in the reactor control room. The other is at a location outside the containment building. Hence, it is possible to initiate ECCS without entry to the reactor building. (Note: The use of the quick-connect hoses minimizes the potential for the inadvertent introduction of chlorinated water to the core tank during normal operation. It also protects against the mixing of primary coolant with potable water. However, that scenario is already precluded because all water supplied to the containment building first passes through a backflow preventer.)

b) Storage Tanks: Flow is initiated using the primary coolant system's auxiliary pump, MM-2. Water would be drawn from the primary storage tank which would in turn be replenished from the makeup water tank.

The ECCS system is redundant in that flow through either of the two nozzles is sufficient to protect the core. The spray nozzles are located above the core and are positioned such that each fuel element will receive at least 20% of the average flow. A series of full-scale out-of-core mockup tests were performed for various in-core experiment configurations. Results showed that the 20% average flow criterion was met for the current nozzle design [6-2].

The emergency spray system is normally lined up to the city water system, which is the preferred supply. It must be revalved in order to use the other source of supply.

Calculations were performed to analyze the capacity of the ECCS spray system for the MITR. The system design is based on the initiating event being an experiment malfunction in one of the beam ports, which causes a break of 2.5 inches (63.5 mm) ID in the core tank. This analysis includes the following:

a) The estimated time to drain the core tank was calculated using the Bernoulli equation.

b) The decay heat at the time of drainage was calculated using point depletion code ORIGEN-S in SCALE 6.1 package [6-3]. It was assumed that the reactor had been operating at 7.35 MW with 4,200 MWD fuel depletion. It is also assumed that 93.2% of the decay power is deposited in the fuel [6-4]. The remaining 6.8% is deposited in the reflector and biological shield.

c) A check was made to determine if the decay of activated aluminum would contribute to the heat load.

d) An evaluation of the flooding limit was made to ensure that the cooling was adequate.

A 20% flow distribution factor was used to take into account the minimum flow into each element. A safety factor of 1.5 was conservatively adopted to ensure an adequate safety margin. Thus,

$$\dot{m}_{design} = \frac{1}{20\%} \times 1.5 \times \dot{m}_{calculated} \qquad \textbf{Eq. 6-1}$$

where $\dot{m}_{calculated}$ is the calculated flow rate to remove decay heat by evaporation from the average channel, and $\dot{m}_{design}$ is the design flow rate.

It was determined that the time to drain the core tank was 411 seconds (starting from 4 inches below overflow). The power produced from decay heat 300 seconds after scram is 186.2 kW. The decay power from aluminum activation by the fast neutron flux was found to be negligible (0.2 W). The ECCS design flow rate was thus 9.5 gpm [6-5].

To assure that this design flow rate was capable of cooling the fuel, the flooding limit was also analyzed. Flooding refers to the stalling of a liquid downflow by a sufficient rate of gas upflow

[6-6]. The spray will not be able to enter the hot channel if the flooding limit is exceeded (i.e., predicted hot channel vapor flow rate greater than that of the flooding condition). The calculated result showed that the vapor velocity in the hot channel was lower than that of the flooding limit by a factor of four.

The effect of a non-uniform flow distribution within a fuel element was also evaluated. This calculation assumed that one of the fuel plates was not wetted by water and that the only effective heat removal path was conduction to the side plate, which is cooled by the flow in the adjacent channels. The calculation assumed that, for the worst case, the flow rate in the adjacent channels was 20% of the average flow. The calculated maximum fuel centerline temperature was about 253.2 °C, which is far below the fuel temperature safety limit of 350 °C presented in Chapter 13.

References

[6-1] MITR-Staff, Safety Analysis Report for the MIT Research Reactor, MIT-NRL-13-01, 2013, MIT Nuclear Reactor Laboratory.

[6-2] Modification of Emergency Core Cooling System Spray Nozzles, MITR Safety Review #0-94-3, 1994.

[6-3] SCALE Official Website: http://scale.ornl.gov/

[6-4] K. Sun, Y. Zeng, T. Newton, L. Hu, A. Bergeron, F. Dunn, and E. Wilson, Neutronic and Thermal-Hydraulic Analyses for Conversion of the MIT Research Reactor (MITR) from Highly Enriched Uranium to Low Enriched Uranium using an Unfinned Fuel Element, MIT-NRL-16-01, Rev.1, May, 2016.

[6-5] K. Sun, File Memo, MITR ECCS Cooling Calculations for 7 MW LEU (19B25) Core, MIT Nuclear Reactor Laboratory, 2016.

[6-6] N.E. Todreas and M.S. Kazimi, Nuclear Systems (I) - Thermal Hydraulic Fundamentals, Hemisphere Publishing Corp., 1990.

7.0 Instrumentation and Control Systems

There are no changes to Chapter 7 (Instrumentation and Control Systems) as a result of LEU conversion **except Sections 7.2.2.1, 7.2.2.2, 7.4.1, 7.4.2, 7.6.2**; information on this subject can be found in the current MITR-II SAR.

7.2 Design of Instrumentation and Control System

7.2.2 Design Basis Requirements

7.2.2.1 Reactor Control System

The Reactor Control System (RCS) has two modes: manual and automatic. The manual mode is used for both transient operation (startup, power-maneuvering, shutdown) between source range and full power (7 MW), and steady-state operation. The automatic mode is normally used only for steady-state operation at power levels in excess of 10 kW. Manual control allows the console operator to manipulate all control devices (six shim blades and the regulating rod). Under automatic control, only the regulating rod is moved. Certain safety features are designed into the system. These are (1) that only one shim blade can be withdrawn at a time, (2) that the shim blades can be dropped for a scram from any position of travel, (3) that the shim blades may be run in simultaneously at normal speed, and (4) that the console operator can take manual control at any time simply by moving the control switch for the regulating rod. There are a number of interlocks associated with the RCS:

a) Startup Interlocks: A reactor startup cannot be initiated unless certain prerequisites are met. This is done to ensure that operating conditions are stable prior to a startup, even though some of these conditions need not be met continuously during actual operation. The prerequisites are that all scrams are reset, that all control devices are fully inserted, that the core and reflector tanks are at overflow, and that the building differential pressure is below its setpoint. Once all conditions are met, a "reactor start" pushbutton is depressed. This bypasses all of the preceding except the scram reset requirements and allows withdrawal of the control devices.

b) Subcritical Interlock: This interlock applies to the shim blades. In order for any blade to be withdrawn above five inches, all blades must first be at five inches. The purpose of this interlock is to ensure that the shim blades are at a uniform bank height prior to the final approach to criticality.

c) Automatic Control: The MITR cannot be placed or maintained on automatic control unless certain criteria are met. These are that all shim blades be above the subcritical interlock position, that the deviation between the power setpoint and the actual power be less than 1.5%, that the regulating rod control switch be in the neutral position, and that the regulating rod be above its near-in position. Once on automatic control, failure to meet any of these conditions causes a transfer to manual control and an alarm.

d) Automatic Rundown: This interlock causes a shim blade to be inserted at its normal speed if the reactor is on automatic control and if the regulating rod reaches its near-in position. This scenario could occur if xenon were being burned out as the result of a

startup following a brief shutdown. The concern is that if the operator did not reshim the control devices, power would rise because the automatic controller could not compensate by driving the regulating rod in any further as xenon poisoning continued to decrease.

Readouts from instruments associated with the RCS are located on the reactor console. These include indication of reactor power from a fission chamber and hence accurate from the source range to full power, indication of reactor period, and a differential galvanometer that shows the deviation from a power setpoint. Also located on the console are the shim blade selector switch, control switches for both the shim blades and regulating rod, the automatic control setpoint switch, and the automatic control transfer pushbutton.

The console is also equipped with controls to shut the reactor down. These are the all-rods-in pushbutton, a minor scram pushbutton, a major scram button, the reflector dump switch, and the reflector dump air-bleed valve. The minor scram causes all blades to drop into the core. The major scram does that and it also causes building isolation and dumps the reflector. The reflector dump switch de-energizes the solenoid that keeps the dump valve closed. The reflector dump air-bleed valve interrupts the air supply that keeps the dump valve closed. Further information on these shutdown features is given in Section 7.3.2.4 of this report.

7.2.2.2 Reactor Protection System

The purpose of the RPS is to ensure that the limiting safety system settings are not exceeded as the result of transients of the type discussed in Chapter 13 of this report. The principal parameters of concern are the reactor period, the reactor power, the primary coolant flow, the coolant outlet temperature, and the core tank level. In addition to these signals, the RPS also monitors many other process system parameters such as the reflector and shield coolant flow, the status of the personnel lock gaskets, and the status of the upper grid plate's latch mechanism. A complete list is given in Section 7.3.1.1 (Table 7-1) of the MITR-II SAR.

The setpoints at which RPS action activates are well within the envelope of the limiting safety system settings. This conservative approach provides further assurance that a safety limit will not be approached. For example, the normal operating power level is 7.0 MW. The scram is set at 7.7 MW, the Limiting Safety System Setting is 8.7 MW, and the Safety Limit is 10.6 MW.

The LSSS and safety limit are calculated for a primary coolant outlet temperature of 60 °C, a primary coolant flow of 2,200 gpm, and a primary coolant height of 10 feet.

The MITR can operate under either forced or natural convection. Accordingly, the RPS also has two modes. The standard mode is forced convection. All scram circuits are active and at their normal values. For natural convection heat removal, the maximum allowed power is 100 kW. Accordingly, two of the three amplifiers that provide a scram on power level are replaced with units that contain additional amplification. This allows the power level scram setpoint to be reset to a value that is consistent with the maximum allowed power for natural convection heat removal. Once these low-range amplifiers are installed, the primary flow scrams may be bypassed.

The RPS is both redundant and diverse as noted in Section 7.2.1 of the MITR-II SAR.

7.4 Reactor Protection System

7.4.1 Nuclear Safety System

The nuclear instrumentation system for the MITR consists of nine neutron or gamma flux monitoring channels. Each channel consists of a detector, high voltage and signal cabling, an output display device, and associated alarm, scram, or control circuitry. Channels 1 and 2 are used as startup channels, and with channel 3, have associated scram trips at a period of 10–11 seconds. Channels 4, 5, and 6 are used as power-range channels and have high flux scram trips corresponding to a reactor power level of 7.7 MW as determined by correlating the previous equilibrium value of each detector's output with the thermal power. These six instruments comprise the reactor's nuclear safety system. Channels 7 and 8 are part of the control/console display instrumentation system. Channel 7 provides a linear indication of the flux level, and channel 8 provides a flux indication if electrical power is lost. Channel 9 is part of the reactor control system. It provides a signal to the automatic control circuit.

All neutron detectors are mounted in either instrument ports or vertical thimbles. The detectors monitor the leakage flux in the reflector region. The degree of overlap between the channels from source range to full power operation is shown in a bar chart in Figure 7-3 of the MITR-II SAR.

Power to all nuclear instrumentation channels except channels 3 and 8 is supplied as unregulated voltage from loads L21/L22 via Panel 1. (See Figure 8-1 of the MITR-II SAR). These loads are supplied by emergency power in the event of a loss of the off-site electrical power. Channels 3 and 8 are supplied by their own self-contained power supplies and do not depend on either off-site or emergency electrical power for operation.

7.4.1.1 Period Channels

Channels 1 and 2 are of the same design and are interchangeable. Each uses a fission chamber and an uncompensated ion chamber as the neutron sensing elements. The fission chamber is operated as a pulsed counter in the source range to provide visible neutron level indication at reactor startup. The uncompensated chamber is operated in the power range once the fission chamber saturates after a four-decade power increase.

The output pulses from the fission chamber are amplified by a preamplifier and are then fed to a logarithmic count-rate amplifier. This amplifier first converts the pulses into a d.c. signal that is proportional to the counting rate and then amplifies the d.c. signal in a logarithmic manner. The output is indicated on a meter on the amplifier chassis and on a duplicate console-mounted meter that displays either channel 1 or 2 level as selected by the console operator. A differentiating circuit in the amplifier chassis is used to derive reactor period that is indicated on a meter on the amplifier chassis and on a duplicate console-mounted meter that displays either channel 1 or 2 period as selected by the operator. The channel output may also be recorded on a strip chart recorder that monitors channel 1, 2, or 3 as selected by the operator.

The d.c. output signal of the period-deriving network is fed to a scram amplifier as part of the nuclear safety system. Each of channels 1 and 2 has an associated safety system scram initiated by its associated scram amplifier at a period between 10 and 11 seconds.

When the fission chambers saturate at the end of their four-decade range following startup, the channel is switched over to the uncompensated ion chamber. The two fission chambers are physically connected to the channel at all times and change-over is accomplished by turning down the gain on the fission chamber. This removes the fission chamber component of the signal, leaving the ion chamber, whose signal has just come on scale, as sole input to the channel. The change-over process is coordinated so that there are two operable period channels available at all times.

Channel 3 uses an uncompensated ion chamber, the output of which is fed directly to a logarithmic amplifier. The output is indicated on a meter in the amplifier chassis and on a duplicate console meter. A differentiating circuit in the amplifier chassis is used to derive reactor period with the output displayed on a meter in the amplifier chassis and on a duplicate console meter. The d.c. output of the period network is fed to a scram amplifier as part of the nuclear safety system. Channel 3 provides a safety system scram initiated by its associated scram amplifier at a period between 10 and 11 seconds. Power to channel 3 is supplied by a replaceable gel cell battery pack. A console meter displays a signal proportional to channel 3 chamber voltage.

A redundant scram has been added to the three period channels (1, 2, and 3) to ensure that the minimum number of channels monitoring reactor period will be on line and functional. The reactor will scram if two or more of the three period channels are off-scale, in any combination of high or low, simultaneously.

7.4.1.2 Level Channels

Channels 4, 5, and 6 use uncompensated boron-lined ion chambers as the neutron sensing elements. The positive d.c. current output of each channel is fed directly to an associated scram amplifier with the magnitude of the output current indicated on an edgewise meter on the front of the amplifier chassis. Each high flux trip is set to provide a reactor scram at a detector output for that channel that corresponds to a reactor power of 7.7 MW.

7.4.1.3 Natural Convection Operation

There are two low-range amplifiers for use when the reactor is to be operated in the natural convection mode or when certain procedures such as refuelings or blade absorber changes are performed that require work in the core tank. The low-range amplifiers allow the primary system pressure scrams on MP-6 and MP-6A to be bypassed with key switches. These amplifiers are more sensitive than the high range amplifiers because their entire range of operation is only one-twentieth that of the full-range amplifiers.

7.4.1.4 Scram Amplifier Operation

Separate scram amplifiers associated with each of the reactor period and level monitoring channels provide a scram capability for the nuclear safety system in the event of a short reactor period or a high neutron flux level. In the case of the period-monitoring channels, a derived positive d.c. signal that is proportional to inverse period is fed to the scram amplifier. In the case of the flux level channels, the positive d.c. chamber output current is fed directly to the scram amplifier.

The principle of operation of the scram amplifiers is that the positive d.c. input current is compared with a negative d.c. reference current with both the input signal and the reference current being indicated on edgewise meters on the front panel of the amplifier. The differential current produced provides a bias to control the gating operation of a field effect transistor (FET). The bias signal is positive (channel input less then reference current scram trip) during normal operation, and the FET will remain on, allowing a small-amplitude, high-frequency a.c. source signal to pass to an amplification and rectifying circuit where it is changed into a d.c. current to energize the shim blade electromagnets.

Each scram amplifier directly controls the power supply to its corresponding shim blade magnet (channel 1 supplies shim blade 1, etc.) and to two separate scram relays. The amount of current supplied to each magnet is controlled by a potentiometer and is displayed on an edgewise meter mounted on the face of the corresponding scram amplifier. When the positive d.c. input signal reaches the same level as the negative d.c. reference scram setting, the FET bias drops to zero thereby shutting the FET off. This stops the flow of high frequency a.c. to the d.c. rectifier network. This in turn cuts off d.c. current to the corresponding magnet, drops the associated shim blade, and de-energizes the two downstream d.c. powered scram relays. One relay cuts off all power to the paired magnet power supply (blade No. 4 for channel 1, etc.), and drops that shim blade, while the other relay opens the withdraw permit circuit thereby dropping the remaining shim blades. As a secondary action, when the withdraw permit circuit opens, the rundown relays de- energize and drop out. This causes all six shim blade drives and the regulating rod drive to be driven to their full-in positions.

7.4.2 Non-Nuclear Safety System

Table 7-2 lists the scrams associated with operation of the MITR. The instruments associated with the non-nuclear scrams are described here.

a) Low Pressure Reactor Inlet: MP-6 and MP-6A are both Bourdon tube pressure gauges that measure the primary coolant static pressure in the inlet plenum of the light-water core tank. This pressure correlates with primary coolant flow and hence MP-6 and MP-6A are protection against a loss of coolant flow.

b) Low Flow Primary Coolant: MF-1 is a flow nozzle that is mounted in a straight section of the primary piping. A strain gauge circuit that is coupled to the differential pressure transmitter's diaphragm provides a signal proportional to the pressure drop across the nozzle. The flow rate is proportional to the square root of this pressure drop (Bernoulli equation). Both the MF-1 and the MP-6/6A scrams are set above the LSSS of 2,200 gpm.

c) Low Level Core Tank: ML-3 is a float switch that is mounted within the core tank. ML-3 causes a scram if the coolant level drops four inches below overflow.

d) High Temperature Reactor Outlet: MTS-1 andMTS-1A are thermocouples. Both measure the temperature of the coolant as it exits the core tank.

e) High Temperature Reactor Outlet Recorder: MT-5A is a platinum resistance temperature detector (RTD). It is mounted in the primary piping at the suction of the primary coolant pumps. MT-5A, MTS-1, and MTS-1A are all set to scram below the LSSS of 60 °C.

f) Low Flow D2O: DF-1 is an orifice plate that generates a signal using the same principal as MF-1. DF-1 causes a scram above the minimum required value of 75 gpm.

g) Low Level D2O Reflector: DL-6 is an insulated stainless steel conductance probe that is mounted in the reflector's overflow line. DL-6 causes a scram if the reflector level drops four inches below overflow.

h) Low Flow Secondary: HF-1 is an orifice plate that generates a signal using the same principal as MF-1. HF-1 and HF-1A scrams on low flow, although this is not required by the technical specifications.

i) Low Flow Shield Coolant: PF-1 is an orifice plate that generates a signal using the same principal as MF-1.

j) Low Pressure Shield Inlet: PPS-1 is a Bourdon-tube pressure switch that measures the pressure at the discharge of the shield coolant pump. This pressure corresponds to the shield flow. Both PF-1 and PPS-1 cause a scram above the minimum required value of 50 gpm.

k) Building Overpressure: XPS-3 is a pressure switch that measures the differential pressure between the reactor control room and the atmosphere. It causes a scram below the maximum allowed value of 3 inches of water.

l) Hold-Down Grid Unlatched: In order to latch the grid, it is necessary to reset a mechanical switch. If the grid becomes unlatched, the switch opens and causes a scram.

Table 7-2. List of Reactor Scrams

Scram Condition	Scram Setpoint
Withdraw Permit Circuit Open*	Minor, major, or medical facility scram pushbutton depressed Key switch off Dump valve open
Nuclear Safety System Scram Period Power	 ≥ 7 sec ≤ 7.7 MW
Period Channel Level Signal Off-scale	Less than two period channel level signals on scale
Low Pressure Reactor Inlet, MP-6, MP-6A	Pressure corresponding to > 2,200 gpm
Low Flow Primary Coolant, MF-1	⩾ 2,200 gpm
Low Level Core Tank, ML-3	≥ -4 inches
High Temperature Reactor Outlet, MTS-1, MTS-1A	≤ 60 °C
High Temperature Reactor Outlet, MT-5A	≤ 60 °C
Low Flow D2O, DF-1	≥ 75 gpm

Low Level D2O Reflector, DL-6	≥ -4 inches
Low Flow Secondary, HF-1, HF-1A	≥ 400 gpm
Low Flow Shield Coolant, PF-1	≥ 50 gpm
Low Pressure Shield Inlet, PPS-1	Pressure corresponding to ≥ 50 gpm
Building Overpressure, XPS-3	≤ 3" water above atmospheric
Main Personnel Lock Gaskets Deflated	Both gaskets deflated
Basement Personnel Lock Gaskets Deflated	Both gaskets deflated
Hold-Down Grid Unlatched	Grid unlatched
Low Flow Fission Converter	≥ 45 gpm (forced circulation mode only)
Low Level Fission Converter	≥ 2.1 meters (forced circulation mode) ≥ 2.5 meters (natural circulation mode)
High Power Fission Converter	≤ 20 kW (natural convection mode only)
Remote Scram Pushbutton Depressed	
Seismic Scram	
City Water Pressure	< 10 psig for more than three minutes
Ion / Fission Chamber Power Supplies	
Core Purge Flow	< 2.5 cfm for more than two minutes
Experimental Scrams Trip	

* The withdraw permit circuit open alarm activates on all scrams. For the conditions listed here it will be the only indication of the scram.

7.6 Control Console Display Instruments

7.6.2 Channel 8

This channel utilizes an uncompensated ion chamber as its neutron-sensing element. Its principal function is to provide an indication of the reactor power level when off-site electrical power has been lost. In addition, it provides a backup to the linear flux channel when the reactor is above a few kilowatts and it provides an alarm if the reactor power exceeds its setpoint.

All power required by channel 8 is supplied by a battery mounted in the back of the control console in the control room. A trickle charger, which keeps a constant voltage across the battery, maintains the battery at full charge. The battery level for channel 8 can be read on the rear of the console. The high voltage required to operate this chamber is supplied by means of a d.c. to d.c. voltage converter. The output current of the chamber is fed to a linear scale microammeter and to a meter relay. The microammeter provides power indication above a 500 kW threshold level. A signal taken from this meter is fed to a log range digital picoammeter. This picoammeter has seven pushbutton-controlled range switches that provide a digital output indication from 0.1–100% power.

The meter relay is used to provide a high level alarm that is set at a power level above the operating point (7.0 MW) and below the scram setpoint (7.7 MW) by comparing the previous

channel 8 equilibrium value (steady-state conditions) with the equilibrium thermal power (calorimetric result).

8.0 Electrical Power Systems

There are no changes to Chapter 8 (Electrical Power Systems) as a result of LEU conversion; information on this subject can be found in the current MITR-II SAR.

9.0 Auxiliary Systems

There are no changes to Chapter 9 (Auxiliary Systems) as a result of LEU conversion **except for Section 9.5.2** where upon converting to LEU the expectation is that authorization for the possession of U-235 will be updated based on more detailed transition plans to be analyzed prior to conversion.

10.0 Experimental Facilities and Utilization

There are no changes to Chapter 10 (Experimental Facilities and Utilization) as a result of LEU conversion; information on this subject can be found in the current MITR-II SAR.

11.0 Radiation Protection and Waste Management

There are no changes to Chapter 11 (Radiation Protection and Waste Management) as a result of LEU conversion **except Section 11.2.3**; information on this subject can be found in the current MITR-II SAR.

11.2 Radioactive Waste Management

11.2.3 Release of Radioactive Waste

The release of radioactive waste is described in Section 11.2.2 of the MITR-II SAR. In summary, airborne releases are primarily through the ventilation system exhaust stack. Continuous air monitoring is coupled with sample analysis. Automatic actions for containment isolation based on signal input from the plenum effluent monitors ensure that no releases would exceed any established limits. The sample analysis verifies the isotopic distribution and concentrations of the releases as measured by the effluent air monitoring system. Liquid wastes, which are discharged to the sanitary sewer, use a discharge permit process which requires sampling and continuous monitoring during the discharge process. This ensures that the discharge is in accordance with the provisions set forth within 10 CFR 20. Solid wastes are transferred to designated burial sites and all wastes are prepared for transfer and disposal in accordance with 10 CFR 61.

Annual reports filed in accordance with the MITR Technical Specifications have demonstrated that all releases and waste generation are within limits and that ALARA provisions are met. The increase in reactor power from 6 MW to 7 MW is expected to result in a 17% increase for airborne releases. This level is still maintained well below allowable limits. Releases via the sanitary sewer and for transfer to a licensed facility for disposal should not increase proportional to the power level increase and are maintained within applicable regulatory requirements.

12.0 Conduct of Operations

There are no changes to Chapter 12 (Conduct of Operations) as a result of LEU conversion; information on this subject can be found in the current MITR-II SAR.

The future updated LEU SAR will contain material as an appendix that details start-up testing and fuel management transition plans based on analysis that will be performed and submitted for regulatory review prior to conversion.

13.0 Accident Analysis

13.1 Accident-Initialing Events and Scenarios

A summary is provided here of accident-initiating events. Analysis of these events and determination of consequences is given in Section 13.2 of this report. One of the events listed below, the Maximum Hypothetical Accident, involves a scenario that causes fuel damage. None of the other events that are listed below result in core damage.

13.1.1 Maximum Hypothetical Accident

The maximum hypothetical accident (MHA) for the MITR is postulated to be a coolant flow blockage in the fuel element that contains the hottest fuel plate. It is assumed that the entire active portion of five LEU fuel plates melts [13-1, 13-2]. This accident could occur if a foreign object were to fall into the core tank and be undetected. In order to cause damage, the object would have to fall through the lower grid plate. This could only occur during a refueling when an element position was open. Fuel element nozzles have multiple openings to allow coolant flow. For the foreign object to block flow to the fuel plates, it would have to pass through one opening, thus putting an effective size limit on the object. Hence, a maximum of only five plates would be affected. If this accident were to occur, the following indications, automatic protective actions, and corrective actions would occur:

a) Boiling might occur in the blocked channels. If so, the formation and collapse of vapor bubbles would create noise that should be observed on the linear flux channels. MITR operators are directed by procedure to lower reactor power if this is observed.

b) If power is not lowered, then melting of the fuel plates is postulated to occur. Fission product gases would be detected by the core purge monitor that provides an alarm in the control room. MITR operators are directed by procedure to shut the reactor down if elevated core purge radiation levels exist.

c) If reactor operation were continued, the fission product activity would be merged with the building exhaust ventilation. The plenum radiation monitors would become elevated and alarm. Building ventilation would be tripped and the ventilation dampers would close, thereby sealing the building and stopping any release.

d) If the main ventilation dampers failed to close, the auxiliary intake and exhaust ventilation dampers would close, thereby sealing the building and stopping any release.

To summarize, there would be at least three distinct indications to the console operator for this accident. These are noise on the linear flux channels, elevated core purge radiation levels, and elevated plenum effluent monitor levels. In addition, an engineered safeguards feature, the plenum monitor building isolation interlock, would automatically stop the release even if the operator failed to act.

13.1.2 Insertion of Excess Reactivity

Damage to the core from this type of accident is not considered credible because of both administrative controls and reactor design features. Initiating scenarios are:

a) Step Reactivity Insertion: An initiation event could be the failure of an in-core sample assembly or ICSA. For example, an ICSA thimble could fail open and the force of the coolant could lift the sample out of the facility thereby inserting positive reactivity. The MITR is protected against this type of occurrence by (1) careful design of all such facilities and (2) limitations on the allowed reactivity worth of all ICSA samples. Thus, even if an ICSA failed, the consequences could not create a step reactivity insertion greater than the maximum allowed.

b) Ramp Reactivity Insertion: An initiating event could be the overspeed of a shim blade drive. The MITR is protected against this type of occurrence as follows:

   (i) During normal operation, the shim blade speed is locked to the frequency of the electric power grid. Operation at other than the design speed is not possible.

   (ii) During the performance of digital control experiments, shim blade speed can be varied up to a maximum. Protection against overspeed is provided by use of a special trip on reactor period and the careful design of all such experiments.

13.1.3 Loss of Primary Coolant

Damage to the core from this type of accident is not considered credible because the core is contained in two concentric tanks, both of which would have to fail to cause a complete loss of primary coolant. In addition, the reactor is equipped with an emergency core cooling system that would provide cooling to the fuel elements if a complete loss of coolant were to occur. Initiating scenarios are:

a) Break of Primary Coolant Piping: This is unlikely given the design of the piping. Were it to occur, the core would be unaffected because the reactor would scram on low primary flow and the anti-siphon valves would open to prevent the siphoning of coolant from the core tank.

b) Break in Core Tank: The core would remain covered because the reactor is contained in two concentric tanks, the light-water core tank and the heavy-water reflector tank. Light water and heavy water would mix and cause a negative insertion of reactivity.

c) Sample Malfunction in Proximity to Core Tank: Administrative procedures are implemented to exclude samples that could cause any damage to the core tank during an irradiation.

13.1.4 Loss of Primary Coolant Flow

Damage to the core from this type of accident is not considered credible. A loss of primary coolant flow could (and has) resulted from a loss of normal electrical power and/or a failure of a

primary coolant pump. Both events cause the reactor to shut down automatically and natural convection cooling is established and removes the decay heat.

13.1.5 Mishandling or Malfunction of Fuel

Mishandling of fuel is unlikely because of the careful design of the fuel handling tools and because of written schedules that are followed whenever fuel is to be handled. Incipient fuel element cladding failures have occurred during normal reactor operation. They are quickly detected by the core purge monitoring system. The corrective action is to shut the reactor down, to identify the fuel element in question, and to remove it from the core. This action occurs well before any 10 CFR 20 limit is approached.

13.1.6 Experiment Malfunction

Damage to the core from this type of accident is not considered credible because of the careful design of all in-core experiment facilities and the administrative limits imposed on all experiments, in-core and ex-core.

13.1.7 External Events

Damage to the core from external events (lightning, floods, meteorological disturbances, and seismic events) is not considered credible because the core is contained within two concentric tanks and a full containment building.

13.1.8 Mishandling or Malfunction of Equipment

Damage to the core from accidents of this type is not considered credible because of the reactor's passive safety features. The reactor is designed so that instrument or equipment failures generally result in a reactor shutdown. In addition, strict administrative and procedural controls are implemented for situations for which it is not possible to devise interlocks and/or a fail-safe response.

13.2 Accident Analysis and Determination of Consequences

The MITR is one of a number of research reactors that are operated across the United States by universities, government laboratories, and private industry. Research reactors constitute a distinct class of reactor. Other classes are test, power, military, and spacecraft. Each reactor class is subject to certain restrictions on its design and operation. For research reactors, these are that the power level be no more than 10 MW, that in-core experiments have a cross-sectional area of less than sixteen square inches, and that there be no fueled loops. These restrictions result in a type of reactor that is suitable for siting on university campuses where they can be used for both teaching (physics laboratories, reactor physics demonstrations, radiological health education, etc.) and research (nuclear medicine and cancer therapy, identification of air pollutants, archaeological studies, etc.).

In addition to the above noted general characteristics of research reactors, the MITR has several other features that greatly limit its potential for creating accidents, especially accidents with off-site consequences. These are:

a) The fuel alloy behaves stably and predictably under irradiation, and maintains a lattice of nanobubbles under the conditions where MITR operates. These retain fission product gases. Hence, should there be a cladding failure, the fission product gas must diffuse through the fuel grains and to the breach in order to escape.

b) The reactor core is contained within a closed primary system. This system is not airtight, but it would retard the release of fission products should there be a cladding failure. (See Sections 4.3 and 5.2 of the MITR-II SAR.)

c) The entire reactor is contained in a gas-tight containment building that is sealed automatically should effluent radiation levels be abnormal. (See Section 6.5 of the MITR-II SAR.)

The absence of a significant source term, the lack of a driving force for fission product release, the use of a stable fuel form, the presence of a closed primary system, and the use of a full containment minimize the potential for any accident at the MITR to have off-site radiological consequences.

13.2.1 Maximum Hypothetical Accident

The maximum hypothetical accident (MHA) for the MITR is postulated to be a coolant flow blockage in the fuel element that contains the hottest fuel plate. This could occur as the result of some foreign material falling into the core tank during a refueling. After the primary pumps are started, the object would be swept from the bottom of the tank up to the fuel element nozzle so that flow to the fuel plates was obstructed. In order for this to happen, the foreign material would have to fall through the lower grid plate. This could only occur during a refueling, when a fuel element was removed so that the corresponding position was open. The size of the openings in the lower grid plate would restrict the dimensions of the foreign object to those of a fuel element nozzle. Coolant can pass through either a nozzle's end or side openings. Hence, the foreign object could not block all coolant flow through the nozzle. However, if the material were small enough to enter the triangular entrance in the nozzle, it might possibly block the flow to a maximum of six coolant channels (seven LEU plates). Because the two fuel plates on the outer regions of the blocked area will be cooled from one side, the only melting that might occur would involve the inner five fuel plates. It is conservatively assumed that all six coolant channels are blocked and that the entire active portion of the five associated plates melts completely. This is a very conservative assumption because the coolant channels can only be partially blocked because of the geometry of the nozzle. Experience with fuel plate melting both at the Materials Testing Reactor (MTR) and at the Oak Ridge Research Reactor has shown that fuel plate melting because of flow blockage does not propagate beyond the affected flow channels. Although nearby plates were discolored, cooling by the unaffected channels was sufficient to prevent propagation of the melting [13-3, 13-4].

An analysis of fission product release and radiation dose to the off-site population was previously performed by Mull for the MITR-II [13-5]. That analysis was redone by Li both for higher reactor powers and with an updated source term [13-6]. Recently, Plumer carried out the same set of MHA analysis for an earlier version LEU core/fuel design [13-7] and the ORIGEN-S point depletion code in the SCALE-6.1 code package has been adopted for the study [13-8]. In

all three analyses, the fission products in the fuel at the time of the accident were assumed to be in equilibrium for the steady-state reactor power. This assumption is conservative for the MITR because the reactor is shut down periodically for maintenance and refueling. Table 13-1 lists the equilibrium (after 4,200 MWD irradiation) fission product activity inventories for five fuel plates at peak power locations. Reactor power of 7.35 MW (5% overpower due to uncertainty in power measurement) is conservatively used and the radial peaking factor for 5 adjacent plates is determined to be 1.41 [13-2]. This table includes all the nuclides with important contributions (over 99% total activities) [13-2], taking into account the fuel-to-containment release fractions (see Table 13-2).

Table 13-1. Fission product inventory for 5 Adjacent LEU plates at peak power locations

Major Nuclides	Half-Life	Discharge Activity (Ci)
Xe131m	11.93 d	3.77E+01
Xe133	5.25 d	6.99E+03
Xe133m	2.19 d	8.19E+01
Xe135	9.14 h	4.15E+03
Xe135m	15.29 m	9.55E+02
Xe137	3.82 m	6.31E+03
Xe138	14.08 m	6.25E+03
Kr83m	1.83 h	4.98E+02
Kr85	10.78 y	3.37E+01
Kr85m	4.48 h	1.20E+03
Kr87	76.3 m	2.30E+03
Kr88	2.84 h	3.09E+03
Kr89	3.15 m	3.92E+03
I131	8.02 d	9.64E+01
I132	2.30 h	1.43E+02
I133	20.8 h	2.09E+02
I134	52.5 m	2.40E+02
I135	6.57 h	1.97E+02
Cs138	33.41 m	1.83E+02
Te132	3.20 d	3.26E+01
Te134	41.8 m	4.71E+01
Rb88	17.77 m	8.44E+01
Rb89	15.15 m	1.12E+02
Br84	31.80 m	2.62E+01

13.2.1.1 Containment Source Term

Table 13-2 lists the fission product release fraction from the melted fuel (F_f), the fraction released from the primary coolant system (F_p), and the fraction remaining airborne in the containment atmosphere (F_c). These values, which are used in the current analysis, were taken from the MITR-II SAR. The only exception is to assume 100% halogens will be released from the melted fuel, instead of 90% used previously, which leads to a more conservative consideration. These values were chosen based on power reactor accident scenarios that involved severe accidents initiated from coolant system failure that eventually lead to core melt [13-9]. The MITR's MHA, which is initiated by coolant channel blockage, does not involve a primary coolant system failure. However, the primary coolant system is not leak tight. Hence volatiles, such as noble gases, may be released to the containment. In addition, non-volatile fission product transport from the core tank to the containment is possible through coolant evaporation from the reactor core tank. (Note: Both the loss of volatiles and the evaporative release mechanism for non-volatiles ignore the presence of the reactor top shield lid, which is required to be in place if reactor power exceeds 100 kW. The presence of this lid makes the primary system a barrier to fission product release.)

A calculation was made to estimate the amount of fission product release to the containment through evaporation during a two-hour period [13-10]. Assumptions for this calculation are that the coolant temperature is 60 °C, the relative humidity in the upper core tank air space is 10%, the temperature in the air space is 20 °C, and the fission products mix uniformly with the primary coolant in the core tank (about 700 gallons). The first assumption specifies the highest possible coolant temperature (LSSS), the second and third assumptions establish the lower bound of air conditions that would result in a higher evaporation rate, and the last assumption conservatively uses only the coolant volume in the core tank instead of the total coolant volume in the primary coolant system. This calculation shows that about 1.6 gallons of primary coolant would be lost through evaporation during a two-hour period. This is equivalent to about 0.3% of the primary coolant in the core tank. The actual fraction would be lower because both the pool of water above the core and the presence of the reactor top shield lid would limit the release rate.

A coolant system release fraction of 3% is adopted to conservatively bound the non-volatile fission product release. It should be noted that a linear evaporation process for the coolant-to-containment radiation source release (noble gas elements excluded) is assumed in the current a, analysis whereas an instantaneous release scenario is adopted in the MITR-II SAR. The effect of applying a linear evaporation rate of primary coolant has been quantified in the Ref [13-2]. In any case, the linear evaporation process is still considered a very conservative model since no delay time for the fission product release is accounted for during the MHA development. Another conservative consideration is that it is assumed that 100% of the noble gases are released to the containment.

Table 13-2. Fission product release fractions

Element Group	Fraction Released from Melted Fuel F_f	Fraction Released from Primary Coolant System F_p	Fraction Remaining Airborne in Containment Atmosphere F_c
Noble Gases	1.0	1.0	1.0
Halogens	1.0	0.03	0.3
Alkali Metals	0.9	0.03	0.3
Tellurium group	0.23	0.03	0.9
Barium, Strontium	0.01	0.03	0.9
Noble Metals	0.01	0.03	0.9
Lanthanides	0.0001	0.03	0.9
Cerium group	0.0001	0.03	0.9

Because the MITR has no containment spray or other engineered safeguards features to reduce the quantity of fission products in the containment atmosphere, depletion of the radioactive isotopes released to the containment occurs through natural processes. These include agglomeration and sedimentation. Agglomeration is the process by which the size distribution of airborne particulate tends to shift with time to larger sizes until an equilibrium condition is reached. This process affects sedimentation which is deposition because of gravitation. The noble gases are not expected to undergo either of these depletion process and thus they remain in the containment atmosphere.

The fission product activities in the containment atmosphere will vary with time. Activity initially increases as more fission products are released from the melted plates. A maximum occurs when a balance is reached with the depletion processes described above. The activity then starts to decrease because the natural depletion processes and leakage continue while the source is finite. As mentioned earlier, a linear evaporation process for the coolant-to-containment radiation source release (noble gas elements excluded) is assumed in the current analysis. The natural depletion processes start to take place simultaneously from the beginning of the accident. In this analysis, fission product leakage from the containment was neglected as a removal mechanism. During the two-hour period, it was assumed that the depletion for iodine and cesium was 70%, and that depletion for the other non-volatile elements was 10% [13-6].

13.2.1.2 Off-Site Radiation Dose Calculations

The following approaches were used to evaluate effects of the major release paths to the exclusion area during the maximum hypothetical accident:

a) An analysis was made to determine the atmospheric release from the containment building. The radiation doses that result from leakage (including external gamma dose from plume and containment leakage) were calculated using a standard Gaussian diffusion model and local meteorological data.

b) Gamma radiation reaching the boundary area by direct penetration of the containment shell was calculated using standard shielding calculations. A Compton scattering model was developed and applied to photon scattering from the steel containment roof.

c) Radiation streaming for the truck airlock, which is the largest containment penetration, was confirmed to have negligible dose contribution [13-7].

10 CFR Part 20.1301 lists the annual dose limits for the public from normal operation of a reactor. The specific value cited is 0.1 rem Total Effective Dose Equivalent (TEDE). However, this document also mentions authorization up to an annual dose limit of 0.5 rem based on additional information required of the licensee [13-11]. The limit of 0.5 rem (or 500 mrem) TEDE corresponds directly to the 0.5 rem whole body annual dose limit cited from NUREG-1537 [13-12]. In this study, the TEDE levels will be calculated for a two-hour exposure period at the Exclusion Area Boundary (EAB).

13.2.1.3 Atmospheric Release

There are two paths for the fission products in the containment building to be released to the outside. One is a controlled release through the stack via the containment's pressure relief system. The other is containment leakage which is not controllable.

The containment building was designed to withstand internal pressures up to 2.0 psi above atmospheric and 0.1 psi lower than atmospheric. The building is normally maintained at a pressure slightly less than atmospheric in order to prevent out-leakage. If high radiation levels were detected by the plenum gas or particulate monitors, the building ventilation system's intake and exhaust fans would stop and both isolation dampers would close automatically. The maximum permissible leakage rate is 1% of the building volume per day per psi of overpressure. An integral air leakage test of the containment building is performed periodically to ensure that this criterion is satisfied. It is assumed conservatively in the containment leakage calculation that the containment pressure remains constant at 2.0 psig during the accident and that this results in a continuous release of the fission products to the environment at the maximum permissible leakage rate.

The containment building is equipped with a pressure relief system which consists of a blower, roughing filters, two high-efficiency absolute particulate air filters, and an activated charcoal filter for removal of elemental iodine (See Section 6.5.4.2 of this report.). The volumetric flow rate through this system was obtained from experimental data [13-13]. The fractions of radionuclides penetrating through the filters of the pressure relief system are: 100% of noble gases and bromine, 5% of iodine, 50% of all the others [13-6].

Atmospheric dispersion of a pollutant is primarily dependent on (1) meteorological conditions such as ambient temperature, wind speed, time of day, insulation, and cloud cover (atmospheric stability), and (2) pollutant stack emission parameters such as effluent velocity and temperature. The stability of the atmosphere is determined by the atmospheric thermal gradient, which is called the lapse rate. Neutral stability exists for a vertical temperature gradient of -1 °C/100 meters. Unstable conditions with lapse rates greater than -1 °C/100 m add to the buoyancy of an emission, and stable conditions (lapse rates less than -1 °C/100 m) tend to inhibit downward

vertical motion of the pollutant gases (plume). Dispersion from an elevated source (stack) is affected by the mixing and dilution of polluted gases with the atmosphere.

For a stack release, the maximum ground-level concentration in a sector may occur beyond the exclusion area boundary distance. Therefore, for stack releases, the atmospheric relative concentration values are calculated at various distances. Values of dispersion coefficients, which depend on the downwind distance and the atmospheric stability category, can be determined from the Pasquill curves [13-14] (a set of diffusion coefficient curves versus plume travel distance). In most references, the dispersion coefficients are given as a set of curves over the range of 102 to 105 meters. It is impossible to extrapolate these curves accurately to the range of the MITR's exclusion area distance, 8 to 21 meters. One alternative is to use the interpolation formulas for σ_y and σ_z developed by Briggs which fit the Pasquill curves [13-15].

The meteorological data needed for the atmospheric relative concentration calculation include wind speed, wind direction, and a measure of atmospheric stability. The meteorological data used in this report were recorded at the Boston Station, MA 240BS 93-95. The wind speed data are expressed in the units of knots, where one knot equals 1,853 meters/hour. The annual average wind speed for each stability category in the Boston area is listed in Table 13-3. It is shown that class D (neutral stability) is the most frequent stability condition, accounting for about 74% of the total events.

For release from the stack (see Figure 13-1), the more unstable an atmospheric condition, the more a pollutant will be deposited in a shorter range with a higher concentration. In contrast, a more stable atmosphere would disperse the pollutant over a wider range and thus result in a lower concentration. From the meteorological data for the Boston area, it was found that the dose rates at 8 and 21 m are negligible based on class C, D, and E which account for most of the atmospheric conditions (frequency of 94%).

For containment release, the model ("exact" model) proposed in the U.S. NRC Regulatory Guide 1.145 is adopted [13-16]. Figure 13-2 shows the comparison of atmospheric relative concentrations for class A, B, C, D, E, and F versus distance. Class F represents a conservative estimate for both the site boundary and the restricted area and is therefore adopted as the limiting case of the ground release. It is noted that the calculated doses for class F stability would give a conservative estimate of the release with frequency greater than 99.9% [13-2] [13-6].

Table 13-4 shows the two-hour dose from containment leakage at the MITR EABs. As mentioned earlier, Pasquill Stability Class F (a stable class) is adopted for the calculations. In addition, full wake effect treatment is used. This methodology, which was used for the previous dose calculations in the MITR-II SAR, is again used in the current LEU analysis. As can be seen, the two-hour TEDE doses from containment leakage of 8.2 mrem and 8.1 mrem at the back fence (8 m) and front fence (21 m), respectively. These dose contributions will be taken into account for the total radiation release estimation.

Table 13-3. Wind speed for each stability category (knots) averaged over all directions

Directions / Categories	A	B	C	D	E	F
N	0.0	5.4	7.7	10.3	7.2	4.8
NNE	0.0	6.1	8.2	11.0	6.3	4.5
NE	0.0	5.0	8.4	12.4	6.0	3.8
ENE	5.0	6.3	9.6	11.8	6.5	3.8
E	5.0	6.6	9.8	10.4	6.8	3.8
ESE	5.0	6.2	9.6	10.8	6.9	3.8
SE	4.5	7.1	8.4	9.4	6.3	4.1
SSE	5.0	5.8	7.3	9.0	6.3	4.4
S	1.0	5.0	8.5	10.6	6.6	4.8
SSW	4.5	5.6	9.1	12.1	7.4	5.1
SW	5.0	6.6	9.9	12.0	7.9	5.1
WSW	0.0	6.5	9.7	12.0	8.1	5.3
W	5.0	6.7	9.7	13.2	8.4	5.0
WNW	3.0	6.7	9.0	13.4	8.4	5.0
NW	5.0	6.1	10.0	13.2	8.3	5.0
NNW	4.0	6.5	9.0	12.5	8.2	4.6
Average	3.8	6.4	9.2	11.9	7.7	4.6
Relative Frequency (%)	0.00823	1.8254	8.3007	73.9423	12.0338	3.8154

Note: A: Extremely unstable, B: Moderately unstable, C: Slightly unstable, D: Neutral,
E: Slightly stable, F: Moderately stable.

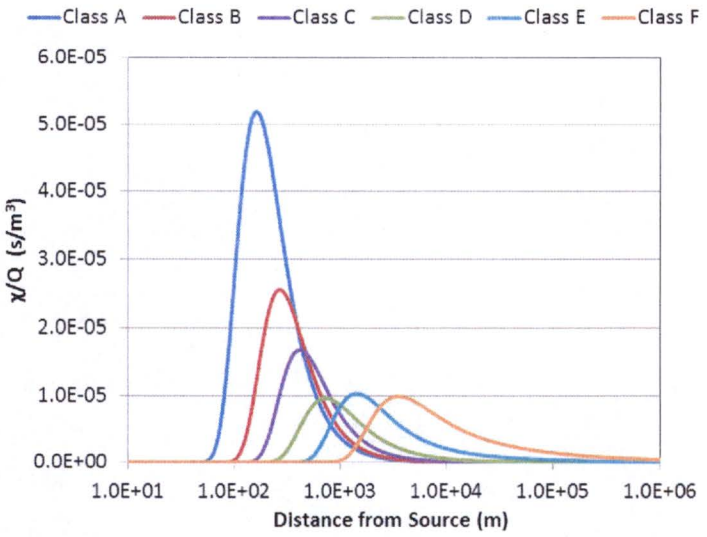

Figure 13-1. χ/Q distributions with different atmospheric stability conditions for stack release. χ: Ground level concentration (Ci/m^3) Q: Pollutant exit rate from containment (Ci/s)

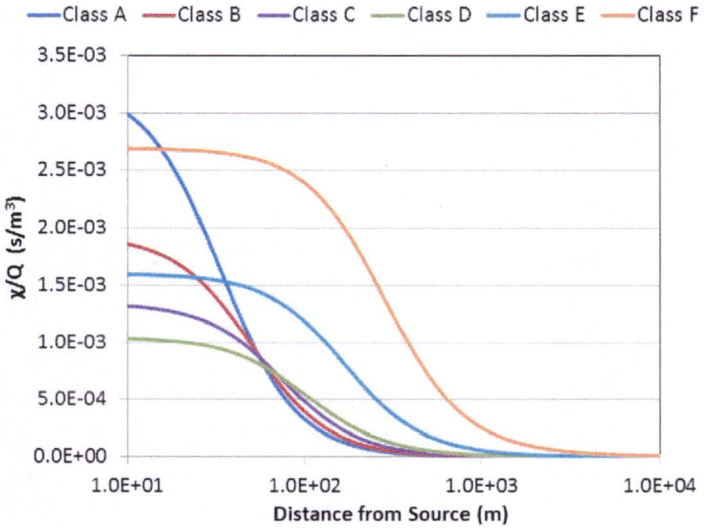

Figure 13-2. χ/Q distributions with different atmospheric stability conditions for containment leakage release considering full wake effect.

Table 13-4. Two-hour dose from containment leakage at two MITR exclusion area boundaries

MITR Boundaries	χ/Q (s/m^3)	Two-hour CEDE Dose (mrem)	Two-hour DDE Dose (mrem)	Two-hour TEDE Dose (mrem)
Back Fence (8 m)	2.69E-03	1.3	6.9	8.2
Front Fence (21 m)	2.68E-03	1.2	6.9	8.1

CEDE: Committed Effective Dose Equivalent (from inhalation)
DDE: Deep Dose Equivalent (from immersion in semi-infinite cloud)
TEDE: Total Effective Dose Equivalent (CEDE + DDE)

13.2.1.4 Direct and Scattered Gamma Dose from Contained Source

Those radionuclides that are retained in the containment building constitute a source of gamma radiation. The gamma dose at the exclusion boundary consists of direct gamma dose and scattered gamma dose (gamma dose through the truck lock was confirmed to be negligible according to Ref [13-7]. The four gamma Deep Dose Equivalent (DDE) components, a) direct gamma flux through steel dome penetration, b) direct gamma flux through shadow shield penetration, c) scattered gamma flux after interaction with air, and d) scattered gamma flux after interaction with steel dome, are analyzed. The contribution from each gamma energy group and the photon flux at the EABs are presented in Ref [13-2]. These are to provide complete information of the MHA estimated doses for the LEU-fueled MITR core.

13.2.1.5 Conclusion for the Maximum Hypothetical Accident

Table 13-5 shows the estimated doses from all modes of radiation release for the LEU-fueled MITR core with power level of 7.35 MW after 4,200 MWD operation. It is seen that the primary contribution to the total TEDE dose is from the scattering terms. The overall dose is 302.1 mrem total TEDE at 8 m EAB and a higher dose of 392.8 mrem total TEDE is found at 21 m EAB. As mentioned in the MITR-II SAR, the maximum dose peaks at 16 m with an approximately 21% increase in addition to the 21 m dose level. By taking into account this effect, the maximum dose from the LEU core MHA is still less than 480 mrem total TEDE, which is under the 500 mrem total TEDE limit goal for public exposure cited from NUREG-1537 [13-12].

Concentration of Ar-41 is predicted to be 2.09×10^{-3} μCi/ml for 7 MW. This estimate is extrapolated from measurements performed for the MITR at 5 MW. Compared to fission products released from the fuel, this concentration is lower by a factor of 5 to 7. Therefore, the contribution of Ar-41 to the off-site dose is negligible [13-6].

Table 13-5. Estimated Doses from all Modes of Radiation Release during an MITR Maximum Hypothetical Accident

Component of the Dose	Dose (mrem) [a]	
	8 m [b]	21 m [c]
Leakage TEDE	8.2	8.1
Gamma DDE	—	—
Steel Dome Penetration	3.3	25.1
Shadow Shield Penetration	47.9	22.5
Air Scattering	103.1	120.9
Steel Scattering	139.7	216.1
Total TEDE [d]	302.1	392.8

[a] Calculation assumes that radiation emergency plan

for protection of the public will be implemented in less than two hours. (b) Boundary of restricted area (c) Nearest point of public occupancy (d) The maximum TEDE is 480 mrem at 16 m.		

13.2.2 Insertion of Excess Reactivity

In order for an insertion of excess reactivity to cause a reactor transient, it is necessary for the reactor to be at or near critical. The MITR core is designed with a mechanical interlock (the upper grid plate) that forces any operation that involves a large reactivity insertion to be done when the reactor is shut down. Specifically, access to the core is possible only if the upper grid is rotated, and that action is in turn possible only if all shim blades are fully inserted. Thus, refuelings can be performed only after the shim blades have been fully inserted. In addition, in-core experimental facilities are fixed in place so that they too can be moved only when the grid is rotated. Excess reactivity transients are therefore unlikely because of the interlock between the shim blades and the grid itself. Hence, initiating events for such a transient are limited to control device malfunctions such as continuous withdrawals and/or the unanticipated movement of a sample contained within an in-core sample assembly.

Analyses of the MITR's response to step and ramp reactivity insertions indicated that the reactor could be shut down safely without damage to the core in the event of a transient up to a limiting value of either inserting reactivity in a step (conservatively assuming insertion time of 0.5 s for simulation) or ramp reactivity insertion (i.e., with much slower rate). These values are the basis of both the step reactivity limit for any single experiment or component, which could credibly cause a reactivity effect by failure or ejection, and by the ramp reactivity insertion limit.

13.2.2.1 Step Reactivity Insertion

Step reactivity insertion analyses were performed for the MITR-II in the 1970s using a correlation derived from SPERT experiments [13-17]. The SPERT experiments span a range of core configurations sufficiently similar to the MITR-II core, such that the correlation was expected to give a good prediction of the MITR-II transient response.

The estimated step reactivity limit of the MITR-II core was 1.8% $\Delta k/k$ or 2.3 β.

The step reactivity insertion limits for the LEU MITR core were evaluated using the PARET code, which provides coupled thermal, hydrodynamic, and point kinetics capability for research reactors under loss-of-flow and reactivity insertion transients [13-18]. Reactivity insertion transients were analyzed for research reactors utilizing both LEU and HEU cores using the PARET code by Woodruff [13-18]. Experimental data from the SPERT series of reactivity insertion tests have been used to benchmark the PARET code. For the HEU benchmark core, a step insertion of approximately 2.35 β was found to be the limiting case (i.e., for reactivity insertions larger than this limit, the peak temperature of the cladding is predicted to exceed the cladding melting temperature for Al-6061 alloy).

The initial power was assumed to be 80 kW for natural convection and 7 MW for forced convection. The step reactivity is inserted within 0.5 seconds in these calculations. This is based on a standard of fast reactivity transients used in other reactors such as the National Bureau of Standards Reactor [13-19].

The most limiting case for a step reactivity insertion transient was identified to be the cases with overly conservative trip circuit delay time and initial shim bank position [13-2]. These cases both result in a delay of the safety system response (triggered by period less than 7.0 s) that would terminate any transients. Hence, taking into account these conservative assumptions, there is more time for the reactor power to rise. For the reference step insertion under forced convection (1.8% Δk/k insertion within 0.5 s), the highest cladding surface temperature (101.6 °C) is found in a T-plate; whereas the highest fuel temperature (120.2 °C) is found in a F-plate. Both temperatures are well below the fuel blistering threshold temperature of 350 °C Ref [13-2]. By increasing the reactivity insertion magnitude from 1.8% Δk/k to 3.0% Δk/k, the maximum temperature increment during the accident is less than 30 °C. The effects caused by the fuel depletion have been addressed in terms of fuel core swelling and thermal conductivity degradation. However, both effects are found to be insignificant to the core behavior during a step reactivity insertion event. The step reactivity insertion is better mitigated under natural convection conditions. More detailed results of the step reactivity insertion analyses can be found in Ref [13-2].

In summary, the LEU core adopts the same step reactivity insertion limits as the HEU core (i.e., 1.2% Δk/k (or 1.5 β) for natural convection mode and 1.8% Δk/k (or 2.3 β) with forced convection established before the reactor is made critical).

13.2.2.2 Ramp Reactivity Insertion

Ramp reactivity insertions are quite different to step insertion, since the time scale is sufficiently longer. According to Ref [13-20], the reference slow ramp reactivity insertion accident consists of a 3% Δk/k reactivity insertion over 60 seconds (i.e. an LSSS insertion rate of 5×10^{-4} Δk/k/s). The time scale of the ramp reactivity insertion is much longer than that of the step reactivity insertion (~ 2 seconds vs. ~ 0.2 seconds). The reactor, during a ramp reactivity insertion, would not be tripped by a short period (less than 7.0 seconds) condition in the case of a step insertion, but rather by the 20% over-power trip.

In the ramp reactivity insertion case the maximum cladding surface temperature reaches ~ 100 °C and the maximum fuel centerline temperature rises close to 120 °C. These peak temperatures are strongly correlated with the higher energy release in the absence of a period trip. No safety limit is exceeded during the ramp insertion scenarios and no sub-cooled boiling occurs. Increases in the reactivity insertion rate during the slow ramp scenario (but without triggering the period trip of 7.0 seconds) did not lead to more limiting conditions. More detailed results of ramp reactivity insertion analyses can be found in Ref [13-2].

In summary, the LEU core adopts the same ramp reactivity insertion limits as the HEU core (i.e., 5×10^{-4} Δk/k/s). This figure is conservative given the above analysis, and provides adequate safety margin for the purposes of operating the MITR.

13.2.2.3 Limitations on Excess Reactivity

Reactivity information on the MITR's shim blades and regulating rod is given in sections 4.2.2.5 and 4.5.1.5 of this report. As is noted in those sections, a refueled core normally attains criticality at a shim bank height of 8 to 10 inches. A typical value of the excess reactivity is about 6 to 7 β. This is utilized to offset the effects of temperature, xenon, and fuel burnup. It should be noted that there are two design features that limit the potential possible impact of excess reactivity on the MITR:

a) Subcritical Interlock: Observance of this interlock means that the infinite period shim bank height is at least 5 inches. This places an upper limit on the excess reactivity.

b) Shim Blade Withdrawal Limitation: There are six shim blades. It is not physically possible to withdraw more than one at a time. Hence, the excess reactivity per blade is quite modest.

13.2.3 Loss of Primary Coolant

A loss of primary coolant accident is not credible for the MITR for the reasons discussed in Chapters 4, 5, and 6 of the MITR-II SAR. To summarize:

a) All penetrations to the light-water core tank occur well above the core. Hence, a break in the primary outlet piping could not uncover the core. (See Section 4.3 of the MITR-II SAR.)

b) A break in the primary inlet piping could establish a siphon that would draw coolant through the core and up through the inlet plenum that is formed by the wall of the core tank and the core shroud. Such a siphon would be broken by the two redundant anti-siphon valves that are installed at the inlet penetration. (See Section 6.3 of the MITR-II SAR.) Hence, a break in the primary inlet piping could not uncover the core.

c) A break in the core tank itself would not uncover the core because the light-water tank is wholly contained by the heavy- water reflector tank. (See Section 4.3 of the MITR-II SAR.)

For the above reasons, a loss of coolant accident is not credible. Nevertheless, the MITR is equipped with an emergency core cooling system (ECCS) as described in Sections 5.2.5 of the MITR-II SAR. An analysis of the ECCS is given in Section 6.4 of the MITR-II SAR. The ECCS is capable of removing the decay heat that would be present following extended operation at full power.

Analyses are given below of three events that were considered during the design of the MITR as possible initiators of a loss of coolant accident. In each case, the core remains both covered and properly cooled. Therefore, a complete loss of coolant accident is not considered to be credible.

13.2.3.1 Break in Primary Coolant Piping

A low-level core tank scram would occur when the coolant level drops four inches below the overflow level. If the break is in the outlet piping, the coolant level will drop until the outlet penetrations, which are about seven feet above the top of the core, are uncovered. If the break is in an inlet line, the coolant level will drop until the anti- siphon valves are uncovered. These are about six feet above the top of the core. In both cases, decay heat will be removed by natural circulation as described in Section 6.2 of the MITR-II SAR.

13.2.3.2 Break in Light-Water Core Tank

Primary coolant would leak into the heavy water reflector where it would cause a strong negative reactivity effect as described in Section 4.5.1.6. The light-water coolant level would decrease to the height determined by the helium vent line from the D_2O reflector tank. This vent line returns to the basement at the same level as the primary coolant inlet and outlet pipes. (See Section 5.3.1.5 of the MITR-II SAR.) The level of the coolant above the core would be at least 6 feet and decay heat would be removed by natural circulation. If the D_2O reflector dump system should be activated, then the light water would flow through the dump system and the vent lines to fill both the dump tank and the D_2O storage tank. The level of the coolant in the core tank would then drop to three or four feet above the core, depending on the volume in storage. Natural convection would still cool the core but the total heat capacity of the coolant in the core tank and its radiation shielding capability would be reduced and action to increase the water volume might be required.

13.2.3.3 Sample Malfunction in Proximity to Core Tank

The MITR contains a pneumatic tube in position 6RH1. This tube terminates inside a reflector tank reentrant thimble, thereby placing the sample in close proximity to the core tank. The consequences of a failure of this facility were examined by performing a planned failure within a laboratory mock-up. This mock-up consisted of the pneumatic system in a beam port adjacent to the core tank wall, all immersed in water to simulate the D_2O reflector. The MIT pneumatic tube rabbit is a polyethylene sample container with threaded cap ends. Samples may be sealed within an aluminum inner container. Two types of explosive failures were postulated. The first was the overpressurization of the polyethylene container and the second was the overpressurization of the aluminum container within the polyethylene container. Both accidents were simulated in an operating model. The first test, which used the polyethylene rabbit only, resulted in the end cap blowing off suddenly at 700 psi pressure. There was no evidence of damage to the pneumatic tube system. In the second test, the pressure reached 800 psi before the ends blew out of both the aluminum can and the rabbit. (This pressure rise is equivalent to about 280 mg of TNT.) Again, there was no evidence of damage to the pneumatic tube. Thus, in both experiments, damage was limited to the sample container and no measurable effect was found on the beam tube or the core tank wall. The potential energy that was released during these tests was greater than that which could possibly be generated by an approved sample. The hazard to the core tank is further reduced because any projectile must in turn go through the inner pneumatic tube, the outer pneumatic tube, the heavy-water reflector tank thimble and then reach the core tank wall.

13.2.4 Loss of Primary Coolant Flow

The MITR is designed so that a low primary flow (less than 2,200 gpm or higher) will automatically initiate a scram. There are two initiating events that can cause a loss of primary coolant flow accident. The first is a loss of off-site electrical power which will stop the primary pumps and scram the reactor by dropping all six shim blades simultaneously. This is a credible scenario. The second is a pump coast down accident that occurs because of primary pump power supply failures or malfunctions of the pump motors. This is not considered to be a credible accident because the probability for both pumps to fail at the same time is very small.

The reactor will shut down automatically upon receiving a low primary coolant flow scram signal. The trip circuit delay time is less than 0.1 second.

An analysis was performed for a loss-of-flow accident subject to the assumption that the power supply to both primary coolant pumps was interrupted at the same time. The initial conditions and assumptions made in this analysis were as follows:

a) The steady-state equilibrium reactor power was 7.1 MW. This is the maximum steady-state power compatible with an LSSS of 8.68 MW and a primary coolant flow of 2,200 gpm. It was chosen because the loss of flow is more severe if initiated from high power.

b) The primary coolant outlet temperature was 55 °C (scram setpoint).

c) The hot channel received the minimum flow among all coolant channels. This conservative assumption simplified the calculation by eliminating the need for analyzing individual coolant channels.

d) The axial power distribution was assumed uniform in both the average and the hot channel. (See Section 4.6.7 of the MITR-II SAR.)

e) The steady-state primary coolant flow rate was 2,200 gpm. The coast-down curves for interior and end channels are shown in Figure 13-3.

f) The reactor scram was activated one second after the primary flow reached below 2,200 gpm. It is conservatively assumed that the low-flow trip resulted in the start of shim blade motion (scram) one second later (see Figure 13-3).

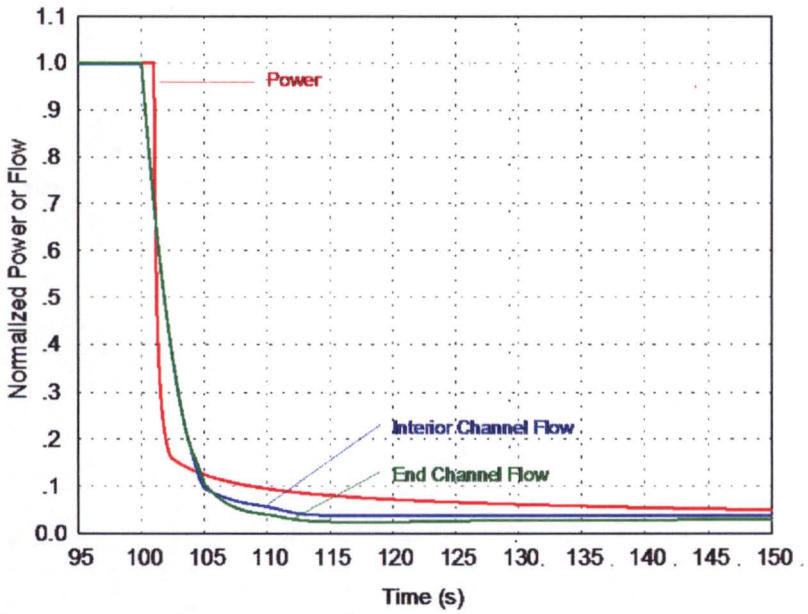

Figure 13-3. Normalized power and flow for loss of primary flow analysis

The calculation was performed using the RELAP5/MOD3.3 code [13-21], which is developed for the best-estimate transient simulation of light water systems. Figure 13-4 shows the fuel plate and coolant temperature evolutions during loss of primary flow. There are two peaks in the temperatures. The temperatures rise when the pump coastdown starts and the pump flow rate drops rapidly. The first peak occurs at 1 second after loss of flow when the control blades start moving in and the power drops rapidly. After a few seconds the power drops to decay heat levels and then drops more slowly, but the coolant mass flow rate continues dropping rapidly until natural circulation flow develops. The second temperature peak occurs approximately 16 seconds after loss of flow as natural circulation has been established and the decay heat power continues to drop slowly. The first peak represents higher plate temperatures but lower coolant bulk temperatures than the second peak. These temperatures are all well below the fuel blistering threshold temperature of 350 °C. It is concluded that the LEU core fuel performs well during loss of primary flow events after nominal operation at up to 7.0 MW.

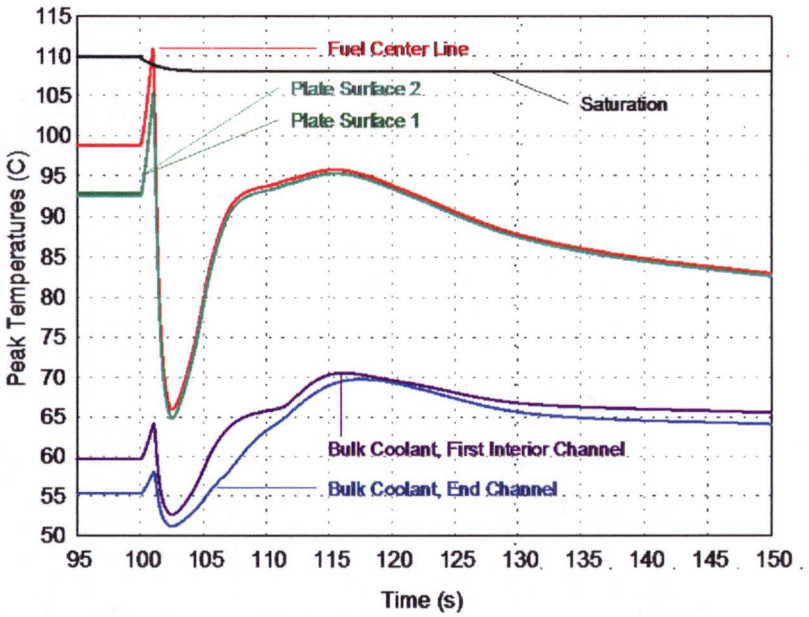

Figure 13-4. Fuel plate and coolant temperature evolutions for loss of primary flow analysis

13.2.5 Mishandling or Malfunction of Fuel

13.2.5.1 Mishandling of Fuel

The tools used for the handling of MITR fuel are described in Section 9.2.3 of the MITR-II SAR. These tools are designed to prevent damage, such as scratches, to the cladding during fuel movement. Also, they are designed to prevent the inadvertent drop of an element. These tool designs have been used since 1974 and no fuel damage has occurred during handling. If damage were to occur, or if it were suspected to have occurred, the element in question would not be utilized until an evaluation was performed. This could probably be done by visual inspection (through water for shielding) and, if felt necessary, by element sipping. The latter process entails placing the element in an approved storage location, such as the fuel storage ring, where it is immersed in water that is not subject to forced convection. If damage has occurred, fission products such as iodine will accumulate in the water. A sample of this water can be drawn after several days and counted for activity. Water from several control elements (ones with no suspected damage) would also be drawn for comparison.

Mishandling of MITR fuel would not cause a sudden radiological problem because the fuel alloy provides a means of retention of fission product gases below the melting temperature of the cladding. Fission products must diffuse through the fuel in order to be released.

13.2.5.2 Malfunction of Fuel

Operating experience with MITR fuel is summarized in Section 4.2.1 of the MITR-II SAR. A few plates, almost all from a former supplier, were identified as showing incipient excess outgassing. This was determined from the radioactivity in the purge gas (air) that is drawn across the core outlet plenum as described in Sections 5.2.1.7 and 9.1.5.2 of the MITR-II SAR. Confirmation of the problem and identification of the fuel element involved was done through

use of the fuel sipping method described above. Once confirmation was made, the element that contained the affected plate was removed from service. Malfunction of fuel does not engender serious radiological consequences because the MITR is equipped to identify any such malfunction in its incipient stages. Also, MITR operation does not impose significant thermal stress on the fuel. There is no mechanism (such as water-logging followed by a pulse) whereby an incipient condition could suddenly worsen. Specifically, the MITR does not operate in a pulse mode and the temperature change of the fuel from cold shutdown to hot operating conditions is about 30 °C.

13.2.6 Experiment Malfunction

Experimental facilities and the review process for the use of these facilities is discussed in Chapter 10 of the MITR-II SAR. From the perspective of reactor safety, these facilities may be divided into three groups. These are:

a) Ex-Reflector Facilities: These facilities are decoupled from the reactor so that they cannot affect either the thermal-hydraulic or the neutronic performance of the core. Examples include the medical irradiation rooms, any equipment monitored at the exterior of a beam port, pneumatic tubes that terminate in the graphite reflector, the sample processing areas, the in-reflector (graphite) irradiation facilities, the reactor floor hot cell, and the gamma irradiation facility.

b) In-Reflector Facilities: These facilities are in sufficient proximity to the reactor so that administrative limits are warranted to ensure that a malfunction could not affect the core. The principal facility in this category is the 2PH1 pneumatic tube that terminates in the 6RH1 reentrant thimble. An analysis of a malfunction of a sample in this tube is given in Section 13.2.3.3 of this report. That analysis showed that a severe overpressurization would not cause damage to the reactor. Nevertheless, administrative limits have been imposed on samples allowed in this (and all other) facilities. These address behaviors such as explosive energy, corrosion potential, radiolytic decomposition, and internal heating.

c) In-Core Facilities: These facilities are within the core itself. A fundamental principal of their design is that, despite their location, they be decoupled to the maximum extent possible from the core. Thus, in-core sample assemblies are often designed with a thimble that eliminates or restricts thermal interaction. In addition, ICSAs often have dedicated cooling. Some coupling, such as neutronic, is, of course, unavoidable. ICSAs have been designed and installed in the MITR to do the following:

   i) Serve as a sample irradiation facility.

   ii) Serve as a temperature-controlled irradiation facility.

   iii) Replicate Pressurized Water Reactor (PWR) conditions to allow study of coolant chemistries for dose reduction.

   iv) Replicate Boiling Water Reactor (BWR) conditions to allow study of coolant chemistries for dose reduction.

v) Replicate conditions that would result in Intergranular Accelerated Stress Corrosion Cracking (IASCC) and allow in-pile mechanical property testing.

Each of these facilities has been the subject of its own Safety Evaluation Report (SER) that documents the design, operation, safety, and accident potential of the facility. Appendix A to MITR-II SAR Chapter 13 is a condensed version of the SER for one of these ICSAs, the Boiling Coolant Chemistry Loop (BCCL). The BCCL SER is illustrative of the issues addressed for all in-core facilities.

13.2.7 Loss of Normal Electrical Power

The MITR was designed with the expectation that there would be interruptions of offsite electrical power. Passive safety features exist so that on loss of electricity the reactor will shut down. Specifically,

a) The six shim blades are attached to their drives by electromagnets. On loss of power, the electromagnets deenergize and the blades drop into the core under influence of gravity.

b) The air pressure that keeps the heavy-water reflector's dump valve closed is in turn controlled by an electrically-operated solenoid valve. On loss of electrical power, it opens thereby dumping the reflector and shutting the reactor down.

The MITR is also designed for the removal of decay heat by natural convection cooling. This is Mode #1 of the four modes of emergency cooling that are described in Section 5.2.5 of the MITR-II SAR. Finally, both the main and auxiliary containment building ventilation dampers close on loss of offsite power, thereby precluding the release of any radioactive effluent to the environment.

The MITR is also equipped with an emergency power system as described in Section 8.2 of the MITR-II SAR. Its principal purpose is to provide power for reactor and radiological instrumentation, auxiliary pump MM-2 which can be used for decay heat removal and lighting. None of these functions is essential to safety because:

a) The MITR's power level, coolant temperature (core outlet plenum), and core tank level are available either from battery-operated devices or instruments that do not use electricity.

b) Information on radioactive effluents is not required because the building is sealed (dampers closed).

c) Decay heat removal is achievable via natural convection within the core tank.

d) Battery-operated lights provide sufficient illumination for safety of personnel.

13.2.8 External Events

The MITR is protected from the impact of external events by the containment building, the design of which is given in Section 6.5 of the MITR-II SAR. To summarize, it is a domed

cylindrical structure with a diameter of 74 feet (22.5 m) and a height between grade elevation and the top of the dome of 49 feet (14.9 m). The shell is constructed of steel plate that is 3/8 inch (9.5 mm) thick on the sides and 5/8 inch (15.8 mm) thick on the dome. A cylindrical concrete wall, 2.0 feet thick and 31.5 feet high, is contained within the shell. The building is gas-tight and can withstand an internal pressure 2 psi above atmospheric pressure and an external pressure differential corresponding to -0.1 psi.

13.2.8.1 Lightning

The steel containment shell is grounded to a heavy copper conductor that is buried below the natural water table. Lightning arresters are attached to the ventilation exhaust stack and are grounded to the buried copper conductor. Hence, lightning does not pose a direct threat to the facility. It could cause a loss of offsite electrical power. However, for the reasons discussed in Section 13.2.7 of this report, such a loss will not initiate a safety challenge.

13.2.8.2 Floods

The MITR is located in Cambridge, Massachusetts, which lies in a basin formed by a low-lying chain of hills. The basin, which opens into Boston Harbor and Massachusetts Bay, is drained by the Charles River. As discussed in Section 2.4 of this report, this drainage to the ocean means that the MITR site is not subject to flooding.

13.2.8.3 Meteorological Disturbances

Tornadoes are very rare in the metropolitan Boston area. In comparison, hurricanes are fairly common, although high sustained wind speeds are rare in this area. The containment building effectively isolates the reactor from meteorological disturbances. The relevant considerations are:

a) The containment building was conservatively designed to conform to the wind load criteria of Massachusetts building codes.

b) The reactor ventilation stack was designed to withstand wind loads in excess of 100 mph.

c) The containment building is protected against excessive pressure variations by the vacuum relief breakers and by the pressure relief system. (See Sections 6.5.4.1 and 6.5.4.2 of the MITR-II SAR.)

d) The building and ventilation stack have not sustained any damage from any meteorological condition that has occurred since their construction in 1958. Moreover, both are maintained in excellent condition through regular painting of the building and use of cathodic protection, as well as through periodic inspection of stack.

13.2.8.4 Seismic Event

The MITR is protected against the consequences of a seismic event provided that the core tank remains functional. Other types of damage such as disruption of process systems and lack of electrical power may or may not occur. However, these will not result in core damage for the reasons summarized in Sections 13.2.3, 13.2.4, and 13.2.7 of this report. Specifically, the

location of core tank penetrations, the presence of redundant anti-siphon valves, the provisions for natural convection cooling, and the shutdown of the reactor on loss of electricity protect the core against damage to piping and power supplies. Disruption of process systems would, at most, result in the spillage of primary coolant or heavy water. Any such spills would be contained within the reactor building. A seismic event would also not interfere with the capability to shut the MITR down. The six shim blades cannot be withdrawn so far that the blades are ever completely out of the blade slots. Thus, blade insertion would not be jeopardized by seismic activity. This is further discussed in Section 13.2.8.6 of this report. The issue therefore is the integrity of the core tank. The impact of a seismic event on the tank is summarized below:

a) Support Structure: The MITR's light-water core tank is supported by the heavy-water reflector tank, which in turn rests on the lower annular ring. The lower annular ring is supported by the inner section of the radial thermal shield which is contained within the biological shield. The biological shield is an integral part of the remainder of the reactor containment building. The building, which is 70 feet in diameter, rests on a three-foot thick concrete pad that sits on compacted gravel that is above a layer of "Boston" blue clay that is over a hundred feet deep. (See Section 2.5.2 of the MITR-II SAR for a summary of soil conditions.) Because of this construction, it is expected that the shield and pad will shift as a unit rather than crack under seismic shock.

b) Design Acceleration: Analysis of the New England area's geologic history suggests that, for design purposes, a reasonable peak acceleration for a seismic event is 0.15 g. (See Section 2.5.4 of this report.) The MITR is built on Class B soil and such ground tends to amplify seismic motion. Accordingly, a site modification factor of 1.5 is applied. (See Section 2.5.6 of this report.) Hence, the design value applicable to the MITR is 0.225 g.

c) Method of Analysis and Results: Both the light-water core tank and the interior structures (shroud and core support housing) were analyzed to determine the accelerations (horizontal and vertical) that would cause the components to experience their limiting stress. Each structure was divided into a number of elements or nodes for purposes of the calculation. In order to simplify the calculation, it was assumed, as is reasonable in earthquake analysis, that for all cases, the vertical acceleration was two-thirds of the horizontal. It was found that the light- water tank (and not the shroud or core support housing) is the limiting factor. Horizontal and vertical accelerations of 5.1 g and 3.4 g respectively would cause the weakest point in the tank to reach its yield stress of 9,500 psia. If one takes a safety factor of fifty percent into account, then a "working" stress limit of 6,250 psi is used in lieu of the actual yield stress. This figure is attained for horizontal and vertical accelerations of 2.9 g and 2.0 g, respectively. The location at which this limiting stress is attained is the section of the light-water core tank that supports the core support housing. Details of the calculations are given by Allen [13-22]. The effect of heavier LEU fuel was particularly addressed and the results indicated negligible impact on the yield stress.

d) Conclusion: The MITR light-water core tank is capable of withstanding (at yield stresses) static forces corresponding to 5.1 g horizontal acceleration and simultaneously 3.4 g vertically. It is not conceivable, even under the most unfavorable circumstances, that the response to earthquake motions would be more than a small fraction of these amounts.

A seismic analysis was also performed of the MITR's 150-foot ventilation exhaust stack. For this analysis, it was assumed that the seismic event occurred simultaneously with a 100 mph wind. The allowable shear stress was found to be greater than the total (seismic plus wind) for all elevations. Hence, a collapse of the stack would not be expected [13-22].

13.2.8.5 Mechanical Impact or Collision with Building

Mechanical impacts or collisions of some type could occur with either the side or the domed roof of the reactor containment building. The latter is more limiting because the dome consists of 5/8-inch steel plate while the sides are made of 3/8-inch steel plate that encloses two feet of concrete. Accordingly, notwithstanding the design features that preclude such a collapse, an analysis is given here of the effect of a failure of the MITR's exhaust ventilation stack such that the stack falls onto the domed section of the containment.

For purposes of this analysis, the stack was assumed to be hinged at its base and to fall as a unit toward the containment. The masses of the upper two portions were doubled to account for the effect of impact. In addition, the lower section of the stack (height < 39 feet) was not included in the calculation because it can strike only the side of the building. Table 4-1 gives the loads used in the analysis. The maximum total loading is 5.65 psi.

Table 13-6. Loads Used in Stack Collapse

Zone Section Struck by Mass of Stack	Equivalent Mass of Stack Hitting Section (lbs)	Area Struck (ft^2)	Equivalent Load (psi)
1 and 2	113,700 *	160	5.0
3	37,900	90	3.0
4	64,900	104	4.3
5	69,200	112	4.3
6	90,000	119	5.3
* Equivalent mass is increased by a factor of two to simulate dynamic impact effects.			

The question then arises as to whether the dome will either buckle or fracture.

a) Buckling: The critical pressure to cause local buckling of a spherical shell is:

$$P_{cr} = 0.365 \cdot E \cdot (t/R)^2 \qquad \textbf{Eq. 13-1}$$

where P_{cr} is the critical buckling,

E is the modulus of elasticity

t is the shell thickness, and

R is the shell radius.

For the MITR dome, the values of E, t, and R are 0.3 $\times 10^8$ psi, 3/8 inches, and 840 inches, respectively. The critical pressure is therefore 2.3 psi. This is less than the loading calculated in Table 13-5. Hence, local buckling of the containment dome can be expected.

b) Fracture: The dome is made of A-283-C steel for which the yield point and ultimate tensile strength are 33,000 psi and 60,000–72,000 psi, respectively. The peak stress on the dome, which will occur on the inside surface, was calculated using the same approach as outlined in Section 13.2.8.4 of this report. The peak values are about one-third of the yield point [13-22]. Hence, fracture will not occur. (Note: The figures for the yield point and ultimate tensile strength assume that the steel is above its null ductility transition temperature of -18 °C (0 °F). The containment building is always kept at room temperature (~22 °C). Hence, the temperature of the shell is always above the transition temperature.)

To summarize, local buckling of the domed portion of the containment is likely if the stack should topple onto it. However, fracture will not occur. The twenty-ton polar crane, which is supported by the two-foot thick concrete wall that forms part of the side of the containment, would limit any buckling of the roof. Further protection to the reactor core would be provided by the biological shielding and the reactor top shield lid. (Note: The above analysis assumed a uniform 3/8-inch thick steel shell. The actual thickness is greater over most of the dome.)

13.2.8.6 Seismic Effects on Shim Blades

An analysis of seismic effects on shim blade operation was performed by Allen [13-22]. The principal findings were:

a) Each control blade is connected to a guide rod that traverses a guide tube during vertical movement of the blade. The rods are keyed in the guide tube and thus no rotary motion is possible even during lateral ground movement.

b) Jamming of the guide rod in its tube is not an issue because the length of the guide rod is insufficient to have an angle sufficient to permit jamming.

c) The shim blades are not prone to whip because they are constrained at the top by the guide rod and at the bottom by the blade slots. The displacement of the end of the blade resulting from a 1 g lateral load was calculated to be only 0.0063 inches (0.16 mm), which is negligible.

d) Vertical ground displacement could cause a temporary upward force on the shim blades. If this force occurs at the exact moment of blade release and if the blade has an initial upward velocity of 0.3 ft/sec (0.1 m/sec) (which is a reasonable value for a strong earthquake), the blade drop time will only be delayed by 0.02 seconds, which is negligible when compared to a typical blade drop time of 0.7 seconds.

13.2.8.7 Pipe Vibrations

Piping in the reactor was also analyzed to determine if seismic vibrations could cause damage [13-22]. The longest unrestrained run of a major pipe is the light water coolant pipe that runs

from the equipment room to the core tank. (The pipe is actually restrained against large motions by the compactness of the area through which it passes.) The fundamental frequency of this pipe is 23 cycles per second, well above normal earthquake frequencies. (Note: Even if a failure of this pipe were to occur, it would not result in core damage because of the anti-siphon valves.)

13.2.8.8 Explosions or Toxic Releases

The containment building would protect the reactor and those utilizing it from both explosions and toxic release.

a) Explosion: For an explosion to have effect, it would have to penetrate both the containment's steel shell and the two-foot thick concrete wall, propagate across the open space within the containment building, then penetrate the 5.5-foot thick biological shield that is made of high density concrete, and then still have sufficient effect to damage the steel thermal shield that is the basis of support for the core tank.

b) Toxic Release: Protection could be obtained against any such release by sealing the containment building. The MIT Environmental Health and Safety Office, local industries, and the City of Cambridge's Department of Emergency Preparedness exchange information and conduct drills/exercises that involve toxic release scenarios.

13.2.9 Mishandling or Malfunction of Equipment

The MITR has been designed to exploit passive safety features. Thus, instrument or equipment failures have been anticipated and generally result in a reactor shutdown. For example, both the safety system and the instruments that monitor radioactive effluents are themselves monitored for power and on-scale indication. If these are lacking, a reactor scram and/or a building isolation occurs. However, there are some situations for which it has not been possible to devise interlocks and/or a fail-safe response. For these, administrative procedures are observed. These situations are discussed here.

13.2.9.1 Operation with Shim Blades in a Non-Uniform Bank Position

It is intended that, whenever the MITR is at a power level in excess of 100 kW, the six shim blades be within ±2 inches of an average bank height. This is done in order to achieve a uniform distribution of the neutron flux. An interlock is used during reactor startups to assist the console operator in achieving this objective. Specifically, the subcritical interlock, which is described in Section 7.3.1.2 of the MITR-II SAR, blocks blade withdrawal beyond five inches unless all blades are first brought to the five-inch position. Once all blades are above five inches, satisfaction of the requirement to maintain a uniform bank height is achieved by administrative procedure. Hence, either operator error or an incorrect indication of blade position could result in a non-uniform bank. This would in turn cause a tilt in the power distribution.

Calculations have been performed for the scenarios with one blade full out and the other five maintaining criticality. These were done using the computational code MCNP5 [13-23]. All the calculations assume the reactor operates at LSSS power. Both the fresh core (22 fuel elements) and equilibrium cores (24 fuel elements) have been considered. Fuel stripes (1/4 in lateral and 1/16 in axial of a plate) were tallied throughout the core. The peak values and their locations

were studied. It is found that the peak stripe powers in the fresh core are generally higher than those in the equilibrium core. This is primarily due to power concentrating in fewer total elements. It is also found that the peak stripe in the fresh core occurs in the A-ring for the reference case, but the location shifts to the C-ring for the scenarios with the shim bank fully withdrawn. The peak stripe in the equilibrium cores occurs in the B-ring and its location is unaffected by shim bank position. Fresh fuel is homogeneously loaded in the fresh core so the power of the fuel plates facing the withdrawn shim blades increases significantly. The equilibrium core loads fresh fuel in to the B-ring, and the C-ring elements are typically deeply burned. This is the explanation for why the peak stripe is not shifted to the core periphery with increased shim bank height. The most important observation is that all the peak stripes in the studied cases are lower in power, with sufficient margin, than the corresponding safety limit power level of 10.05 kW per stripe in the fresh core and of 9.21 kW per stripe in the equilibrium cores. More detailed results including the analysis methods can be found in Ref [13-2].

The case with one blade fully inserted is generally less operationally significant compared to the case with one blade fully withdrawn since the most significant power deformation corresponds to a power decrease due to the fully inserted shim blade. Very limited power increase is expected on the opposite core side of the fully inserted blade. It should also be noted that the MITR Technical Specification Rev.6 (TS.3.1.4.5) [13-24] only allows high power operation (power level greater than 100 kW) with five shim blades when the inoperable blade is at the average shim bank height or higher. This specification practically eliminates the possibility of forming an excessive peak power stripe under the scenario with one shim blade fully inserted.

13.2.9.2 Use of Lead Fixtures Over the Core Tank

The MITR is a tank-type reactor. Storage for spent fuel is provided by a pool that is separate from the tank (i.e., there is no canal that connects the two). In order to transfer spent fuel from the core to the pool, a lead transfer cask is used. The procedure is done with the reactor shut down. The reactor top shield lid is removed and the element in question, which is normally already in the fuel storage ring, is placed in a protective basket.

The lid is replaced and the plug to one of the ports that penetrates the lid removed. A lead sleeve is lowered through the port and supported on the port's lip. The sleeve provides shielding. The fuel transfer cask, which is a lead-filled annulus, is then placed over the port so it rests on the lid. The basket is drawn into the cask, the cask shutter is closed, and the cask transferred to the spent fuel pool. The various lead fixtures are moved using the overhead polar crane. Certain administrative requirements are imposed on the above procedure:

a) The lead fixtures are not moved across the top of the core tank unless the reactor top shield lid is in place.

b) The bottom of the fuel transfer cask is kept within 6 inches of the upper surface of the reactor top shield lid.

If these requirements are met, analysis has shown that no damage will occur to the core should one of the lead fixtures and/or the cask drop onto the lid. The lid would deform but it would not rupture [13-25].

13.2.9.3 Spill of Heavy Water

Leakage from the heavy water reflector is of concern because of the tritium contained in the heavy water. The heavy water system is equipped with a leak detection system that will sound an alarm to notify the operator of any moisture that may result from a leak. This system is documented in Section 5.3.1.10 of the MITR-II SAR.

The maximum allowable tritium content in the heavy water is 5 Ci/liter as indicated in Section 5.3.1.6 of the MITR-II SAR. An evaporation rate of 5.1 liters per hour is estimated for a heavy water temperature of 60 °C, a relative humidity of 20%, and a spill area of 6 feet in diameter. This evaporation rate corresponds to a total volume of 122 liters, or a maximum activity of 610 Curies, in 24 hours. This is higher than would actually occur and hence conservative.

The effluent concentration (EC) for tritium concentrations in air in unrestricted areas is 1×10^{-7} μCi/ml. Using this value, a conservative dilution factor of 15,000, and assuming the containment building ventilation is operating, it is calculated that approximately 1.2 EC / 0.2 mrem exposure off-site would be attained over 24 hours [13-26].

13.2.9.4 Mixing of Light and Heavy Water

The current MITR core is moderated and cooled by light water and reflected by heavy water. Light water has both a higher moderating power and a larger absorption cross-section than heavy water does. In an under-moderated core with a hardened neutron energy spectrum such as the MITR, the effect of the high moderating power of light water outweighs its absorption effects, and, consequently, replacing coolant in the core with heavy water results in a negative reactivity effect. In the exterior regions of the light water core tank, where the neutron energy spectrum is much softer, neutron absorption by light water dominates over moderation so that replacing the light water with D_2O in the plenum above the fuel elements and along the walls and bottom of the core tank results in a momentary positive reactivity effect which is followed by a negative effect as the D_2O enters the core proper, i.e., the active region. Replacement of the heavy water in the reflector tank with light water will always result in a negative reactivity effect.

In Figure 13-5, the heavy water reflector contamination results are presented for the LEU case: 1) negative reactivity insertion with linear correlation to the percentage of light water leakage and 2) magnitude of ~ -1.6 β in case of 10% mixing. It should be noted that the calculation assumes homogeneous mixing of the light water with the heavy water in the reflector region. Local effects of H_2O leakage cannot, therefore, be inferred from this data.

In Figure 13-6, the light water system contamination results are presented for the LEU case: 1) positive reactivity insertion, when the heavy water leaks into either the light water above or below the core, or the light water annular space between the core and the sides of the core tank, and 2) significantly negative reactivity insertion, when heavy water mixes into the primary coolant of the core proper or progressively replaces the entire light water system.

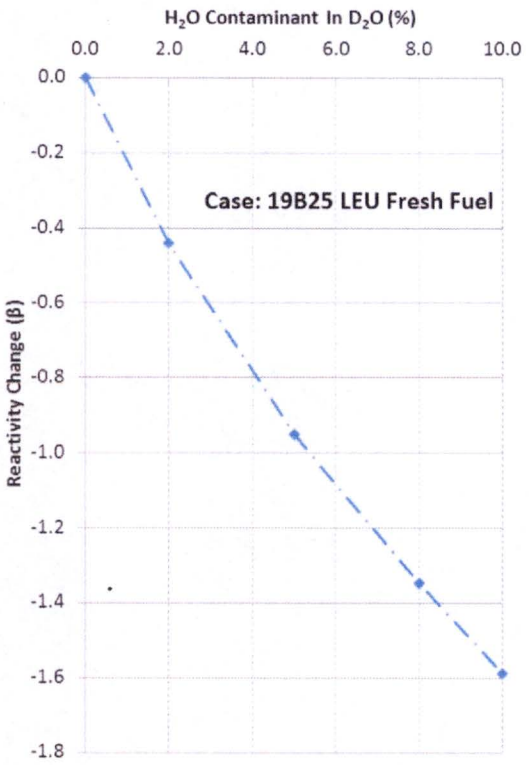

Figure 13-5. Effect of light water leakage into the heavy water reflector

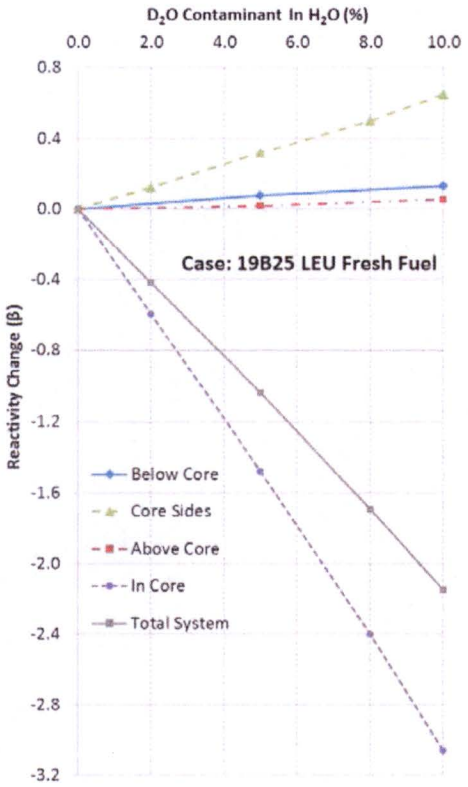

Figure 13-6. Effect of heavy water leakage into the light water system

13.3 Summary and Conclusions

This chapter contains conservative analyses of different types of accidents that are related to the MITR and its surrounding environment. There is no projected damage to the reactor core as an outcome of the accidents evaluated, except when the core damage is assumed to be part of the accident scenario, as described in Section 13.2.1 of this report, the maximum hypothetical accident. No radiation exposure to the public is expected except in the maximum hypothetical accident, for which the maximum Total Effective Dose Equivalent to the general public is 392.8 mrem during a two-hour period at 21 m from the containment building.

The robustness of the MITR is the result of the use of passive and engineered safety features in its design. These features are enumerated in Section 1.2.3 of the MITR-II SAR.

References

[13-1] A. Bergeron, E.H. Wilson, G. Yesilyurt, F.E. Dunn, J.G. Stevens, L. Hu, and T. H. Newton, "Low Enriched Uranium Core Design for the Massachusetts Institute of Technology Reactor (MITR) with Un-finned 12 mil-thick Clad UMo Monolithic Fuel", ANL/GTRI/TM-13/15, Argonne National Laboratory, November 2013.

[13-2] K. Sun, S. Don, T. Newton, L. Hu, F. Dunn, E. Wilson. Preliminary accident analyses for the MIT Research Reactor (MITR) conversion using 19B25 LEU fuel design. MITR-NRL-14-04, Rev. 2, June 2017.

[13-3] J.W. Dykes et al., A Summary of the 1962 Fuel Element Fission Break in the MTR, IDO-17064, February 1965.

[13-4] W.H. Tabor, Fuel Plate Melting at the Oak Ridge Research Reactor, ANS Transactions 8 Suppl., 36, July 1965.

[13-5] R.F. Mull, Exclusion Area Radiation Release During the MIT Reactor Design Basis Accident, S.M. Thesis, Nuclear Engineering Department, MIT, May 1983.

[13-6] Q. Li, Estimate of Radiation Release for MIT Research Reactor During Design Basis Accident, S.M. Thesis, Nuclear Engineering Department, MIT, May 1998.

[13-7] K. Plumer, Estimate of Radiation Release from MIT Reactor with Low Enriched Uranium (LEU) Core during Maximum Hypothetical Accident, Master Thesis, 2011, Massachusetts Institute of Technology.

[13-8] SCALE Official Website: http://scale.ornl.gov/.

[13-9] U.S. Nuclear Regulatory Commission, Severe Accident Risks: An Assessment for Five U.S. Nuclear Power Plants, NUREG-1150, June 1989.

[13-10] File Memo (MITR Coolant System Release Fraction during the MHA, March 1999).

[13-11] Regulatory Guide 1.183 – Alternative Radiological Source Terms for Evaluating Design Basis Accidents at Nuclear Power Reactors. 2000.

[13-12] NUREG-1465 – Accident Source Terms for Light-Water Nuclear Power Plants. 1995.

[13-13] J. Gosnell, Modification of Pressure Relief System, Technical Report.

[13-14] F.A. Gifford, An Outline of Theories of Diffusion in the Lower Layers of the Atmosphere, Meteorology and Atomic Energy, July 1968.

[13-15] Reactor Safety Study, Calculations of Reactor Accident Consequences, WASH-1400, October 1975.

[13-16] Atmospheric Dispersion Models for Potential Accident Consequence Assessments at Nuclear Power Plants, U.S. NRC Regulatory Guide 1.145, November 1982.

[13-17] Safety Analysis Report for the MIT Research Reactor (MITR-II), MITNE-115, October 1970.

[13-18] W. Woodruff, A Kinetics and Thermal-Hydraulics Capability for the Analysis of Research Reactors, Nuclear Technology, pp. 196-206, Vol. 64, Feb. 1984.

[13-19] J. Carew, L. Cheng, A. Hanson, J. Xu, D. Rorer, and D. Diamond, "Physics and Safety Analysis for the NIST Research Reactor," BNL-71695-2003-IR, 2003.

[13-20] F. Dunn, et al., Preliminary Accident Analyses for Conversion of the Massachusetts Institute of Technology Reactor (MITR) from Highly Enriched to Low Enriched Uranium, ANL/GTRI/TM-13/5, 2013, Argonne National Laboratory.

[13-21] RELAP5/MOD3.3 Code Manual, March 2006.

[13-22] G. Allen, Jr., Aspects of A Seismic Study of the MITR, S.M. Thesis, Department of Nuclear Engineering, MIT, May 1971.

[13-23] X-5 Monte Carlo Team, MCNP – A General Monte Carlo N-Particle Transport Code, Version 5, Volume II: User's Guide. April 24, 2003.

[13-24] MITR-Staff, Technical Specifications for the MIT Research Reactor (MITR-II), Rev.6, 2010.

[13-25] G. Walgenwitz, Response of the MIT Nuclear Reactor Top Lid to a Fuel Transfer Cask Drop Impact, MIT/NRL Special Report, June 1995.

[13-26] File Memo (Spill of Heavy Water, June 1999).

14.0 Technical Specifications

14.1 Format and Content

Technical specifications for the MITR are contained in a separate document, MITR Technical Specifications. These specifications were developed in accordance with ANSI/ANS-15.1-1990. Normal operation of the MITR within the limits of these technical specifications will not result in offsite radiation exposure in excess of 10 CFR Part 20 guidelines.

Due to LEU conversion, the operating conditions of the MITR will change as outlined in this PSAR. New technical specifications will be developed for the new LEU core operating conditions after the PSAR is approved.

15.0 Financial Qualifications

There are no changes to Chapter 15 (Financial Qualifications) as a result of LEU conversion; information on this subject can be found in the current MITR-II SAR.

16.0 Other License Considerations: Prior Use of Reactor Components

There are no changes to Chapter 16 (Other License Considerations: Prior Use of Reactor Components) as a result of LEU conversion; information on this subject can be found in the current MITR-II SAR.

17.0 Other License Considerations: Medical Use

There are no changes to Chapter 17 (Other License Considerations: Medical Use) as a result of LEU conversion; information on this subject can be found in the current MITR-II SAR.